TECHNISCHE UNIVERSITÄT MÜNCHEN

Lehrstuhl für Experimentelle Genetik

The role of AID and NF-κB for B cell development and lymphomagenesis

Sabine Schmidl

Vollständiger Abdruck der von der Fakultät Wissenschaftszentrum Weihenstephan für Ernährung, Landnutzung und Umwelt der Technischen Universität München zur Erlangung des akademischen Grades eines

Doktors der Naturwissenschaften

genehmigten Dissertation.

Vorsitzender:	Univ.-Prof. Dr. Dr. h.c. J. Bauer
Prüfer der Dissertation:	1. apl. Prof. Dr. J. Adamski 2. Univ.-Prof. Dr. H. H. D. Meyer 3. Univ.-Prof. M.J. Atkinson, Ph.D.

Die Dissertation wurde am 26.11.2010 bei der Technischen Universität München eingereicht und durch die Fakultät Wissenschaftszentrum Weihenstephan für Ernährung, Landnutzung und Umwelt am 28.07.2011 angenommen.

Für meine Familie

Wer nichts Unerwartetes erwartet,

wird das Unerwartete nicht finden.

(Heraklit 540-480 v.Chr.)

Contents

List of figures

List of tables

List of abbreviation

α	anti
A	adenine
AID	activation-induced cytidine deaminase
APC	allophycocyanin
APS	ammonium persulfate
BAFF	B cell activating factor of the TNF family
bp	base pair
B-CLL	B cell chronic lymphoblastic leukemia
BCR	B cell receptor
BrdU	Bromodesoxyuridine
BSA	bovine serum albumine
C	cytosine
CFSE	Carboxy-Fuorescin Diacetate Succinimidyl Ester
CLP	Common lymphoid progenitor
CMP	Common myeloid progenitor
Cre	protein recombinase of the phage *P1*
CSR	class switch recombination
DMEM	Dulbecco's modified minimal essential medium
DMSO	dimethyl sulfoxide
DNA	deoxyribonucleic acid
DNase	deoxyribonuclease
dNTP	desoxyribonucleotide triphosphate
EBV	Epstein-Barr virus
EDTA	ethylenediaminetetraacetate
EMSA	electromobility shift assay
ERK	extracellular signal-regulated kinase
et al	"et alii"
FACS	fluorescence-activated cell scanning/ sorting
FCS	fetal calf serum
FITC	fluorescein isothiocyanate
FoB	follicular B cell
G	guanine
g	gramme
xg	x times gravity
GC	gene conversion
GFP	green fluorescent protein
h	hour
ICAM	intercellular adhesion molecule
Ig	immunoglobulin
IgH	immunoglobulin heavy chain
IgL	immunoglobulin light chain
IL	interleukin
IRES	internal ribosome entry site
JNK	c-Jun N-terminal kinase
kb	kilo base
kDa	kilo dalton

ko	knock-out
l	liter
LMP	latent membrane protein
loxP	locus of crossover (x) of phage P1
M	molar
MACS	magnetic associated cell sorting
MAPK	mitogen activated protein kinase
MHC	major histocompability
min	minute
mg	milligram
MZB	marginal zone B cell
µF	microfaraday
N	amino-terminus
NF-κB	nuclear factor κ B
NLS	nulear localization sequence
PBS	phosphate buffered saline
PCR	polymerase chain reaction
PE	phycoerythrin
PerCP	perdinin chlorophyll protein
RNA	ribonucleic acid
RNase	Ribonuclease
rpm	revolutions per minute
RT	room temperature
SDS	sodium dodecyl sulfate
sec	second
SHM	somatic hypermutation
TAE	Tris-acetate-EDTA
TD	T cell dependent
TdT	terminal desoxynucleotidyl Transferase
TE	Tris-EDTA
TNF-R	tumor necrosis factor receptor
TRAF	TNF receptor associated factor
U	units
UV	ultraviolet light
V	volt
v/v	volume per volume
w/o	without
wt	wildtype
w/v	weight per volume

Summary

Peripheral B cells that encounter a cognate antigen and become activated via CD40 binding start to form germinal centres where they undergo affinity maturation. The affinity maturation process somatic hypermutation (SHM) depends on the activation-induced cytidine deaminase protein (AID) that inserts mutations into the immunoglobulin (Ig) locus, enhancing the genomic variety of antibodies. AID recruitment to the Ig locus and AID mutations must be strictly regulated to ensure genomic stability. However, the specific targeting of AID has not been clarified. In the scope of this project, *cis*- elements included in the Ig locus and potential *trans*- factors involved in the specific AID recruitment were identified. To this end a chicken DT40 cell line was used that solely undergoes somatic hypermutation. The assay for mutation was a *GFP2* reporter system in the Ig locus that accumulates AID-induced mutations. The compact size of the DT40 Igλ locus of 10 kb facilitates a successive deletion analysis.

A deletion of the complete Igλ locus demonstrated that elements essential for SHM are located in the Ig sequence. Via several staggered deletion analyses, the Igλ enhancer was identified as the core sequence essential for AID recruitment and in particular a 200 bp sequence located at the 5' end of the enhancer. This hypermutation core element ('HyCorE') was sufficient for AID recruitment. Multimerization of the element enhanced the mutation frequency. An identification of 'HyCorE' homologes in closely-related species and their efficient recruitment of AID confirmed the exclusive role of this sequence. An *in silico* analysis of the 200 bp core element identified binding sites for E2A, NF-κB, MEF-2, SP1 and Pax5. This is the first time demonstration of a sequence of 200 bp that is sufficient to induce hypermutation and carries binding sites for *trans*-acting factors for a putative AID recruitment complex.

CD40 signalling, that is essential for germinal centre formation and initiation of SHM, was known to be deregulated in several lymphomas. The LMP1/CD40 mouse model, established in our lab, allowed a detailed analysis of constitutive CD40 signalling. The LMP1/CD40 mouse expresses a chimeric protein consisting of the self-activated LMP1 transmembrane domain and the CD40 intracellular domain. It has previously been shown that a constitutive CD40

signal *in vivo* initiates B cell expansion and promotes B cell tumourigenesis. Analysis of signalling pathways in LMP1/CD40 expressing B cells revealed that the MAPK ERK and JNK and the non-canonical NF-κB pathway are activated. To analyze, whether the canonical NF-κB pathway influences B cell expansion and lymphomagenesis, mice with a NEMO or IKK2 null deletion were crossed with LMP1/CD40 mice. The disruption of the canonical NF-κB pathway blocked the LMP1/CD40 induced B cell expansion, reduced the LMP1/CD40 mediated survival and inhibited proliferation. Interestingly, the depletion of NEMO or IKK2 in LMP1/CD40 mice did not influence the translocation of the NF-κB components, but led to diminished pERK and pJNK levels, indicating a cross-talk between the NF-κB and MAPK pathways. Previous publications demonstrated a connection between NEMO/IKK2 and ERK via Tpl2/MEK1, resulting in a specific activation of p65 (Phospho-Ser276). Indeed p65(Ser276) was specifically phosphorylated in LMP1/CD40 mice, but not in NEMO or IKK2 depleted LMP1/CD40 or in wild type mice. These data imply that the canonical NF-κB pathway contributes to LMP1/CD40 mediated B cell expansion via the Tpl2/ERK/pp65(Ser276) regulation mechanism. This result elucidates a completely new role of the canonical NF-κB pathway for CD40 signalling in B cells and creates a foundation for detailed signalling analyses.

Zusammenfassung

Periphere B Zellen, die auf ein passendes Antigen treffen und durch CD40 aktiviert werden, bilden Keimzentren, in denen sie eine Affinitätsreifung durchlaufen. Ein Prozess der Affinitätsreifung, die somatische Hypermutation (SHM), benötigt das Protein Activation-induced cytidine deaminase (AID), welches Mutationen in den Immunglobulinlokus (Ig) einfügt und dabei die genomische Variation erhöht. AID induzierte Mutationen und die Rekrutierung an den Ig Lokus müssen streng reguliert werden, um eine Stabilität des Genoms zu gewährleisten. Allerdings wurde bisher noch nicht aufgeklärt, wie die spezifische Rekrutierung von AID an den Immunglobulinlokus erfolgt. Im Rahmen meines Projektes detektierte ich *cis*-Elemente, die Teil des Ig Lokus sind, und potentielle *trans*-Faktoren, die in die spezifische AID Rekrutierung involviert sein könnten. Dafür verwendete ich eine Hühner DT40 Zelllinie, die nur Hypermutation durchläuft und durch ein *GFP2* Reportersystem AID-induzierte Mutationen verfolgt werden können. Die kompakte Größe des DT40 Igλ Lokus von 10 kb erleichtert eine sukzessive Deletionsanalyse. Die Deletion des kompletten Lokus verdeutlichte, dass Elemente, die unentbehrlich für die SHM sind, innerhalb der Ig Sequenz liegen. Mit Hilfe von schrittweisen Deletionsanalysen, zeichnete sich der Igλ Enhancer als Kernsequenz für die AID Rekrutierung ab und dabei insbesondere eine 200 bp Sequenz, die am 5' Ende des Enhancers liegt. Das Hypermutationskernelement (‚HyCoreE') war ausreichend, um AID zu rekrutieren. Zudem erhöhte eine Multimerisierung dieses Elements die Mutationsfrequenz. Die Identifizierung von ‚HyCorE' homologen Sequenzen in nahverwandten Spezies, bestätigte die einzigartige Rolle dieser Sequenz. Mit Hilfe einer *in silico* Analyse des 200 bp Kernelements ermittelte ich Bindestellen für E2A, NF-κB, MEF-2, SP1 und Pax5. Damit konnte ich zum ersten Mal eine Sequenz von 200 bp detektieren, die hinreichend war, um Hypermutation zu induzieren, und die Bindestellen für *trans*-Faktoren enthält, welche Teil eines AID Rekrutierungskomplexes sein könnten.

Es ist bekannt, dass die CD40 Signaltransduktion essentiell für die Bildung von Keimzentren ist und in diversen Lymphomen in deregulierter Form vorliegt. Das LMP1/CD40 Mausmodell, das in unserem Labor etabliert wurde, eröffnete die Möglichkeit konstitutives CD40 Signal eingehend zu studieren. Es wurde im Vorfeld gezeigt, dass das LMP1/CD40 Signal zur B Zell Expansion und zur Tumorgenese führt. Weiterhin aktiviert es die MAPK ERK und JNK und den

nicht-kanonischen NF-κB Signalweg. Der kanonischen NF-κB Signalweg ist nicht hyperaktiviert. Um festzustellen, ob der kanonischen NF-κB Signalweg die B Zell Expansion und die Lymphomagenese beeinflusst, kreuzte ich Mäuse mit NEMO oder IKK2 Deletionen in den LMP1/CD40 Mausstamm. Eine Unterbrechung des kanonischen NF-κB Signalweges blockierte die LMP1/CD40 induzierte B Zell Expansion, reduzierte das Überleben und inhibierte die Proliferation. Interessanterweise beeinflusste die Deletion von NEMO oder IKK2 in LMP1/CD40 Mäusen nicht die Translokation von NF-κB Komponenten, sondern führte zu verminderten pERK und pJNK Werten. Dies deutet eine Koregulation von NF-κB und MAPK Signalwegen an. In vorhergehenden Publikationen wurde eine Verbindung zwischen NEMO/IKK2 und ERK über Tpl2/MEK1, welche letztlich in einer spezifischen Aktivierung von p65 (Phospho-Ser276) endet, aufgezeigt. Ich konnte eine spezifische Phosphorylierung von p65(Ser276) in LMP1/CD40 Mäusen detektieren, aber nicht in NEMO oder IKK2 deletierten LMP1/CD40 oder in Wildtypmäusen. Diese Daten implizieren, dass der kanonische NF-κB Signalweg über den Tpl2/ERK/pp65(Ser276) Regulationsmechanismus zur LMP1/CD40 vermittelten B Zell Expansion beiträgt. Dieses Ergebnis verdeutlicht, dass der kanonischen NF-κB Signalweg eine komplett neue Rolle in der CD40 Signaltransduktion in B Zellen einnimmt und damit die Grundlage für weitergehende Analysen bildet.

1. Introduction

1.1 The immune system

During evolution, organisms have developed highly sophisticated defence mechanisms to protect themselves from bacteria, virus, parasites and other pathogens. Starting as a very simple enzymatic system in bacteria, it further developed in plants producing molecules as defensins and evolved to very complex systems in vertebrates. In mammals we can distinguish between the innate and the adaptive immune system.

All cells of most of mammalian immune systems start their development in the bone marrow arising from a pluripotente hematopoietic stem cell (HSC) that matures either to a common lymphoid progenitor (CLP) or a common myeloid progenitor (CMP). CLP give raise to B, T and natural killer (NK) cells whereas the myeloid progenitors develop to macrophages, neutrophilic and dendritic cells. Macrophages and neutrophilic cells contribute to the innate immune system and control the early immune response. They rapidly recognize a common pathogen-specific signature, but are not able to eliminate all pathogens. For a specific immune response, the adaptive immune system, consisting of B and T lymphocytes, evolved during evolution. Each lymphocyte presents a different, specific antigen receptor on its surface, creating a repertoire of receptors which recognizes almost every antigen (Janeway et al., 2002).

1.2 The B cell receptor (BCR) and B cell development

In 1891, Paul Ehrlich introduced for the first time the term ‘antibody’ in his work “Experimental studies on Immunity” (reviewed by Winau et al., 2004). Fifty years later Linus Pauling confirmed Ehrlich’s predicted lock-and-key theory of antigen-antibody binding (Pauling et al., 1943). But the source of antibodies, the B cell, was not established until Cooper’s description of chicken bursa of fabricius in 1966 (Cooper et al., 1966). B cell development in most mammals starts in the bone marrow, passing several developmental stages that correspond to a genomic change of the immunoglobulin locus. In 1972, Edelman and Porter received the Nobel Prize in physiology or medicine for their discoveries concerning the chemical structure of antibodies. They demonstrated that antibodies consist

of two identical disulfide bond-linked heavy and light chains and of antibody binding (Fab) and antibody tail (Fc) regions (Olins et al., 1962; Cohen et al., 1964). The Fab region is composed of the variable (displayed in green) and one segment of the constant region (displayed in dark grey) of both light and heavy chain whereas the Fc region contains a variable number of constant domains of both heavy chains (Figure 1.1).

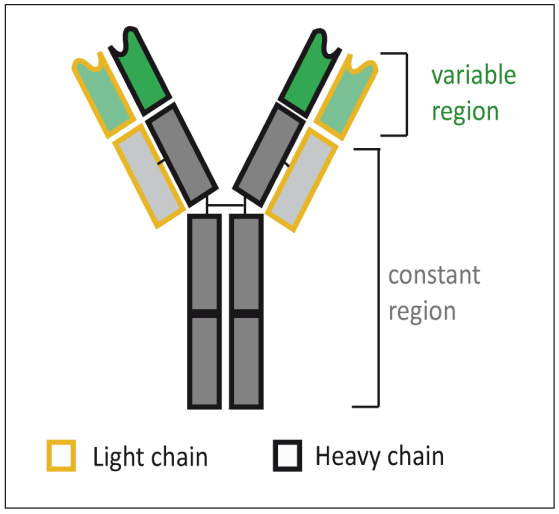

Figure 1.1 Antibody structure adapted from Janeway et al. (2001).
The Ig heavy chain is displayed with a black, the Ig light chain with an orange frame. The variable antigen-binding region is depicted in green, the constant functional region in grey.

The Ig heavy chain locus consists of multiple V (variable), D (diversity) and J (joining) gene segments. The Ig light chain locus only of V and J segments which can recombine in a random process, called somatic recombination (Ehrlich et al., 1995; Ten-Boeckel et al., 1995). During B cell development in the bone marrow D-J recombination of the heavy chain occurs in the early Pro-B cells and the V-DJ recombination in the late Pro B-cells (Hardy et al., 1991). If the Pre-B cell presents a functional rearranged heavy chain together with a surrogate light chain on its surface, it is positively selected and starts recombination of the κ or λ light chain V-J segments (Melchers et al., 1993; Melchers et al., 2000). Allelic exclusion guarantees that only one allele is rearranged per cell (Alt et al., 1984; Loffert et al., 1996; Melchers et al., 1999). If the B cell receptor is not functional or auto-reactive, a secondary gene rearrangement occurs to replace the inappropriate B cell receptor (BCR). This process is called receptor editing. In case the B cell receptor formation fails again, clonal deletion and apoptosis takes place. Immature B cells, expressing a functional BCR, enter the periphery as transitional B cells. In the spleen, B cells have to receive survival signals via the tonic BCR and BAFF (B cell activating factor) receptor to emerge to mature B cells. Only a few percent

of these cells survive and develop to two main mature populations, the follicular B cells (Fo B cells) and the marginal zone B cells (MZ B cells). The cell fate decision is commited by signalling through the BCR, Notch, BAFF and NF-κB (Pillai et al., 2009), but still not completely defined and under intensive investigation. The Fo B cells circulate through the blood and lymphoid organs for several months (Fu et al., 1999). In contrast, MZ B cells remain in the marginal zone of the follicles where they contribute to the early T cell independent immune response to blood borne bacteria.

If a cognate antigen binds to the B cell receptor of a naïve B-cell, the antigen is internalized, processed and presented as a MHCII:peptide-complex on the surface. $CD4^+$ T cells recognize the MHCII:peptide-complex and activate the B-cell via surface-expressed CD40 and other co-stimulatory signals. The cross-linking of BCR via an antigen, together with the co-stimulatory signals, leads to the activation of the B-cell, creating a germinal centre (GC). Within the GC the maturing B cell undergoes affinity-maturation via somatic hypermutation (SHM) to increase the antibody variety. B-cells with an increased affinity and without auto-reactivity survive and undergo class switch to change the functionality of the antibody. Both the somatic hypermutation and class switch processes depend on the activity of the cytidine deaminase enzyme (AID) (Muramatsu et al., 2000). After affinity maturation and positive selection, the B-cell differentiates either to a plasma cell or a memory B cell. Plasma cells secrete high-affinity antibodies leading to the neutralisation, opsonisation or activation of the complement system and finally to an elimination of the pathogen. Memory B cells continue circulating through the secondary lymphoid compartments for a long period of time. Contact of a memory B cell with a specific antigen epitope leads to an immediate secondary immune response and the secretion of high-affinity antibodies.

1.3 Antibody diversification processes

An efficient BCR binding depends on wide repertoire of potential high affinity antibodies to react on the vast variety of pathogens. Therefore, the immune system is equipped with four mechanisms to increase the affinity and diversity of antibodies: somatic recombination, hypermutation, class switch recombination and gene conversion.

The somatic recombination of different V, D and J segments within antibody gene loci, as a first step in diversification, was already detected in 1976 (Hozumi et al., 1976) via restriction

analysis and southern blotting. Vertebrates possess a species-specific number of each of the V, D and J segments (Early et al., 1980). Each of these gene segments is flanked by a 5' recombination signal sequence (RSS), consisting of a conserved heptamer, a spacer (12 or 23 bp) and a conserved nonamer (Max et al., 1979). The recombinase enzymes RAG1 and RAG2 bind to the RSSs containing two different spacers (Agrawal et al., 1997). Via protein interaction, the D and J or V and D segments are co-localized, creating a hairpin structure which is digested after the heptamer sequence. The hairpin is cut and ligated randomly (Shokett et al., 1999), including DNA repair proteins of the non-homologous end joining (NHEJ) pathway like Ku70:Ku80, XRCC4 and the DNA ligase IV (Gu et al., 1997; Li et al., 1995). The activity of terminal deoxynucleotidyl transferase (TdT) additionally enhances the variety by modifying the RSS ends by inserting random nucleotides (Komori et al., 1993). The combinatorial diversity of the BCR during early B cell development is further increased by the combination of the light and the heavy chain creating the variable, antigen-binding region.

After a T cell dependent B cell activation, two additional affinity maturation processes occur in the germinal centre, namely the somatic hypermutation and the class switch recombination. Both of these mechanisms depend on the protein activation-induced cytidine deaminase (AID) (Muramatsu et al., 2000). AID has homology to the family of APOBEC proteins, in particular to that of APOBEC1 (Conticello et al., 2005; Muramatsu et al., 1999). Like the APOBEC family members, AID specifically deaminates cytidine in a polynucleotide context (Beale et al., 2004; Petersen-Mahrt et al., 2003) and exclusively in single-stranded DNA (Bransteitter et al., 2003; Chaudhuri et al., 2003; Dickerson et al., 2003; Pham et al., 2003). The expression of AID is up-regulated by germinal center initiating factors, like CD40 ligand (CD40L) and IL4 (Dedeoglu et al., 2004; Zhou et al., 2003).

In the somatic hypermutation process, AID deaminates cytidine to uracil, primarily at the consensus sequence WRCY (W=A/T, R=A/G, Y=C/T) (Sharpe et al., 1991; Rogozin et al., 1992; Betz et al., 1993). The resulting uracil base is removed by a uracil-DNA glycosylase (UNG) during base excision repair, creating an abasic site that can be repaired either in an error-free or error-prone process (Rada et al., 2002). Somatic hypermutation of the V region occurs with a frequency of 10^{-3} per bp (Neuberger et al., 1995) per generation. Single mutations in the variable region, enhancing the specificity of the BCR, contribute to the B cell survival during the selection process.

Class switch recombination occurs in B cells after activation and following cytokineinduction. It can be directed towards different C regions (C_μ, C_δ, C_γ, C_ε and C_α) of the heavy chain, depending on the cytokine, which specifically initiates transcription of the gene. These sterile transcripts are characterized by a non-coding 'I' exon located at the 5' end of the RNA. They are essential for chromatin access of AID during CSR. AID inserts nicks to the switch regions (S), which are located upstream of each C region. Switch regions are highly repetitive GC rich sequences that recombine in order to change the isotype (IgM, IgD, IgG, IgE and IgA) of the heavy chain (Stavnezer et al., 1996) and therewith its functionality.

In birds and some domesticated species, B cells are required to undergo an additional AID dependent diversification mechanism, namely gene conversion (GC) since the BCR gene has only a single copy of the V and J segments. A cluster of pseudogenes is located upstream of this VJ segment. In the light chain, the pseudogenes contain 25 VL-like segments, in the heavy chain the cluster consists of 80 VHDH-like segments (Reynaud et al., 1987; Reynaud et al., 1989). During gene conversion parts of the pseudogenes are copied and inserted into the V region, whereby the related pseudogen is retained at its original location (Carlson et al., 1990).

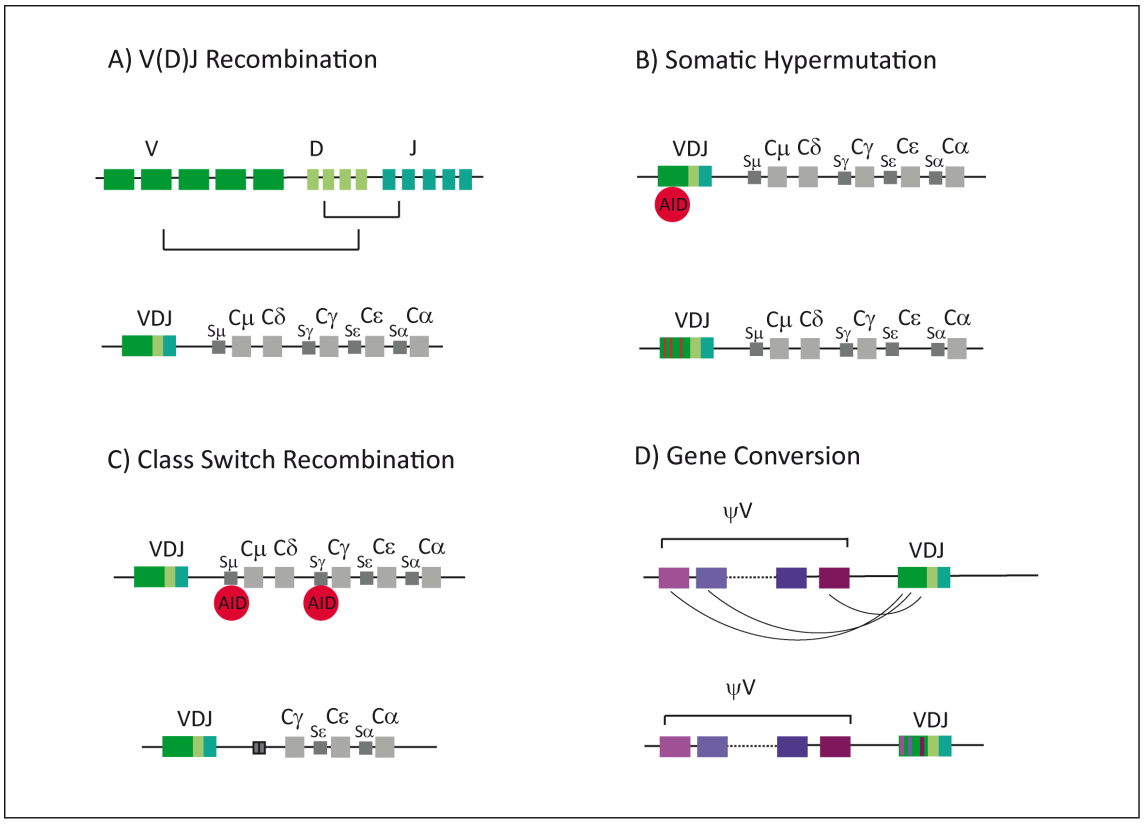

Figure 1.2 Diversification mechanisms adapted from de Yébenes et al. (2006).
A) The RAG-complex binding initiates J to D and (D)J to V recombination. B) AID introduces single mutations in the V region by deaminating cytosine to uracil. C) AID induces CSR by inserting nicks in the switch regions upstream the C regions, thereby changing the functionality of the antibody. D) During gene conversion gene, segments of the pseudo V genes (ψV) are inserted into the V region.

1.4 The activation-induced cytidine deaminase (AID)

Although some processes during antibody diversification depend on AID, it is not completely understood how the mutagenic potential of AID is restricted. One of the control mechanisms is the cell-type specific expression of AID, which is restricted to B cells. The forced expression of AID in fibroblasts was sufficient to induce CSR and SHM initiation in non-lymphocytes (Yoshikawa et al., 2002; Okazaki et al., 2002). A second protective mechanism is that AID is mainly located in the cytoplasm, since its C-terminal domain contains a strong nuclear export signal. This compartimenalizatio prevents access to DNA and prevents unregulated DNA mutation (Rada et al., 2002; Ito et al. 2004; McBride et al., 2004). The C-terminal domain of AID is not only controlling cellular translocation, but is also essential for CSR. Deletion of the C-terminal domain inhibits CSR but does not influence SHM (Ta et al., 2003; Barreto et al., 2003). Conversely, the N-terminal domain of AID is not required for CSR, but essential for SHM (Shinkura et al., 2004). Therefore, the two processes, CSR and SHM, are independently controlled via the different domains of AID. This might indicate that specific CSR and SHM *cis*- or *trans*-elements are involved in each of the different AID activities. It has been reported, that transfected AID was co-immunoprecipitated along with RNA polymerase II (Nambu et al., 2003) and additionally, that the transcription elongation complex directs AID directed mutations (Besmer et al., 2006). Another *trans*-factor that was co-immunoprecipitated with AID is the replication protein A (RPA) (Chaudhri et al., 2004). This is a single-stranded DNA binding protein also involved in the replication process. These results demonstrate that different components of the transcription machinery bind to AID.
Ig genes mutate with 10^5 fold higher mutation rate than non-Ig genes in different B cell lines (Martin et al., 2002). Even in B cell lymphomas with a deregulated AID activation the Ig genes show a 50 times higher mutation-rate than non-Ig genes (Pasqualucci et al., 1998; Shen et al., 1998; Gordon et al., 2003; Landowski et al., 1997; Müschen et al., 2000). However, it is not clear how the B cell specific recruitment of AID to the immunoglobulin locus is accomplished. The specific targeting might result from exclusive *cis*-elements being

involved in AID recruitment. However, substitution of Ig-specific promoter and enhancer sequences with other gene promoters and enhancers did not influence the hypermutation (Yang et al., 2006). However this may be due to a redundancy in the promoter and enhancer sequences within the immunoglobulin locus. Alternatively, *cis*-acting sequences may be distributed over other parts of Ig locus or even outside the Ig locus.

1.5 CD40 Receptor (CD40)

CD40 is a 48 kDa transmembrane type I glycoprotein belonging to the TNF receptor family. Paulie et al. were first to indentify CD40 through a monoclonal antibody reaction with bladder carcinoma cells and B lymphocytes (Paulie et al., 1989). The receptor is not restricted to B cells and is expressed by dendritic cells, monocytes, macrophages as well as non-hematopoietic cells like epithelial cells. (Bourgeois et al., 2002; Déchanet et al., 1997; van Kooten et al., 1997). CD40 activation by CD40L, expressed on activated T cells, triggers B cell proliferation, expansion and differentiation (Banchereau et al., 1994; Barrett et al., 1991; Jabara et al., 1990) and is essential for GC formation as well as initiation of CSR and SHM (Kawabe et al., 1994). It has been shown that a defect in the human CD40 pathway, due to mutation of the *CD40L* gene, leads to an X-linked hyper IgM syndrome. The characteristics of this severe immune deficiency are an impairment of GC formation, defects in the secondary immune response and a high frequency of lymphomas (Callard et al., 1993; Hayward et al., 1997). Since the intracellular cytoplasmic tail of CD40 lacks a kinase activity, the CD40L-mediated activation requires recruitment of additional tumour necrosis factor receptor-associated factors (TRAFs). The TRAF family contains six members, which are recruited to the cytoplasmic tail of CD40. TRAF 1, 2 and 3 bind to the PxQxT binding domain of CD40, TRAF6 binds to the QxPxEx binding domain of, whereas TRAF5 binds indirectly via TRAF3 or TRAF2 (Bishop et al., 2007; Pullen et al., 1998; Pullen et al., 1999). TRAF2 binding initiates JNK, p38, Akt (Hostager et al., 2003; Lee et al., 1997) and the non-canonical NF-κB pathway (Vince et al., 2007). TRAF6 initiates JNK, Erk, p38, Akt and the canonical NF-κB pathway (Davies et al., 2005; Rowland et al., 2007; Bishop et al., 2007), whereas TRAF3 binding selectively inhibits the non-canonical NF-κB pathway (He et al., 2007). The activation of CD40 initiates a degradation of TRAF3 and thereby favours the activation of both the canonical NF-κB pathway via TRAF6 and the non-canonical NF-κB pathway via TRAF2.

The proteins c-Jun N-terminal kinase (JNK), extracellular-regulated kinase (Erk) and p38 are activated by CD40 via a MAPK cascade and regulate several transcription factors including CREB (cAMP response element binding). The CD40 activated NF-κB pathway consists of the canonical and the non-canonical NF-κB pathway. The canonical pathway is activated by the NEMO/IKK1/IKK2 complex, whereas the activation of the non-canonical pathway is mediated via NIK and IKK1.

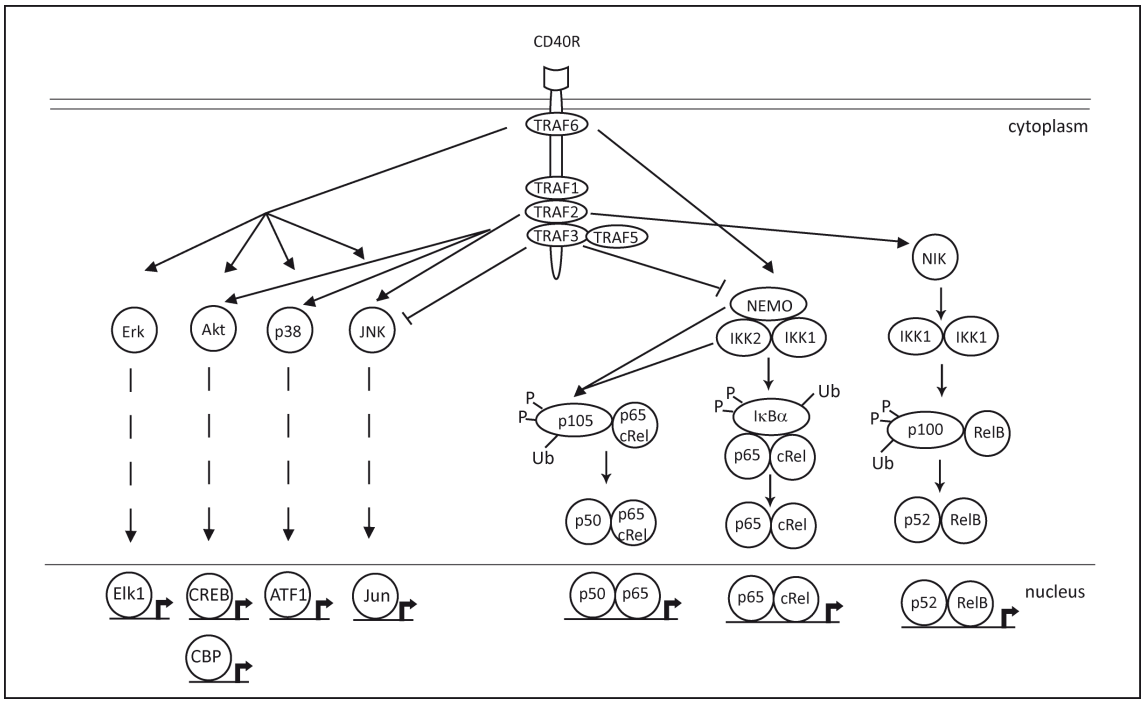

Figure 1.3 CD40 receptor signalling.
TRAF1, 2, 3 and 6 bind directly to the CD40 signalling domain, mediating the activation of Erk, Akt, p38, JNK and NF-κB pathways. Erk, Akt, p38 and JNK activate transcription factors that bind to the DNA, regulating different target genes. After CD40 activation, NF-κB dimers of the canonical and the non-canonical pathway are released from their inhibitors and shuttle to the nucleus, initiating the transcription of different target genes. Erk (extracellular signal regulated kinase), IKK (IκB kinase), JNK (c-Jun N-terminal kinase), NEMO (nuclear factor-κB essential modulator), P (Phosphorylation), Ub (Ubiquitin), TRAF (TNF receptor associated factors).

1.6 The NF-κB pathway

In 1986, NF-κB was identified as a kappa light chain enhancer binding factor (Sen et al., 1986 A and B). Since then, NF-κB has been recognized as one of the key regulators of both the innate and adaptive immune responses (Bonizzi et al., 2004; Karin et al., 2005).

The NF-κB family consists of five different members: the transcriptionally active factors p65 (RelA), RelB and c-Rel and the NF-κB1 (p50 and its precursor p105) and NF-κB2 (p52 and its

precursor p100) molecules, which lack the C-terminal transcription activation domain (TAD). All subcomponents carry a Rel homology domain (RHD) that includes a nuclear localization signal (NLS) and a sequence required for dimer formation. RelB heterodimerizes predominantly with p100 or its processed form p52 (Dobrzanski et al., 1995; Senftleben et al., 2001; Yilmaz et al., 2003), whereas p65 and c-Rel preferentially bind to p50 (Karin et al., 2000).

In resting B cells the translocation of dimers to the nucleus is blocked by an association with inhibitor of κB (IκB) proteins or by an association with p100 or p105. IκB proteins harbour multiple ankyrin repeats, binding to NF-κB dimers and interfering with their NLS (Ghosh et al., 1998). Ankyrin repeats are also found in the C-terminus of p100 and p105 (Dobrzanski et al., 1995; Liou et al., 1992). p100 (IκBδ) preferentially binds to RelB to retain it in the cytoplasm (Bren et al., 2001; Solan et al., 2002). p105 (IκBγ) specifically associates with p50, c-Rel and p65 to inhibit a nuclear translocation (Liou et al., 1992; Mercurio et al., 1993). The initiation of the classical NF-κB pathway requires activation and binding of the catalytic IκB kinases (IKK) IKK1, IKK2 and the regulatory nuclear factor-κB essential modulator (NEMO) (Karin et al., 2000). This trimeric complex phosphorylates IκBα, one of the classical IκB proteins, on Ser32 and Ser36, leading to the addition of a ubiquitin chain to Lys48 and subsequently to proteasomal degradation via the proteasom 26S (Ghosh et al., 2002). IκBα predominantly regulates p65/p50 dimers (Karin et al., 2000). After B cell stimulation, IκBα is degraded rapidly (Hoffmann et al., 2002), releasing the specific dimers. IκBα is also involved in a negative feedback regulatory mechanism. Degradation of IκBα is followed by a NF-κB dependent synthesis of IκBα, a shuttling to the nucleus and binding to deacetylated p65/p50, relocating those to the cytoplasm (Arenzana-Seisdedos et al., 1997; Chen et al., 2001).

The major IκB kinase activity in the classical NF-κB pathway is demonstrated by IKK2. A deficiency of IKK1 merely results in a slightly diminished IKK activity (Hu et al., 1999). However, in the absence of IKK2, IKK1 can provide some residual IKK activity (Li et al., 1999). In the alternative pathway IKK1 plays an exclusive role, independent of IKK2 and NEMO. The NF-κB inducing kinase (NIK) activates IKK1 homodimers which phosphorylate p100 at specific serin residues in the poly-ankyrin region. This is followed by ubiquitination and a C-terminal degradation of p100, releasing p52/RelB dimers (Xiao et al., 2001).

The inhibitor p105 can either be constitutively processed by the proteasome, removing the C-terminus and generating a p50 subunit (Palombella et al., 1994) or it undergoes complete proteasomal degradation. The proteolysis depends on NEMO and IKK2 activation and results in the release of NF-κB subunits without additional p50 production (Beinke et al., 2004; Heissmeyer et al., 2001; Waterfield et al., 2004).

Interestingly, the classical pathway regulates the NF-κB2 and RelB transcription, thereby influencing the alternative pathway (Liptay et al., 1994; Bren et al., 2001).

In the B-cell lineage IKK1 is essential for normal B-cell development (Pasparakis et al., 2002; Kaisho et al., 2001). Bone marrow chimeras, transplanted with *Ikk1-/-* fetal liver progenitors lack mature B cells and show enhanced apoptosis of immature B cells. B cell conditional NEMO and IKK2 knock-outs show normal B cell development in the bone marrow, but have a developmental block from the transitional T1 to T2 stage and therefore reduced numbers of mature B-cells in secondary lymphoid organs (Pasparakis et al., 2002).

1.7 The roles of AID and CD40 in tumourigenesis

CD40 and AID both play an essential role in the germinal center reaction. However, the aberrant expression of both proteins was found to be an initiator for tumour development.

Mistargeted CSR and aberrant SHM are thought to cause chromosomal translocation and mutation of proto-oncogenes. AID initiates the oncogenic translocation of *c-myc* to the IgH locus in multiple myeloma (Chesi et al., 2008). Aberrant SHM is found in more than 50% of diffuse large B cell lymphoma (DLBCLs), leading to mutations in the 5' sequence of several genes (Pasqualucci et al., 2004). Usually AID expression is restricted specifically to GC B cells. AID expression can be initiated by different pathogens outside the GC, thereby contributing to non-GC B cell lymphomas and additionally also to non-lymphoid tumours (Okazaki et al., 2007). To understand how a deregulation of AID can induce these mis-expression and mis-targetings, it is essential to know details about the normal mechanism of AID recruitment to the Ig loci.

An aberrant CD40 expression can be found in Hodgkin lymphomas and non-Hodgkin lymphomas, chronic lymphocytic leukaemia (CLL) (Kato et al., 1998), multiple myeloma (Pellat-Deceunynck et al., 1996; Teoh et al., 2000) and acute myeloid leukaemia (AML) (Aldinucci et al., 2002). In carcinomas such as those of the nasopharynx, cervix and ovary, a

remarkable high level of CD40 expression was detectable (Altenburg et al., 1999; Gallagher et al., 2002; Agathanggelou et al., 1995). Interestingly, several of these tumours were also infected with the Epstein Barr virus (EBV), expressing the oncogenic latent membrane protein (LMP1) that mimicks CD40 signalling by interaction with similar TRAFs than CD40. In contrast to CD40, the activation of LMP1 is independent of ligand binding, since its six transmembrane domains can self-aggregate, leading to a constitutive signal transduction (Eliopoulos et al., 2001) and therefore to a promotion of oncogenic transformation. This also implies an important role of constitutive CD40 signalling for tumour pathogenesis.

1.8 Experimental systems

The DT40 cell line was used as a model to study AID induced somatic hypermutation. The avian leukosis virus (ALV) can induce a bursal lymphoma in chicken which can be cultured as tumour cell line (Baba et al., 1985). One such AVL induced chicken tumour cell line, the DT40 cell line, continues to diversify its light chain genes outside the bursa (Buerstedde et al., 1990), and even during in vitro passage. In this cell line targeted integration of transfected DNA constructs occurs with a high frequency, at least one magnitude higher than that of random integration (Buerstedde et al., 1991). This facilitates experimental genome modification, auch as gene ablation or insertion.
In addition to a high targeted integration ratio, the DT40 cell line offers several advantages for the analysis of the immunoglobulin gene. Thus, DT40 is a cell line with a high genomic stability (Sale et al., 2004), which allows long- term cultivation. Furthermore, a short replication time of 12h abbreviates the duration of experiments. In comparison to human or murine cell lines, whose light chain are of megabasepair size and complex, the chicken light chain gene is only about 10 kb in size which facilitates a detailed sequence analysis.

The LMP1/CD40 transgenic mouse strain was used as a model to study the consequences of constitutive CD40 signalling in B cells. Constitutive CD40 signalling is found in several lymphomas, suggesting a contribution to the tumour pathogenesis. Cornelia Hömig-Hölzel has provided experimental evidence using a mouse model that deregulated CD40 expression is involved in lymphomagenesis (Hömig-Hölzel et al., 2008). The model uses expression of a chimeric protein that consists of the LMP1 transmembrane domain fused to the CD40

intracellular signalling domain (Hömig-Hölzel et al., 2008). A self-aggregation of the transmembrane domains promotes a ligand-independent constitutive CD40 signalling. The *LMP1/CD40* gene was targeted to the ubiquitously active *Rosa26* locus. Upstream of the *LMP1/CD40* gene a loxP flanked stop cassette was inserted. Crossing the LMP1/CD40 mouse to a CD19-Cre mouse line, deletes the stop cassette B cell specifically only in CD19 expressing cells, resulting in the B cell specific expression of LMP1/CD40. Mice expressing LMP1/CD40 in B cells displayed splenomegaly after 8 weeks, an accumulation of mature B and T cells in spleen and other lymphoid organs. The B cells demonstrated an activated phenotype by high surface CD95 and ICAM expression, prolonged survival and enhanced proliferation. The bone marrow B cell population was mostly unaffected, indicating a normal early B cell development. After the age of 80 weeks, more than 50% of the mice developed mono- or oligoclonal B cell lymphoma.

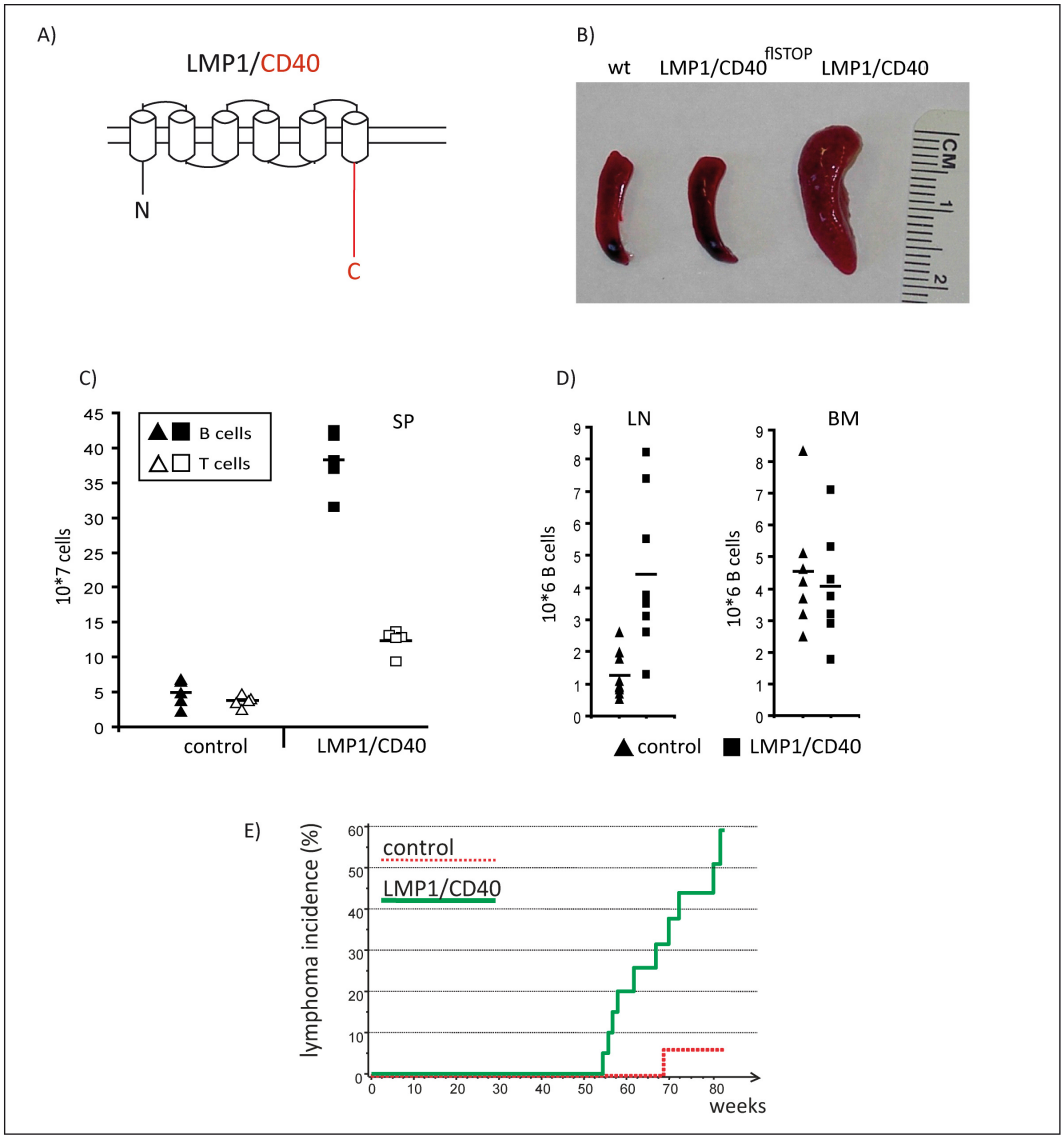

Figure 1.4 LMP1/CD40 mouse model.
A) The LMP1/CD40 mouse expresses a chimeric protein consisting of the EBV LMP1 transmembrane domain (black) and the CD40 intracellular domain(red). B) Mice at the age of 8 weeks, expressing LMP1/CD40 B cell specifically (LMP1/CD40) are characterized by a splenomegaly compared to wildtyp or LMP1/CD40^{flstop} mice. C) The splenomegaly in LMP1/CD40 mice is due to increased splenic (SP) B and T cell numbers. D) LMP1/CD40 B cell numbers are increased in lymph nodes (LN), whereas bone marrow B cells display no significant difference at the age of 8 weeks. E) The Kaplan-Meyer curve indicates a lymphoma incidence of 50% after 80 weeks in LMP1/CD40 mice. Adopted from (Hömig-Hölzel et al., 2008).

The analysis of the signalling pathways revealed that the constitutive CD40 signalling results in an activation of the downstream MAPKs ERK and JNK. *Ex vivo* inhibitor experiments showed that the improved survival of B cells depends more on ERK than on JNK activity. Furthermore, LMP1/CD40 selectively activates the non-canonical NF-κB pathway indicated by enhanced levels of nuclear p52 and RelB. The canonical NF-κB pathway was not

hyperactivated, demonstrated by similar levels of p65 and cRel and reduced levels of pIκBα in LMP1/CD40 B cells (Hömig-Hölzel et al., 2008).

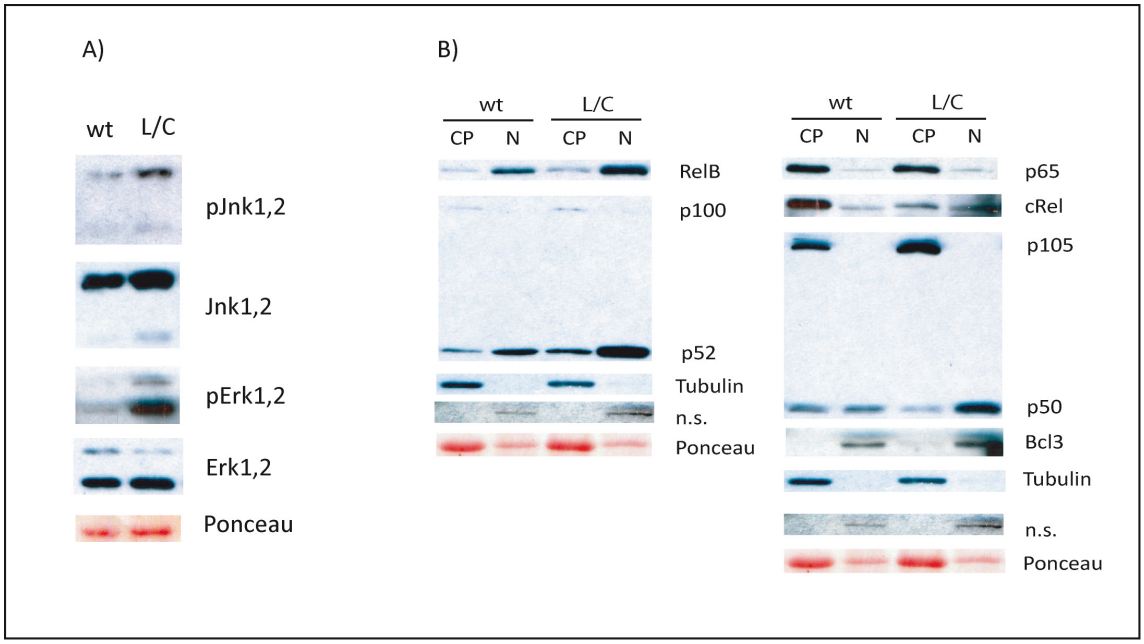

Figure 1.5 LMP1/CD40 protein expression.
A) LMP1/CD40 splenic B cells show enhanced levels of pJNK1/2 and pERK1/2. B) LMP1/CD40 B cells selectively hyperactivate the non-canonical NF-kB pathway, indicated by enhanced levels of nuclear RelB and p52. . Adopted from (Hömig-Hölzel et al., 2008).

2. Project aim

During the T cell dependent (TD) immune response, resting B cells become activated via a CD40 signal, start to expand and undergo affinity maturation. One of the maturation processes, the somatic hypermutation, depends on the protein AID, which induces mutations into the DNA of the Ig locus by cytidine deamination. The AID mutator activity must be strictly regulated to guarantee genomic stability. A deregulation of AID may contribute to oncogene mutations, inducing lymphomagenesis. It is not clear how the specific recruitment of AID to the Ig locus is controlled. AID has been shown to be a B cell specific factor, essential for SHM and it mutates only transcribed genes and single-stranded DNA. The dependence on gene transcription led us to presume a recruitment complex, in which transcription regulatory proteins are involved. The binding of transcription regulating factors occurs usually at *cis*-regulatory elements. Therefore we assume that specific *cis*-elements inside the Ig locus recruit *trans*-acting proteins and ultimately lead to AID binding. So far, it has not been possible to identify these elements. The usage of the DT40 cell line in combination with a *GFP2* reporter system offers for the first time the possibility to perform a detailed sequence analysis of the regulatory elements of the Ig locus. In contrast to human or mouse cells, having an Ig locus of Mbp size, the DT40 chicken B cell Ig locus includes 10 kb, being compact enough for a deletion analysis. The *GFP2* reporter is used to detect AID induced mutations. Mutations inserted into the *GFP* reporter gene lead to a reduction of *GFP* intensity and are correlated with the mutation rate. In the first part of my thesis I will perform a detailed deletion analysis of the Ig locus, detecting the SHM activity via the *GFP2* reporter. The goal of these studies is to identify specific *cis*-regulatory elements and corresponding *trans* factors involved in the AID recruitment process.

The second part of these studies deals with the question of how the CD40 signal responsible for B cell activation and affinity maturation, contributes to tumourigenesis. It was shown *in vivo*, that a constitutive CD40 signal leads to a constitutive activation of B cells, triggering lymphomagenesis (Hömig-Hölzel et al., 2002). A mouse model has been previously generated, allowing the analysis of B cell specific constitutive CD40 signalling. The constitutive CD40 activity was achieved by combining the CD40 intracellular signalling

domain with a self-activating LMP1 transmembrane domain. LMP1/CD40 mice have been shown to hyperactivate the MAPK ERK and JNK and the non-canonical NF-κB pathway. In contrast the canonical NF-κB pathway was not active in LMP1/CD40 mice. This raises the question of whether the canonical NF-κB pathway is dispensable for CD40 mediated B cell activation and whether it has any contribution to lymphomagenesis. A crossing of LMP1/CD40 mice with conditional knock-outs of NEMO or IKK2 mice, both components of the canonical pathway, will be studied to clarify the role of the canonical NF-κB pathway in constitutive CD40 signalling and its contribution to tumourigenesis.

3. Results

3.1 Defining *cis*-regulatory elements that are essential and sufficient for hypermutation

Deletion of the E2A gene (Schötz et al., 2006) in the DT40 cell line reduced the hypermutation rate significantly, demonstrating the involvement of transcription factors in the hypermutation process. Since E2A binding sites (E-box) appear frequently throughout the genome, it can be assumed that additional transcription factors contribute to the AID recruitment. These additional factors could bind to *cis*-elements located inside the Ig locus or in surrounding sequences. At the start of this work it was not clear whether *cis*-elements specific for AID recruitment do exist, and if so, where they are located. To identify the binding sequences we used a reporter construct referred to as *GFP2* (Blagodatski et al., 2009). Transcription of the *GFP2* reporter is driven by a Rous Sarcoma virus long terminal repeat (RSV) promoter and contains a GFP coding region. An internal ribosome entry site (IRES) was included to drive the expression of a downstream blasticidin resistance gene from the same promoter. The blasticidin resistance was used for drug selection of transfected clones and the Simian Virus 40 late polyadenylation signal (SV40 polyA) for efficient polyadenylation reactions. The *GFP2* reporter was inserted upstream of the Igλ locus. An interference of *GFP2* transcription with Ig transcription was excluded, since *GFP2* was inserted in the opposite transcriptional direction than the *Ig* gene, simultaneously deleting the Ig promoter. All constructs that were transfected to the DT40 cell line include the *GFP2* reporter and the IgL region of interest (ROI) and were referred as $pIgL^{ROI, GFP2}$.

All experiments on AID targeting, documented in this work, were performed in the chicken DT40 B cell line.

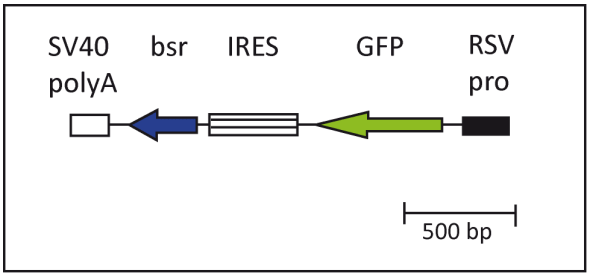

Figure 3.1 The *GFP2* reporter.

The *GFP2* reporter consists of the Simian Virus 40 late polyadenylation signal (SV40 polyA), a blasticidin resistance gene (bsr), driven by an internal ribosome entry site (IRES), and the GFP (green fluorescent protein) gene, driven by an Rous Sarcoma virus long terminal repeat (RSV) promoter.

3.1.1 Specific elements in the Igλ locus are necessary to recruit AID

In previous experiments, performed in our group by Hiroshi Arakawa, the *GFP2* reporter transgene was inserted into the rearranged Ig locus of the DT40 $\psi V^{-}AID^{RI}$ cell line. In this cell line, the pseudogenes upstream of the Igλ locus were deleted to eliminate gene conversion, thereby enhancing the hypermutation frequency. The AID gene was reconstituted to guarantee a constitutive AID expression (Arakawa et al., 2004). The insertion of *GFP2* into $\psi V^{-}AID^{RI}$ upstream the light chain led to an accumulation of mutations in *GFP2*, causing a loss of GFP intensity (Figure 3.2A) in 6.4% of B cells. This result demonstrated that AID does not only introduce mutations into the Ig locus, but also into transcribed genes closely localized like *GFP2*. We assumed, that the percentage of GFP low cells correlates with the hypermutation rate and though with the AID recruitment. Thus, *GFP2* can be used as a read-out assay for hypermutation activity. To detect whether the Igλ locus contains *cis*-elements, essential for AID targeting, Hiroshi Arakawa created a new cell line, in which the Igλ locus was deleted by inserting a puromycin cassette ($\psi V^{-}IgL^{-}$). The puromycin resistance was used to select transfected clones. The insertion of the *GFP2* construct into the $\psi V^{-}IgL^{-}$ cell line, induced a reduction of the percentage of GFP low cells to 0.01% (Figure 3.2B). This indicated, that elements, essential for AID targeting, must be found inside the Igλ locus. To confirm these data, I reconstituted the complete locus ($pIgL^{reconst,\ GFP2}$) and detected a GFP low population of 7.4% (Figure 3.2C). The percentage of GFP low cells in the ψV^{-} $IgL^{reconst}$ cell line was comparable to the percentage of GFP low cells in the precursor cell line cells $\psi V^{-}IgL^{GFP2}$, demonstrating that *cis*-elements, essential for AID targeting, must be located in the Igλ locus.

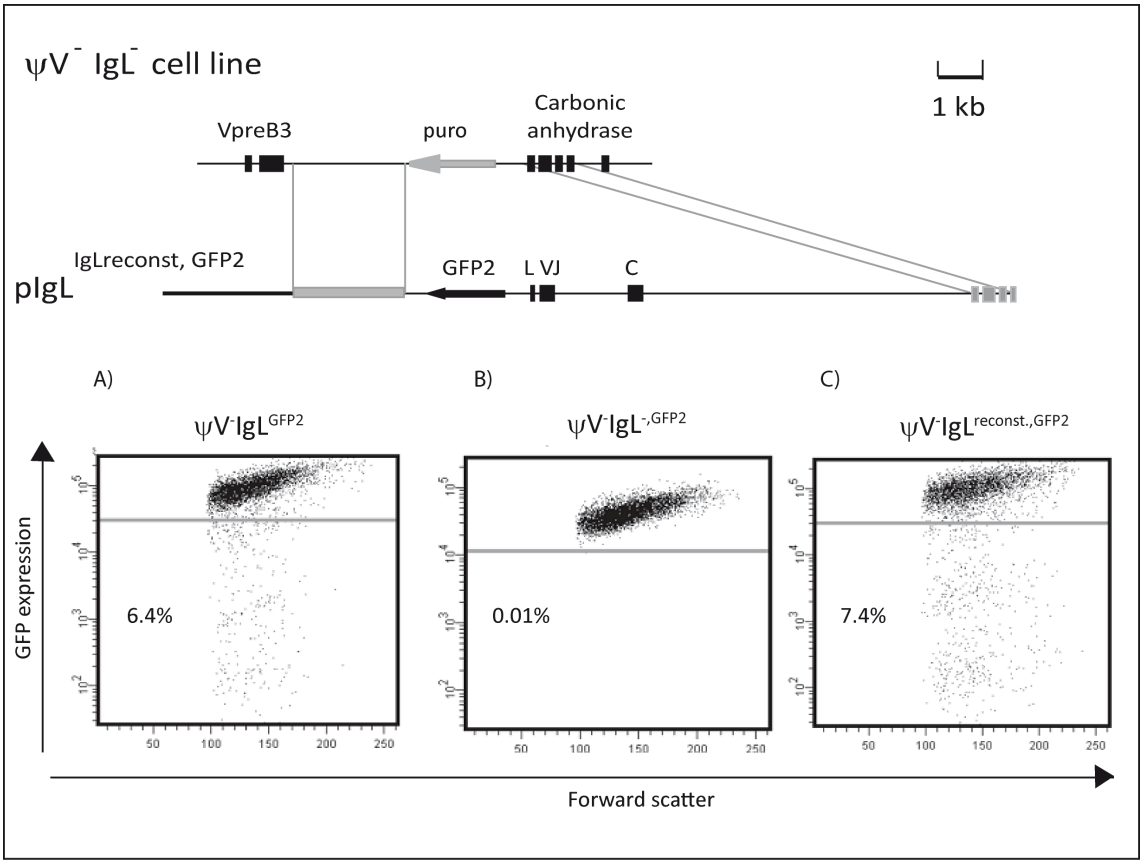

Figure 3.2 Deletion of Igλ inhibited AID induced hypermutation.
The *GFP2* reporter construct was inserted to the ψV⁻IgL⁻ cell line via homologous recombination (grey bars). A) displays the GFP expression of ψV-IgL^{GFP2} cells, in which the GFP2 reporter is inserted in the opposite direction upstream the Igλ locus in the ψV⁻AID^{RI} cell line. B) shows the reduction of GFP negative cells, when the GFP2 reporter is inserted into the ψV⁻IgL⁻ cell line. In C) a reconstituted hypermutation activity is depicted, when the GFP2 coupled to Igλ is inserted to the ψV⁻IgL⁻ cell line. (L= leader sequence, V= variable region, J= joining region, C= constant region)

3.1.2 1 kb fine-mapping of the Igλ locus

To define single *cis*-elements essential for SHM, a detailed deletion analysis of the Igλ locus was performed. In the first approach a fragment ('W'), containing the complete Igλ locus, was created and reinserted by homologous recombination in incremental 1 kb steps from the 5' and the 3' end into ψV⁻IgL⁻ cell line. The fragments were transfected via electroporation as pIgL$^{ROI,\ GFP2}$ plasmids. Two transfected primary cell clones of each construct, positively tested for targeted integration by PCR, were subcloned by limited dilution. 24 subclones of each of the primary clones were analyzed by FACS for GFP expression.

A reinsertion of the sequences located on the fragments ‘A’ and ’B’ demonstrated a very low AID recruiting activity. With increased length of the reinserted fragment the percentage of GFP low cells increased, indicating the presence of cis regulatory elements influencing SHM activity in the original ‘W’ frament. The percentage of GFP low cells, transfected with plasmids containing either the fragment ‘F’ or ‘G’ was similar to that seen with the complete ‘W’ fragment, indicating that ‘F’ and ‘G’ both contain important elements for AID recruitment. These data also reveal a less important role of the remaining 2.8 kb of the ‘W’ fragment (referred as ‘P’). The different clones showed a high variation in their GFP low population, since the percentage depends on the time point and on the position of the mutation. An early mutation or a mutation directly at the chromophore leads to higher percentage of GFP low cells.

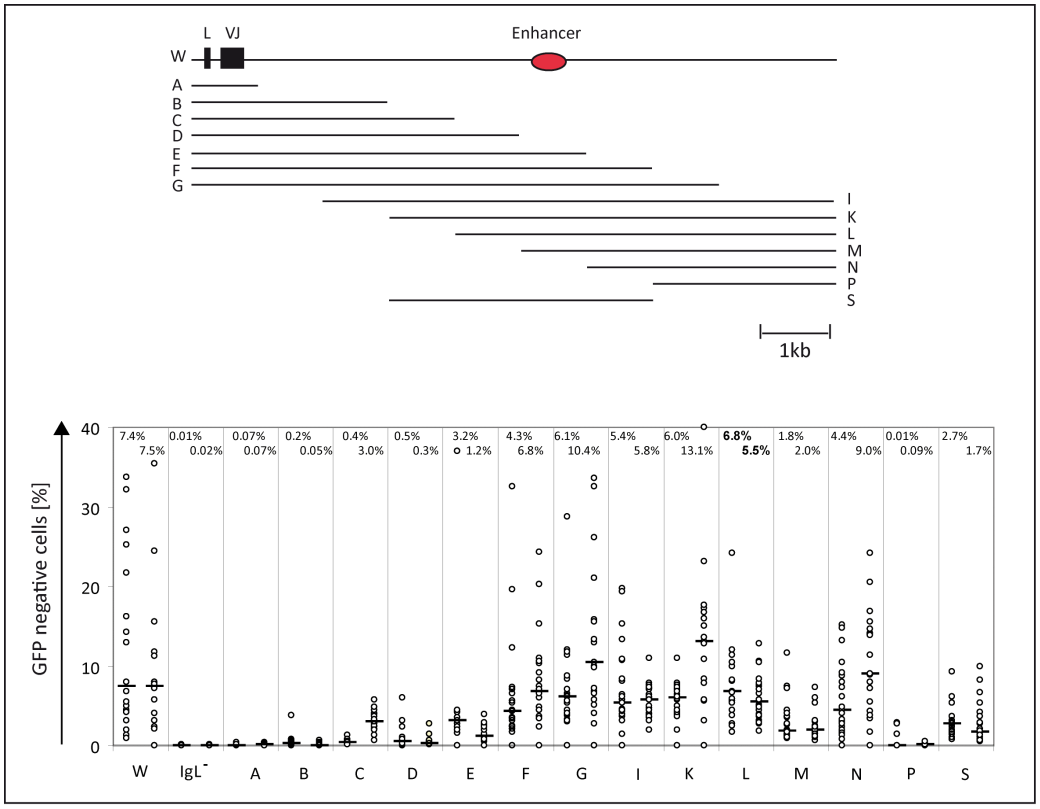

Figure 3.3 Staggered end 1 kb deletion analysis of the Igλ locus.
The Igλ locus was reinserted to the ψV ¯IgL¯ cell line, reconstituting the Igλ locus in 1 kb steps. Of each fragment two independent clones were subcloned and analyzed by FACS after 14 days. The dots represent 24 single subclones, the bars and numbers the median of the subclones.

The results achieved by the reinsertion series starting from the LVJ side were confirmed by reinsertions of fragments of 'W' starting from the 3' end. Cells that were transfected with a plasmid containing the 'P' fragment displayed hardly any GFP low cells, whereas the percentage of GFP low cells, transfected with plasmids containing the fragments 'I', 'K', 'L' and 'N' were similar to wild type percentages. Interestingly, the hypermutation rate decreased again in fragments 'D' and 'M'. This could be explained by the presence of inhibitory elements or an unfavourable conformational change, hindering AID access. Since the first 3 kb ('B') and the last 2.8 kb ('P') of 'W' displayed only a marginal hypermutation activity, the core region of 4 kb size ('S') was also tested. Surprisingly, the percentage of GFP low cells, transfected with a plasmid containing the 'S' fragment, dropped to only one third in comparison to wild type cells. This result supported our assumption of a very complex distribution of *cis*-regulatory elements all over the Igλ locus. Hence, we decided to continue with the analysis of the core region 'S', thereby reducing the number of possible redundant elements.

3.1.3 1 kb fine-mapping of the 'S' core region

The percentage of GFP low cells carrying the core region 'S' revealed one third of GFP low cells compared to wild type cells (2.2% versus 7.4%) and was considered suitable for a more detailed analysis. Plasmids, containing 1 kb incremental fragments of 'S', were transfected into the $\psi V^{-}IgL^{-}$ cell line. Additionally, the 'S' region was subdivided in single 1 kb fragments, which were individually tested for their hypermutation activity in the *GFP2* assay. The significance of the differences to the 'S' values were determined by a Mann-Whitney-U test.

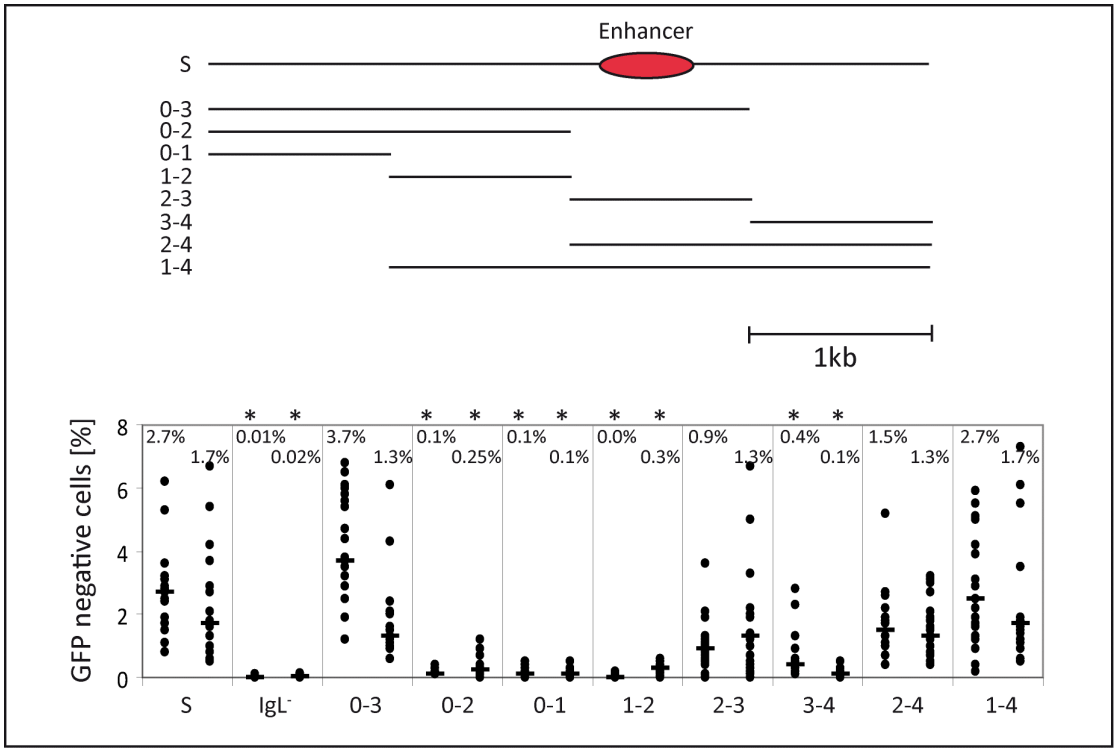

Figure 3.4 Staggered end 1 kb deletion analysis of 'S'.
The 'S' fragment was reinserted into the ψV⁻IgL⁻ cell line in 1 kb steps and additionally as 1 kb single elements. Two independent clones with 24 subclones respectively, were analyzed by FACS after 14 days. Numbers and bars indicate the median of 24 subclones. Significant differences ($p<0.0001$) between 'S' and the deletion fragments were tested by Mann-Whitney-U test and indicated by an asterisk.

A reinsertion of the first 3 kb of the 'S' fragment (referred to as '0-3') resulted in an increased percentage of GFP low cells comparable to 'S'. Cells, transfected with plasmids containing smaller fragments of 2 kb and 1 kb size ('0-2' and '0-1') demonstrated a significantly reduced percentage of GFP low cells. To confirm this result, incremental fragments of 'S' were prepared from the 3' end and inserted into pIgL'^{GFP2}. A transfection of plasmids, carrying only the last 2 kb of 'S' fragment ('2-4'), preserved SHM activity, whereas cells with only the '3-4' fragment showed a significantly reduced percentage of GFP low cells. Since both deletion series indicated an essential role of the '2-3' region, '2-3' fragment was tested alone. The percentage of GFP low cells in '2-3' transfected cells displayed no significant difference to cells transfected with 'S', whereas the percentage of GFP low cells transfected with '0-1', '1-2' and '3-4' were significantly reduced. Interestingly, '2-3' is the only fragment containing the known Ig enhancer.

3.1.4 200 bp internal deletion analysis of the 'S' core region

In parallel, the 'S' fragment was studied in more detail by a series of 200 bp internal deletion steps. For this and subsequent analyses, the number of primary biological replicates were reduced from two to one. The single clone was used to generate 24 subclones as previsously described. Most of the primary clones were unchanged in their hypermutation activity. Three fragments, SΔ1.0-1.2, SΔ2.2-2.4 and SΔ3.6-3.8, shared a significant reduction of GFP low cells. The lowest value (0.4%) was found for SΔ2.2-2.4, which eliminates the 5'-end of the enhancer. The deletion of SΔ2.2-2.4 confirmed the previous result, indicating an important role of the 200 bp fragment '2.2-2.4' in regulating SHM.

Since it was not possible to detect redundant elements using internal deletions and due to the effect that '2-3' played the main regulatory role, it was decided to focus on a detailed staggered analysis of '2-3'.

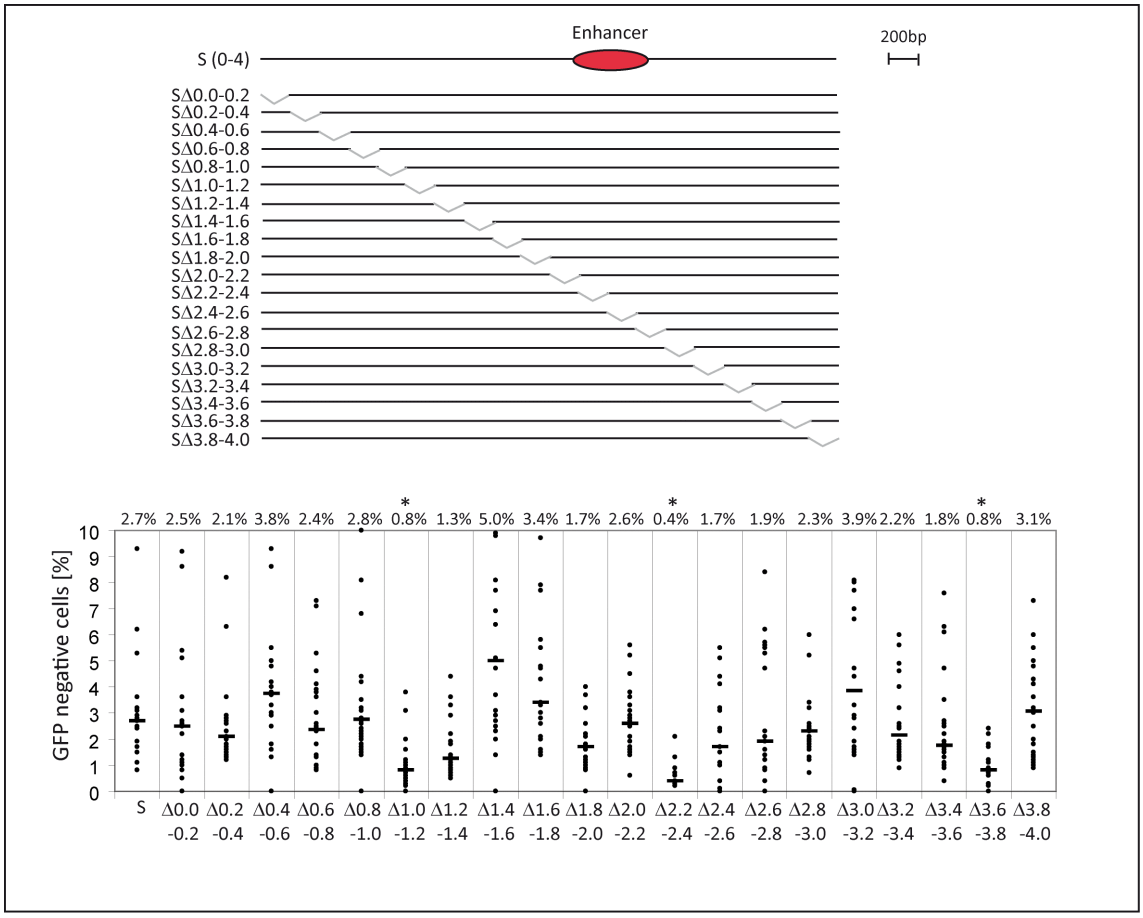

Figure 3.5 200 bp internal deletions of 'S'.

The ‘S’ fragment was inserted with 200 bp internal deletions to the ψV⁻IgL⁻ cell line. One clone of each fragment was subcloned and 24 subclones analyzed by FACS. Numbers and bars indicate the median. Significant reduction ($p<0.0001$) of GFP negative cells is designated by an asterisk.

3.1.5 50 bp fine-mapping of the ‘2-3’ region

Since the deletion analyses of ‘S’ suggested that the hypermutation activity is regulated in cis by the enhancer region we analyzed the ‘2-3’ region in a more precise study. The percent of GFP low cells carrying the fragment ‘2-3’ was 0.9%, which corresponded to about 15% of the complete Igλ locus and was still enough to detect differences in a 50 bp incremental deletion analysis.

Deletions from the 3’-end demonstrated that the fragments ‘2.00-2.05’, ‘2.00-2.10’, ‘2.00-2.15’, ‘2.00-2.20’ and ‘2.00-2.25’ all resulted in a significantly reduced percentage of GFP low cells, whereas an augmentation of the sequence between ‘2.25’ and ‘2.30’ in ‘2.00-2.30’ strongly increased the hypermutation activity. This suggested an important element located between ‘2.25’ and ‘2.30’. Surprisingly, the percentage of GFP low cells dropped again, when the sequence ‘2.70-2.80’ was added to ‘2.00-2.70’. This might indicate either inhibitory elements or a conformational change, retarding AID binding.

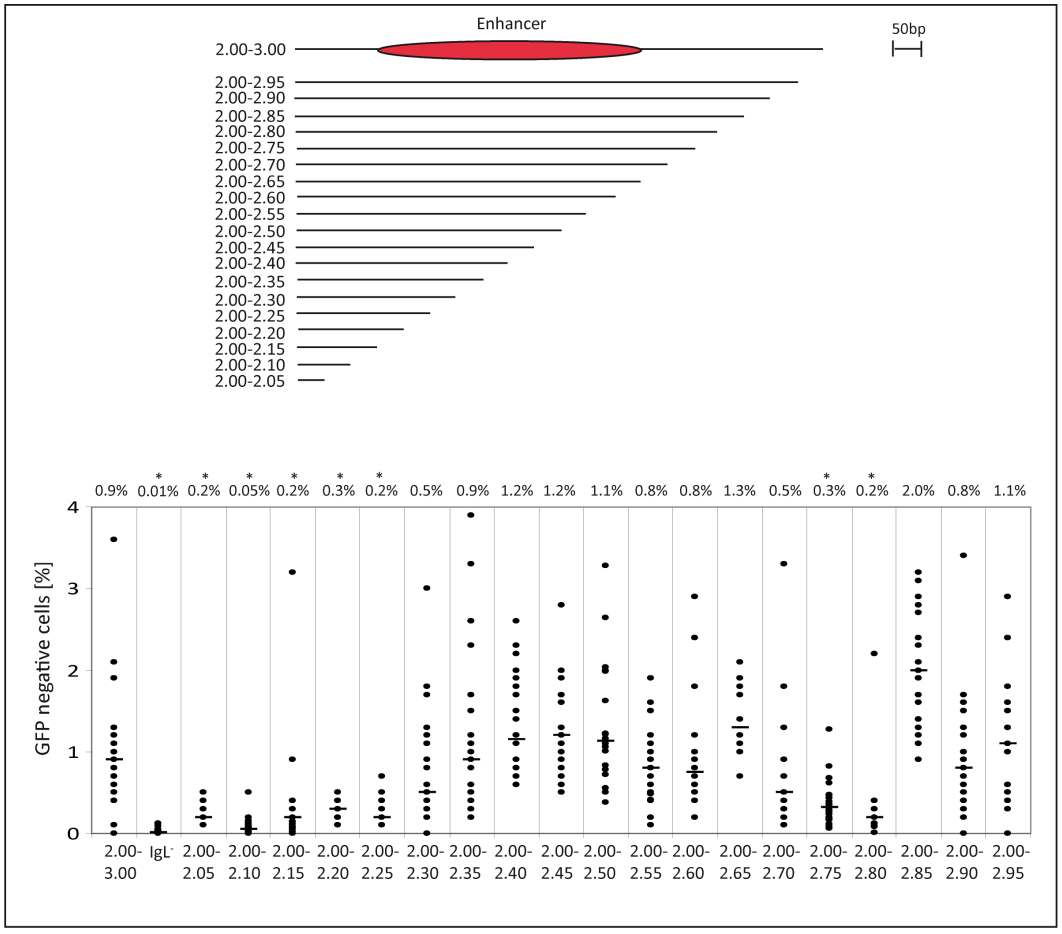

Figure 3.6 5' 50 bp staggered reinsertion analysis of '2-3'.
The fragment '2-3' of 1000 bp size was reinserted into the ψV ⁻IgL⁻ cell in 50 bp steps. One single clone of each fragment was subcloned and 24 subclones were analyzed after 14 days via FACS. Significant ($p<0.0001$) deviations of GFP negative cells are indicated by an asterisk.

In the reinsertion series using sequences from the 3'- end of the fragment '2.25-3.00', as well as all subsequently shortened fragments there of resulted in a significant reduction of GFP low cells. This established that the sequence between '2.25' and '3.00' was inactive to induce hypermutation. This result implied an important *cis*-regulatory element that lies between '2.20' and '2.25', whereas the reinsertion series from the 5'-end established the contiguous '2.25-2.30' as an essential element. Hence, a cooperative effect of '2.20-2.25' and '2.25-2.30' must be assumed. This might reflect an accumulation of different *cis*-elements or a repetition of motives in '2.20-2.30'.

These experiments were done in collaboration with Ulrike Schötz and Hiroshi Arakawa.

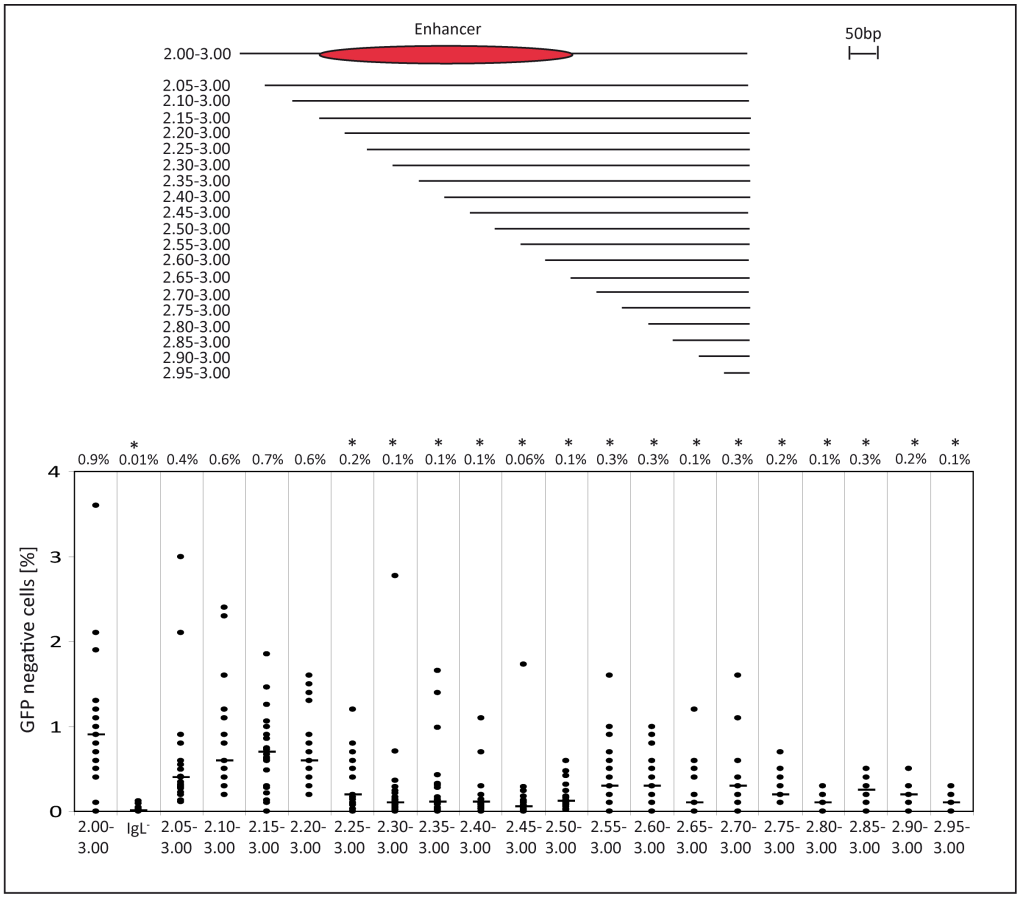

Figure 3.7 3' 50 bp staggered end reinsertion analysis of '2-3'.
The fragment '2-3' of 1000 bp size was reinserted into the ψV⁻IgL⁻ cell in 50 bp steps from 3' end. One single clone of each fragment was subcloned and 24 subclones were analyzed after 14 days via FACS. Significant ($p<0.0001$) deviations of the GFP negative population are indicated by an asterisk.

3.1.6 '2.2-2.4' reinsertion and multimerization analysis

The region '2.2-2.4' was shown to play an important role for SHM activity in the 'S' 200 bp internal deletion analysis. The removal of this sequence led to a reduced percentage of GFP low cells from 2.7% in 'S' to 0.4%. Additionally, the 50 bp stepwise reinsertion analysis of the '2-3' fragment indicated an essential hypermutation activity that is mediated by the fragment '2.20-2.30'. It is not clear whether the sequence of '2.2-2.4' is sufficient to target AID. Therefore, the plasmid pIgL$^{2.2\text{-}2.4,\ GFP2}$ containing the fragment '2.2-2.4' was transfected into the cell line ψV⁻IgL⁻. Furthermore, multiple copies of the sequence were inserted to test whether a repetition of motives influences the SHM activity.

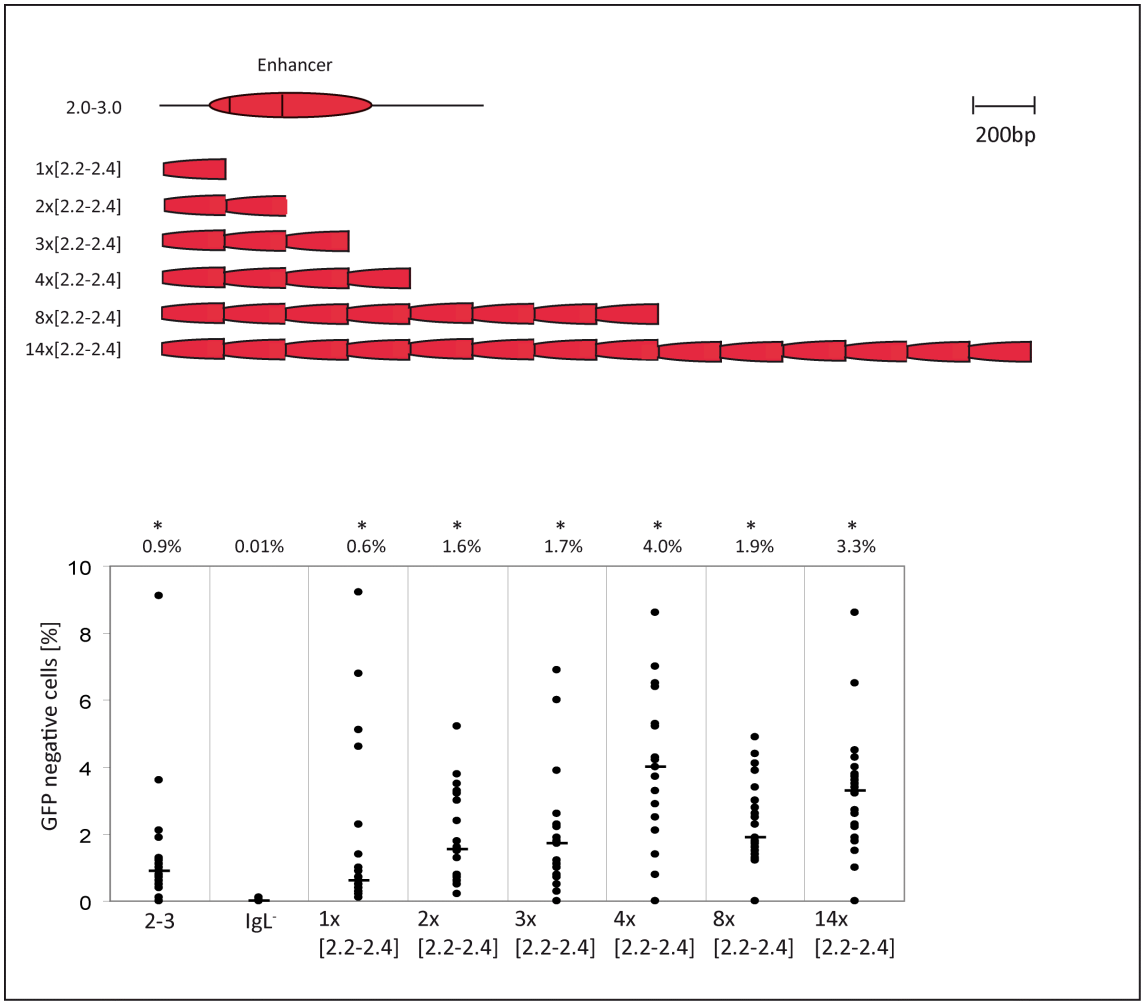

Figure 3.8 Multimerization of '2.2-2.4'.
The fragment '2.2-2.4' and its multimers were reinserted to the cell line ψV$^-$IgL$^-$. One single clone was subcloned and 24 subclones (circles) analyzed after 14 days by FACS. Numbers and bars indicate the median of 24 subclones. Significant differences ($p<0.05$) to the deleted locus (IgL$^-$) were indicated by an asterisk.

Cells transfected with '2.2-2.4' showed some modest SHM activity of 0.6%. The SHM activity could be further increased via multimerization. The addition of few copies of '2.2-2.4' produced a hypermutation rate of 4% (Fig. 3.8) which corresponded to 50% of the rate seen with the complete Igλ locus. However, with higher multimerization a plateau was reached which could not be further increased. This indicated that either a motive repetition or specific distance to the promoter enhances the AID binding ability.

3.1.7 Detection of cis-elements with the bioinformatical tool MEME and MAST

In the reinsertion analyses the fragment '2.2-2.4' was identified as an essential sequence for SHM activity. The working hypothesis suggests that AID binds via multiple trans-activating factors. Therefore, the bioinformatical tools MEME (Multiple Em for Motif Elicitation) and MAST (Motif alignment and search tool) were used to detect via specific algorithms potential *cis*- and *trans*- elements in '2.2-2.4'. For this evaluation the category 'vertebrates' was selected in the MAST matrix database.

At the 5' end of '2.2-2.4' the tool identified an accumulation of putative transcription factor binding sites. Binding sites for Pax5, which is essential for B cell differentiation, were located at the very 5' and 3' end of '2.2-2.4'. The E-Box 'CAGCTG' was found at the 5' end. This is a binding motif for E2A transcription factors. Additionally, an NF-κB binding motif could be identified between '2.2-2.25'. This may be specific for p50/c-Rel heterodimers. A MEF-2 binding site was localized downstream of the NF-kB motif. At the 3' end MEME/MAST additionally detected an SP1 binding site. SP1 has been shown to interact with NF-κB and MEF, enhancing the trans-activating effect.

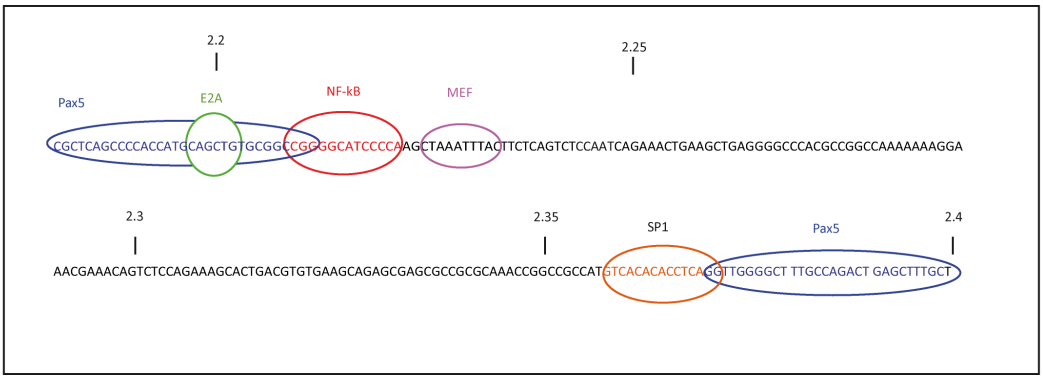

Figure 3.9 Transcription factor binding sites detected via MEME/MAST.
The sequence '2.2-2.4' is depicted together with putative transcription factor binding sites. Pax5 depicted in blue, E2A depicted in green, NF-κB depicted in red, MEF2 depicted in purple and SP1 depicted in orange ellipses.

3.2 The contribution of the canonical NF-κB pathway to LMP1/CD40 induced B cell development and tumorigenesis

The second part of this study describes sutdies into the contribution of the canonical NF-κB pathway in the expansion and lymphomagenesis of B cells expressing constitutivly active CD40. As mentioned in section 1.8, Cornelia Hömig-Hölzel established a conditional, heterozygous LMP1/CD40 mouse model based on the Cre/loxP system, conditionally

expressing LMP1/CD40. B cell specific activation of the transgene was achieved by crossing the LMP1/CD40 mouse to a CD19 Cre mouse line referred to in the following as 'LMP1/CD40'. Since it was not known whether the canonical NF-κB pathway plays any role in LMP1/CD40 mediated B cell expansion and activation, we decided to delete either NEMO or IKK2, as subcomponents of the canonical NF-κB pathway, B cell specifically in LMP1/CD40 mice. Therefore, $NEMO^{fl/fl}$ or $IKK2^{fl/fl}$ mice were crossed to 'LMP1/CD40' mice, referred to in the following as 'NEMOko LMP1/CD40' or 'IKK2ko LMP1/CD40' mice. For subsequent analyses, $CD19^{Cre/+}$ mice were used as wild type controls, referred to as 'wild type' mice. $NEMO^{fl/fl}$ $CD19^{Cre/+}$ and $IKK2^{fl/fl}$ $CD19^{Cre/+}$ mice, referred to as 'NEMOko' and 'IKK2ko' mice, were taken as NEMO or IKK2 ablation controls. Both, NEMOko and IKK2ko, mice were reported to have a deficiency in mature B cell development and demonstrate a block in B cell maturation from the T1 to the T2 stage (Pasparakis et al., 2002).

3.2.1 B cell numbers in the peripheral lymphoid organs

To address whether a loss of NEMO or IKK2 influences the B cell compartments, 8 to 12 - week old mice were sacrificed and the secondary lymphoid organs were analyzed. The B cell specific expression of LMP1/CD40 led to the expected splenomegaly, demonstrated in Fig. 3.10 by an enhanced splenic size, weight and absolute cell number. A depletion of IKK2 in LMP1/CD40 mice, which retain a residual canonical NF-κB pathway activity due to IKK1, showed reduced splenic weight and absolute cell number. The loss of IKK2 resulted in an intermediate phenotype between those of LMP1/CD40 and wild type animals. The deletion of NEMO in LMP1/CD40 expressing B cells, which should block the classical NF-κB pathway completely, had an even stronger effect on LMP1/CD40 induced B cell numbers. The size, weight and the cell number of the spleen were reduced to levels comparable to those of wild type spleens.

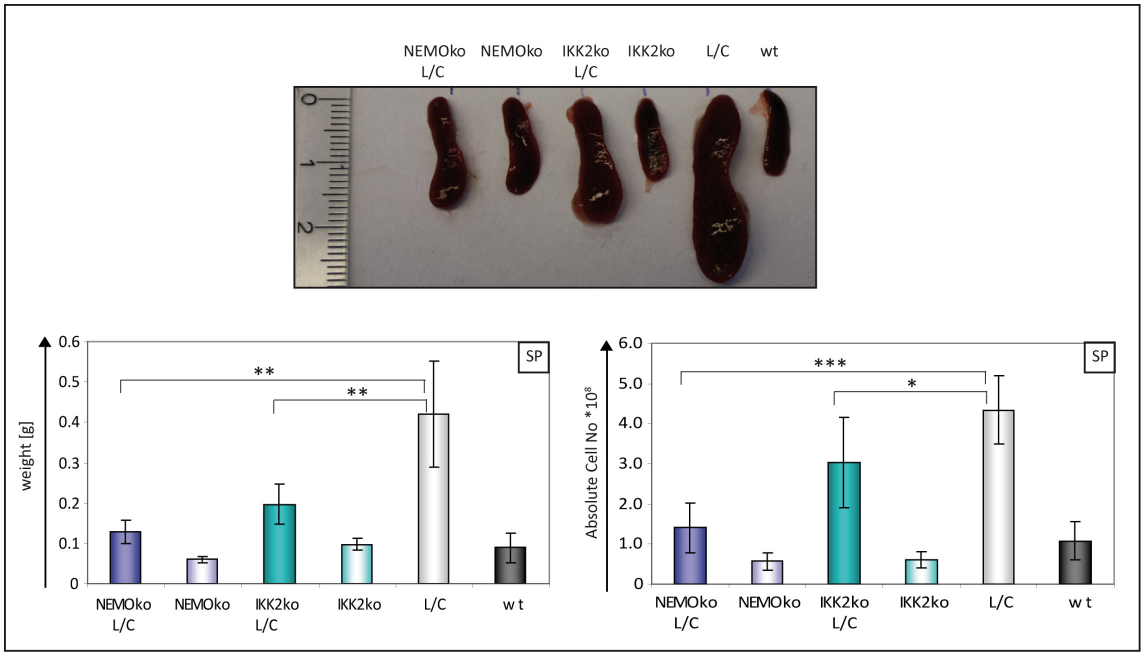

Figure 3.10 The canonical NF-κB pathway is important for LMP1/CD40 induced splenomegaly.
Splenic sizes were measured with a ruler indicating centimetre. Splenic weights of NEMOko LMP/CD40 (dark blue), NEMOko (light blue), IKK2ko LMP1/CD40 (dark green), IKK2ko (light green), LMP1/CD40 (grey) and wild type (black) mice were measured and depicted in a graph. The cell numbers of the spleens were counted and also depicted. The median, indicated by a bar, was calculated from at least three independent experiments and given with a standard deviation as shown. *P<0.05, **P<0.01, ***P<0.001, calculated by two-tailed student's T-test.

To detect, how the canonical NF-κB pathway affects the B cell expansion in the peripheral lymphoid organs, cells were prepared as single cell suspension, counted and the B cell ($B220^+$, $TOPRO\text{-}3^-$) population was detected by FACS analysis.

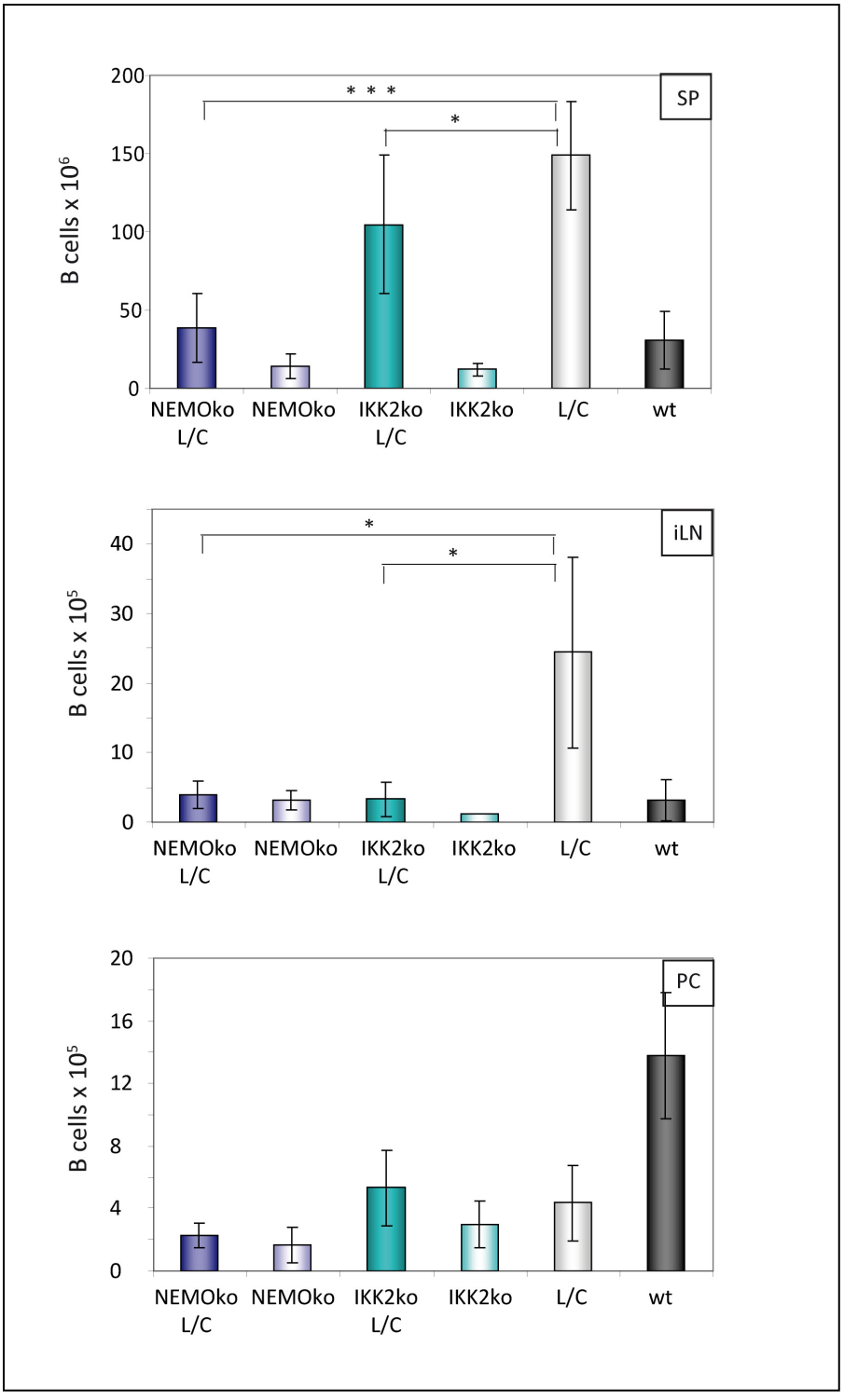

Figure 3.11 B cell numbers of spleen (SP), lymph nodes (LN)) and peritoneal cavity (PC).
B cells were isolated from spleen, lymphnodes and peritoneal cavity of NEMOko LMP1/CD40 (dark blue), NEMOko (light blue), IKK2ko LMP1/CD40 (dark green), IKK2ko (light green), LMP1/CD40 (grey) and wild type (black) mice. The absolute B cell number was calculated by cell counting and B220/TOPRO-3 staining. The median, indicated by a bar, was calculated from at least three independent experiments and given with a standard deviation as shown. *P<0.05 and ***P<0.001, calculated by two-tailed student's T-test.

The splenic B cell numbers of NEMOko LMP1/CD40 and IKK2ko LMP1/CD40 mice exhibited a significant reduction compared to splenic B cells in the LMP1/CD40 mice. The IKK2ko LMP1/CD40 B cell population demonstrated an intermediate phenotype between those of LMP1/CD40 and wild type mice. The depletion of NEMO affected the *in vivo* expansion of LMP1/CD40 expressing B cells to a greater extent and diminished the cell number to those seen in wild type animals. In the inguinal lymph nodes the B cell numbers of NEMOko LMP1/CD40 and IKK2ko LMP1/CD40 mice were both similar to those of wild type mice, namely ten times lower than those in the LMP1/CD40 mice. This indicates that the B cell expansion in LMP1/CD40 mice is dependent upon the functionality of the canonical NF-kB pathway. In the peritoneal cavity LMP1/CD40 expression resulted in an abolished B1 cell expansion and therefore to a reduction of absolute B cell numbers. This result was also seen in NEMOko LMP1/CD40 and IKK2ko LMP1/CD40 mice. In comparison to wild type mice the IKK2ko LMP1/CD40 B cells were reduced to the same extent than LMP1/CD40 B cells. The deletion of NEMO in LMP1/CD40 expressing mice diminished the B cell number additionally, but not significantly to $2.3*10^5$.

3.2.2 Development of early and immature B cells

CD19 is already expressed in the late pro B cell stage, hence leading to a LMP1/CD40 expression and NEMO or IKK2 depletion in the bone marrow (BM). To exclude, that the reduced B cell numbers in the periphery are due to a block in early B cell development, the B cell populations in the bone marrow were examined. Cells from the bone marrow were prepared as single cell suspensions, counted and stained with TOPRO-3 and B220 to detect only living B cells.

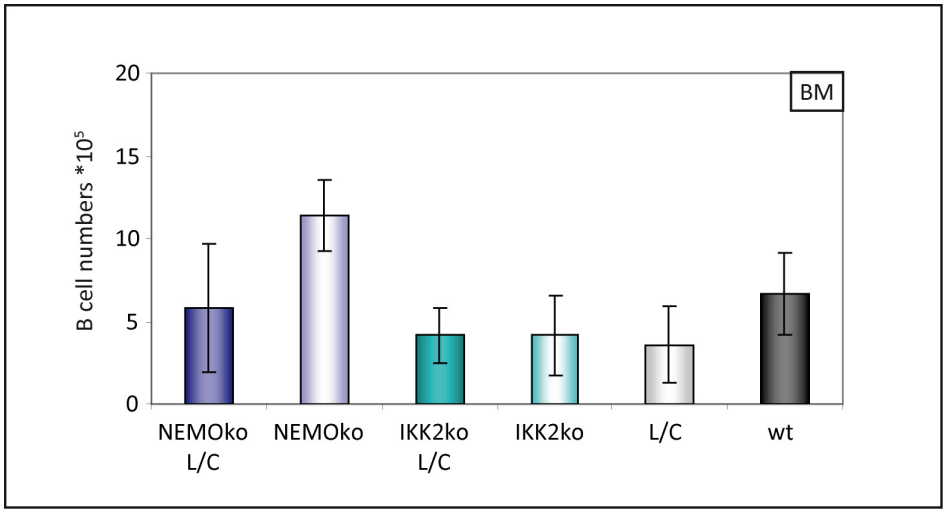

Figure 3.12 Absolute B cell numbers in the bone marrow (BM).
B cells were isolated from the bone marrow of NEMOko LMP1/CD40 (dark blur), NEMOko (light blue), IKK2ko LMP1/CD40 (dark green), IKK2ko (light green), LMP1/CD40 (grey) and wild type (black) mice. The absolute B cell number was calculated by cell counting and B220/TOPRO-3 staining. The median, indicated by a bar, was calculated from at least three independent experiments and given with a standard deviation as shown.

The NEMOko LMP1/CD40, IKK2ko LMP1/CD40 and IKK2ko mice displayed only a small variation in their absolute B cell number ($B220^{high}$) of the bone marrow. The NEMOko B cell population was increased compared to wild type mice. This might reflect a survival disadvantage of NEMOko cells, leading to an enhanced replacement of B cells in the bone marrow. This effect did not appear in the NEMOko LMP1/CD40 mice. The single BM subpopulations were studied to determine if they were influenced by the ablation of NEMO or IKK2.

BM	B cell	Pro	Pre	Im	Rec
[%] of lymphocytes					
NEMOko LMP1/CD40	36±14	9.2±3.3	32±9.6	11±3.4	17±8.3
NEMOko	39±3.3	5.7±2.0	41±5.5	14±4.5	11±2.6
IKK2ko LMP1/CD40	54±24	2.8±0.7	29±3.9	9.9±2.9	23±13
IKK2ko	72±4.8	1.9±1.3	46±14	13±2.9	21±7.4
LMP1/CD40	38±19	5.9±2.9	32±6.0	11±2.6	12±4.9
Wt	50±22	6.1±3.2	41±9.0	17±6.0	17±6.0
[$x10^5$]					
NEMOko LMP1/CD40	5.8±3.8	0.7±0.2	3.6±2.4	1.4±0.8	1.5±0.5
NEMOko	11±2.1	0.9±0.3	9.7±2.5	3.6±2.0	2.2±0.3

IKK2ko LMP1/CD40	4.2±1.7	0.8±0.7	3.6±0.8	1.1±0.4	2.5±1.3
IKK2ko	4.2±2.4	0.9±0.1	5.0±1.6	1.4±0.3	2.3±0.8
LMP1/CD40	3.6±2.3	0.5±0.3	2.7±2.0	1.2±0.9	0.7±0.1
Wt	6.7±2.5	1.6±1.3	6.0±1.8	2.3±0.7	3.0±1.2

Table 3.1 Bone marrow (BM) B cell subpopluations.

B cells were stained with B220, CD43 and IgM to separate Pro- ($B220^{low}$, $CD43^{+}$), Pre- ($B220^{low}$, $CD43^{-}$), Recirculating (Rec; $B220^{high}$, $CD43^{-}$) and Immature (IM; IgM^{high}, $B220^{low}$) B cells. B cell numbers were calculated from at least three independent experiments.

The percentages of the Pro- ($B220^{low}$, $CD43^{+}$), Pre- ($B220^{low}$, $CD43^{-}$), Recirculating- ($B220^{high}$, $CD43^{-}$) and Immature- (IgM^{high}, $B220^{low}$) B cells of NEMOko LMP1/CD40 and IKK2 LMP1/CD40 mice did not reveal a significant difference to wild type and LMP1/CD40 mice. Hence, a depletion of the canonical NF-κB components did not influence early B cell development significantly.

IgM^{+} immature B cells emigrate from the BM and enter the spleen as so called transitional B cells. Transitional B cells are characterized by the expression of the AA4.1 surface marker. The transitional subpopulation T1 is IgM^{high} $CD23^{-}$ and develops during the differentiation to the T2 stage, characterized by IgM^{high} $CD23^{+}$ levels. It was known that in NEMOko and IKK2ko B cells are abolished during the differentiation stage from T1 to T2 cells (Pasparakis et al., 2002). To detect whether the inhibited B cell expansion in the spleens of NEMOko LMP1/CD40 and IKK2ko LMP1/CD40 mice also occurred due to a similar block in B cell differentiation, the transitional B cells and the subpopulations T1 and T2 in the spleen (SP) were analyzed by FACS analysis.

SP						
	Transitional B cells		T1		T2	
	[$x10^6$]	[%]	[$x10^5$]	%	[$x10^5$]	%
NEMOko LMP1/CD40	3.7±1.7	5.0±0.8	6.8±3.8	19±5.8	17±11	39±3.7
NEMOko	1.8±0.9	8.9±2.7	8.1±6.1	40±13	4.2±1.8	24±3.8
IKK2ko LMP1/CD40	5.2±3.4	3.3±1.1	3.5±1.7	27±18	65±46	42±2.0
IKK2ko	2.4±0.7	9.3±3.4	12±9.1	42±13	7.5±4.2	29±1.6
LMP1/CD40	4.5±1.8	2.0±0.5	6.7±4.5	15±7.6	33±29	39±8.4

Wt	5.3±2.5	11±3.8	15±9.1	29±8.7	15±9.4	34±4.8

Table 3.2 Transitional B cell numbers.

Splenic B cells were isolated and stained with B220, AA4.1, IgM and CD23 to separate complete transitional B cells ($B220^+$, $AA4.1^+$), T1 ($B220^+$, $AA4.1^+$, IgM^+, $CD23^-$) and T2 ($B220^+$, $AA4.1^+$, IgM^+, $CD23^+$) B cells. The mean values of at least three independent experiments are displayed in the table.

The absolute number of transitional B cells of NEMOko LMP1/CD40 and IKK2ko LMP1/CD40 was comparable to wild type and LMP1/CD40 B cells. Moreover, the accumulation of T1 cells seen in NEMOko (40.3%) and IKK2ko (42.3%) mice was reversed in NEMOko LMP1/CD40 and IKK2ko LMP1/CD40 mice, leading to a restoration of normal development of T2 cells in both knock-outs lines expressing LMP1/CD40. This indicated that the failure of splenic B cell expansion that is seen in NEMOko LMP1/CD40 and IKK2ko LMP1/CD40 mice (Fig. 3.11) did not arise from a defect during the early splenic differentiation in the transitional state as it was in NEMOko or IKK2ko mice.

3.2.3 The development of B cell subsets in the spleen

In the spleen, two main populations of B cells can be distinguished by their CD21 and CD23 surface marker expression. The marginal zone B cells (MZ B cells) are characterized by a $CD21^{high}$ $CD23^{low}$ phenotype and the follicular B cells (Fo B cells) can be detected as $CD21^{low}$ $CD23^{high}$ population. In wild type spleens the MZ B cells compartment made up 7% of the total splenic B cells and the Fo B cell compartment 62% of B cells, corresponding to an absolute cell number of $2.1x10^6$ and $1.9x10^7$, respectively (Fig. 3.13). In LMP1/CD40 mice the splenic B cell compartments and especially the MZ B cell compartment were highly expanded (MZ B cells: 31%≙$6.2x10^7$ and Fo B cells: 42%≙$6.4x10^7$).

In IKK2ko LMP1/CD40 mice, the follicular B cell number was similar to LMP1/CD40 (68%≙$5.5x10^7$), whereas the MZ B cell compartment (14%≙$1.7x10^7$) was significantly reduced to an intermediate phenotype between LMP1/CD40 and wild type mice.

In NEMO LMP1/CD40 mice the absolute cell numbers of MZ B cells and Fo B cells were both significantly reduced and were comparable to wild type cell numbers (MZ B cells: 10%≙$3.2x10^6$ and Fo B cells: 62%≙$2.2x10^7$). This demonstrates an essential role of the canonical NF-κB pathway mediated by NEMO/IKK2 for LMP1/CD40 induced MZ B cell and Fo B cell expansion.

The B cell numbers of NEMOko (MZ B cells: 8%≙9.2x10^5, Fo B cells: 57%≙6.4x10^6) and IKK2ko (MZ B cells: 8%≙1.2x10^6, Fo B cells: 55%≙8.2x10^6) revealed reduced differentiation as already published (Pasparakis et al., 2002).

These results were also reflected by histological staining (Fig. 3.13C). Cryosections of embedded spleens were stained with antibodies against MoMA (metallophilic macrophages) in blue and IgM (B cells) in red. The metallophilic macrophages are located in the sinus of the individual follicles, separating the FoB cells inside the sinus, and the MZ B cells (highlighted by a black arrowhead) in the mantle zone outside the sinus. Due to the expansion of Fo B and MZ B cells in LMP1/CD40 mice, the individual follicle size of the LMP1/CD40 spleen was increased. This enhanced follicular size was also found in IKK2ko LMP1/CD40 spleens, reflecting the high absolute follicular B cell numbers, since the MZ B cell compartment was diminished. The follicle size and also the extension of the the marginal zone and follicular compartments in the NEMOko LMP1/CD40 spleen were comparable to wild type follicles.

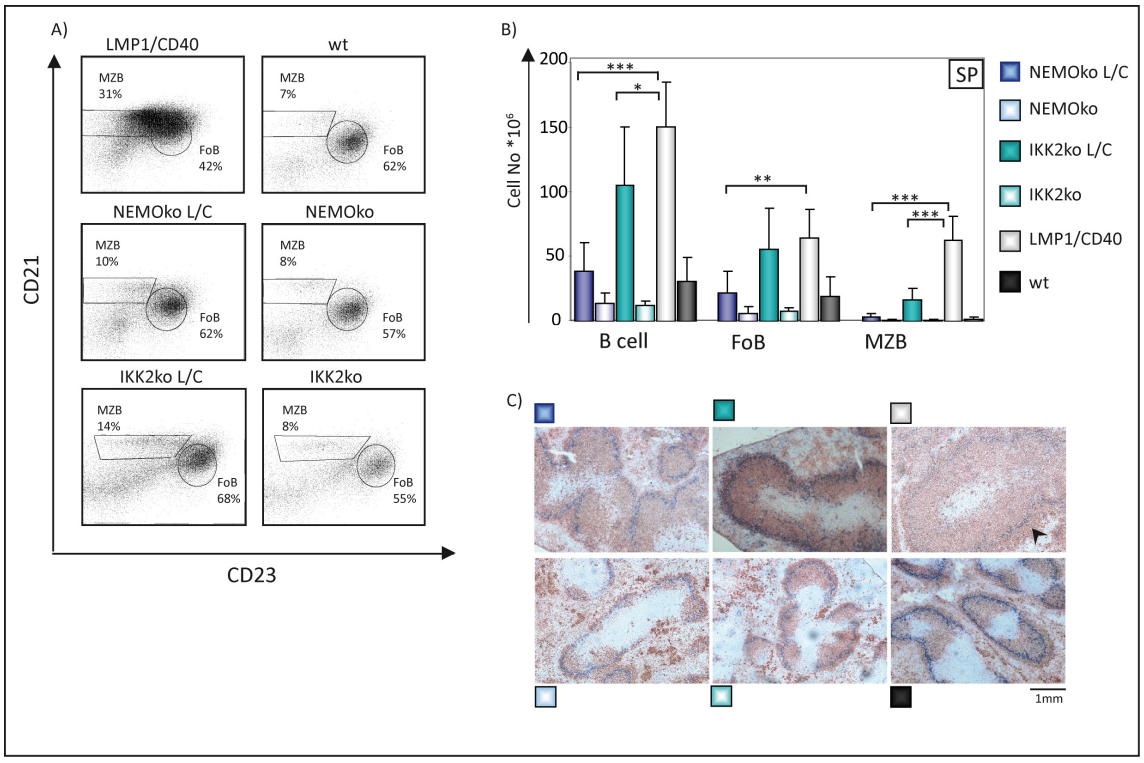

Figure 3.13 The canonical NF-κB pathway is essential for CD40-driven B cell expansion of MZB and FoB.
A) B cells of NEMOko LMP1/CD40, NEMOko, IKK2ko LMP1/CD40, IKK2ko, LMP1/CD40 and wild type were isolated and stained for FACS to distinguish MZB (CD21^{high}, CD23$^-$) from FoB (CD21^{low}, CD23^{high}). B) Isolated B cells of NEMOko LMP1/CD40 (dark blue), NEMOko (light blue), IKK2ko LMP1/CD40 (dark green), IKK2ko (light green), LMP1/CD40 (grey) and wild type (black) were counted and calculated via B220 staining. The mean of the absolute B cell number is depicted in a bar together with the standard deviation. Significance of at least 3 independent experiments was determined by a students T-test (*P<0.05, **P<0.01, ***P<0.001). C) 6 µm

cryosections were stained with antibodies against MoMA (blue) for metallophilic macrophages and IgM (red) for B cells.

3.2.4 The activation status of B cells depends on the canonical NF-κB pathway

LMP1/CD40 splenic B cells have a pre-activated phenotype, indicated by enhanced levels of CD95 and ICAM. CD95 (Fas-receptor) is usually a pro-apoptotic factor (Ejik et al., 2001), but has previously been shown to have a pro-tumouregenic effect (Ribeiro et at., 2002). ICAM (CD54) is an intercellular adhesion molecule, stabilizing cell-cell interaction and facilitating an endothelial transmigration during the immune response (Janeway et al., 2002). Non-stimulated wild type B cells expressed only low levels of CD95 and ICAM, whereas the constitutive CD40 signal in LMP1/CD40 B cells induced a high expression of CD95 and ICAM (Fig. 3.14). IKK2ko LMP1/CD40 B cells also demonstrated elevated levels of CD95 and ICAM on their surface. A NEMO depletion in LMP1/CD40 B cells caused two populations of CD95 and ICAM. The CD95 or ICAM low population was comparable to the wild type population. The CD95 or ICAM higher populations were comparable to those seen in the activated LMP1/CD40 B cells.

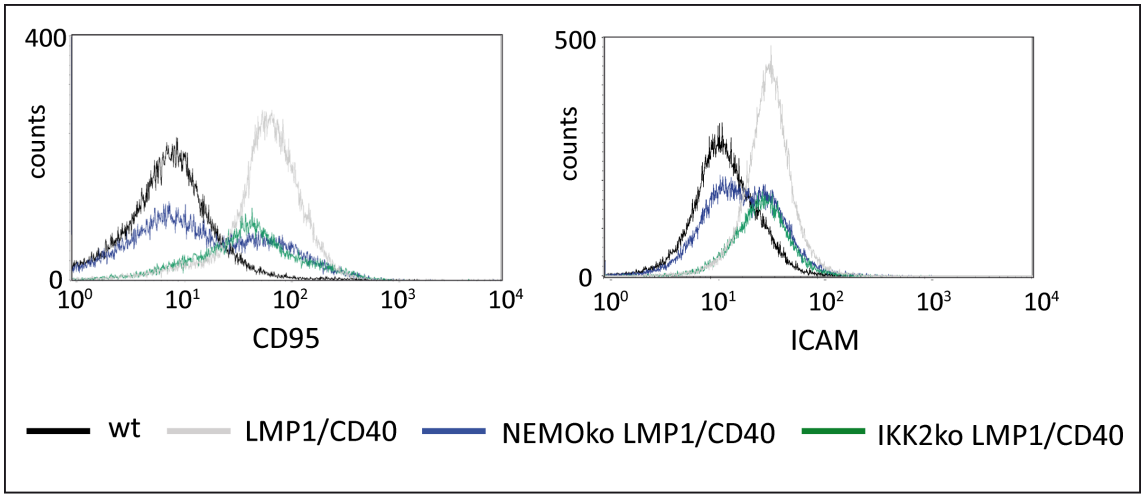

Figure 3.14 The canonical NF-κB pathway influences CD95 and ICAM expression.
B cells of NEMOko LMP1/CD40 (dark blue), IKK2ko LMP1/CD40 (dark green), LMP1/CD40 (grey) and wild type (black) mice were stained for CD95 and ICAM surface marker and were analyzed by FACS. A shift on the x-axis correlates with the expression level, the counts on the y-axis correlate with the cell number. The experiment was performed from at least three sets of mice.

To detect, whether the two different CD95 levels in NEMOko LMP1/CD40 mice correlate with the different B cell populations in the spleen, I pregated the CD95 and ICAM expression

on Fo B cells (CD21^{low} CD23^{high}), MZB (CD21^{high}, CD23^{-}) and MZ B precursor cells (CD21^{high}, CD23^{high}) (Fig. 3.15 and 3.16).

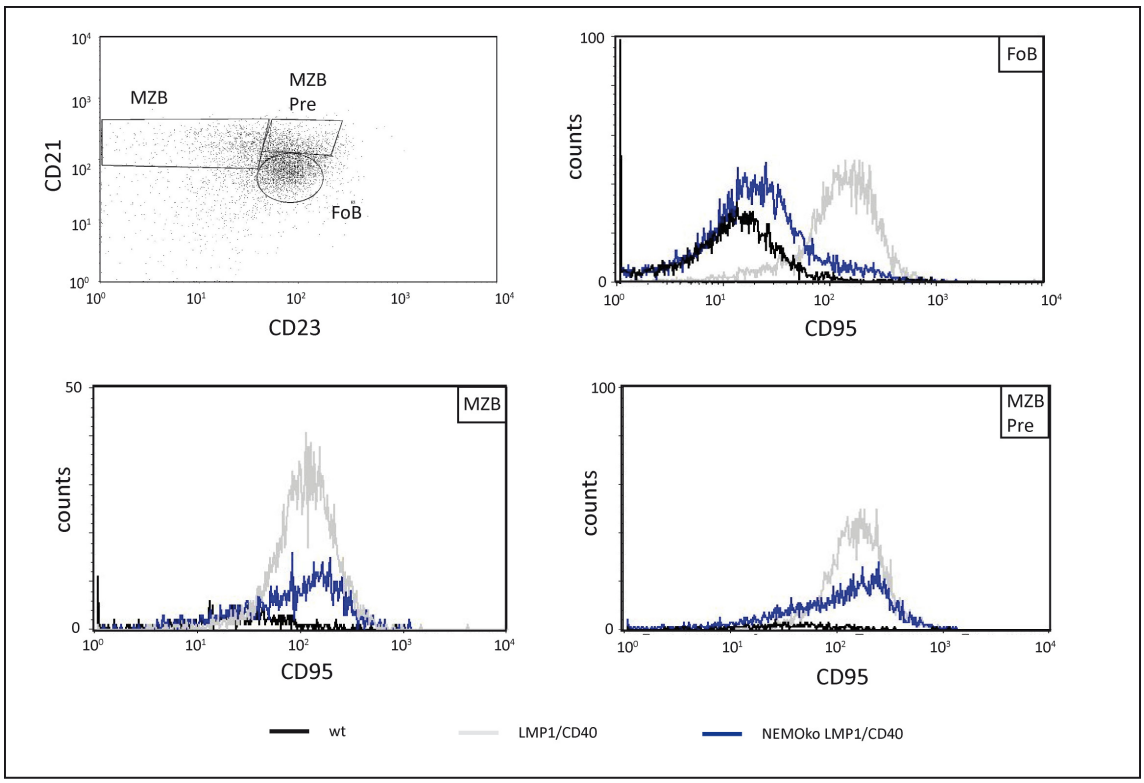

Figure 3.15 The canonical NF-κB pathway is important for the LMP1/CD40 mediated CD95 up-regulation of Fo B cells, but not of MZ B cells and MZ B precursor cells.
Splenic B cells of NEMOko LMP1/CD40 (dark blue), LMP1/CD40 (grey) and wild type (black) mice were isolated and stained with B220, CD21, CD23 and CD95 to separate the populations MZ B, Fo B, MZ precursor B cells and detect their activation status via FACS analysis.

In comparison to wild type B cells, the LMP1/CD40 derived B cells revealed high CD95 and ICAM expression in all subpopulations (Fo B cells, MZ B cells and MZ B cell precursor). In NEMOko LMP1/CD40 mice, the CD95 and ICAM expression on FoB cells was comparable to wild type B cells, whereas the CD95 and ICAM expression on MZ B cells and MZ B cell precursors was comparable to that seen in LMP1/CD40 mice.

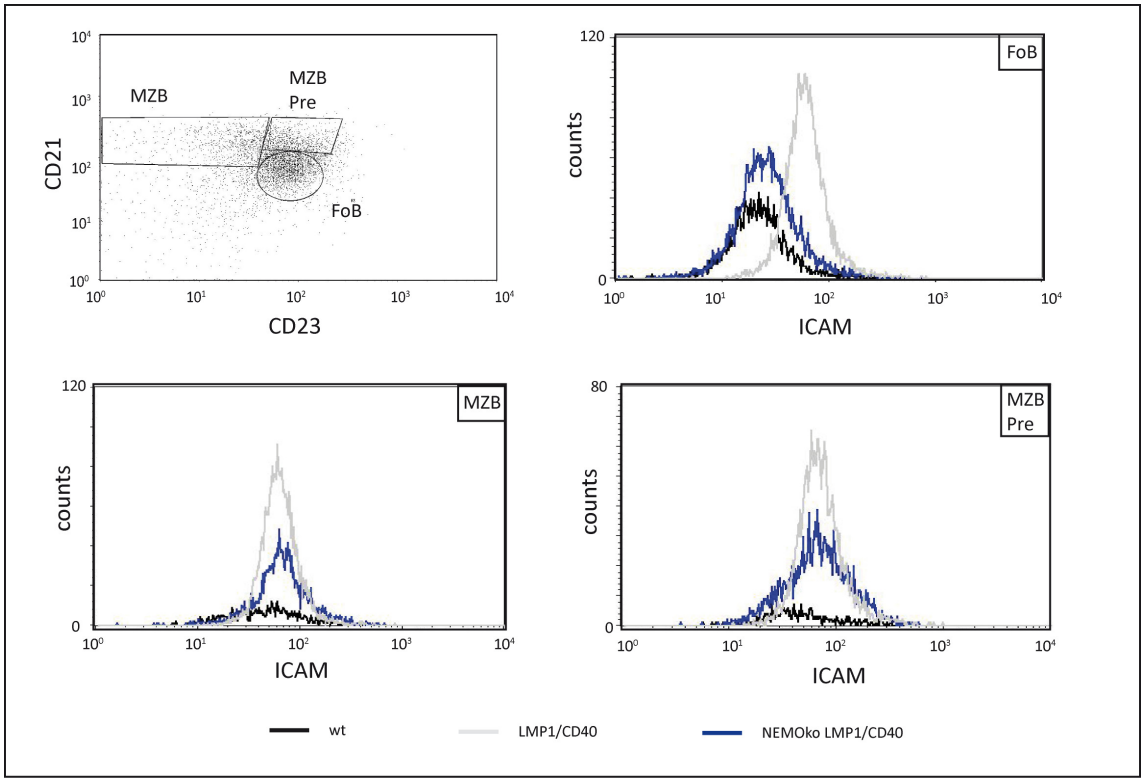

Figure 3.16 The canonical NF-κB pathway is important for the LMP1/CD40 mediated ICAM activation of Fo B cells, but not of MZ B cells and MZ precursor B cells.
Splenic B cells of NEMOko LMP1/CD40 (dark blue), LMP1/CD40 (grey) and wild type (black) mice were isolated and stained with B220, CD21, CD23 and CD95 to separate the populations MZ B cells, Fo B cells, MZ precursor B cells and detect their activation status via FACS analysis.

3.2.5 The canonical NF-κB pathway is important for LMP1/CD40 mediated survival and essential for proliferation *in vitro*

LMP1/CD40 expressing B cells show improved survival and proliferate spontaneously after *ex vivo* isolation (Hömig-Hölzel et al., 2008). To analyze, whether the classical NF-κB pathway is involved in LMP1/CD40 potentiation of B cell survival and proliferation, NEMOko LMP1/CD40 and IKK2ko LMP1/CD40 splenic B cells were isolated and cultured for 5 days. In the following experiments the NEMOko and IKK2ko controls were omitted. Living cells were detected by FACS analysis after TOPRO-3 staining. The percentage of TOPRO-3 negative cells, which corresponds to the living cells, decreased faster for NEMOko LMP1/CD40 and IKK2ko LMP1/CD40 mice than for LMP1/CD40 mice, indicating that these proteins are required for LMP1/CD40 mediated survival. However, NEMOko LMP1/CD40 and IKK2ko LMP1/CD40 B cells still demonstrated a better survival rate than that seen for wild type B cells. Hence the

canonical NF-κB pathway contributes to some extend to the enhanced B cell survival caused by LMP1/CD40.

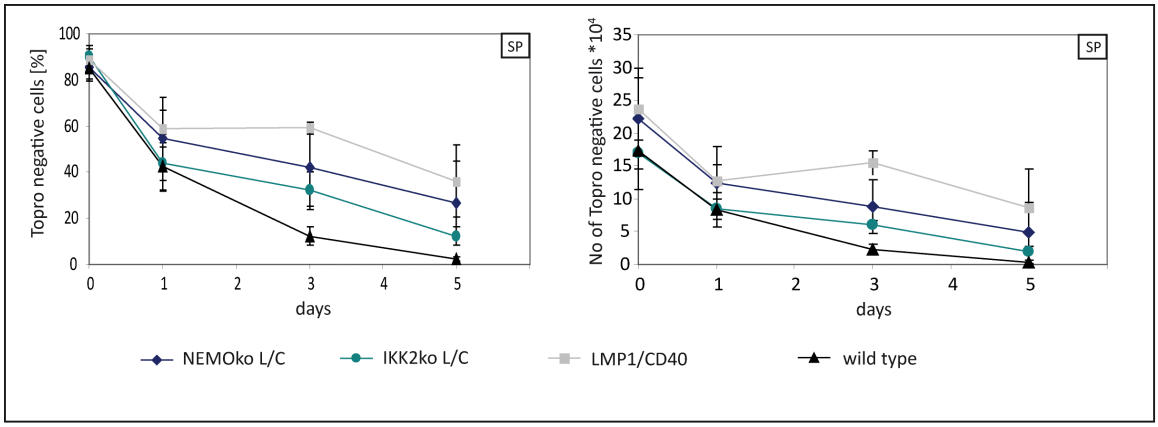

Figure 3.17 The canonical NF-κB is necessary for LMP1 induced prolonged survival.
B cells of NEMOko LMP1/CD40 (blue rhomb), IKK2ko LMP1/CD40 (green circle), LMP1/CD40 (grey square) and wild type (black triangle) mice were isolated and taken in culture for five days. Cells were stained with TOPRO-3 to detect dead cells and were analyzed by FACS on day 0, 1, 3 and 5. The graphs display the mean values with associated standard deviations of three independent experiments.

To detect whether the canonical NF-κB pathway is involved in LMP1/CD40 induced proliferation, NEMOko LMP1/CD40, IKK2ko LMP1/CD40, LMP1/CD40 and wild type splenic B cells were studied *ex vivo* and proliferation activity determined by staining with Carboxyfluorescein succinimidyl ester (CFSE), a fluorescent dye that can be used to follow proliferation. In this assay the labelling of the cell membrane progressively declines due to an equal transmission to daughter cells with each cell division. This allows tracking of the proliferating cells over several days. The percentage of CFSE negative cells in cultures of LMP1/CD40-derived B cells increased and reached after five days a proliferation rate of 13.3%, whereas the wild type level stagnated at 3.1%. The restricted canonical NF-κB pathway in IKK2ko LMP1/CD40 mice reduced the excess proliferation rate of LMP1/CD40 B cells to an intermediate level of 5.5% after 3 days. In contrast to LMP1/CD40 B cells the proliferation rate did not further increase after 5 days, but arrested at 6.2%. The CFSE negative population of NEMOko LMP1/CD40 B cells was about 3.2% during the 5 days culture and therewith similar to non-proliferating wild type B cells. This indicated an essential role of the canonical NF-κB components for proliferation.

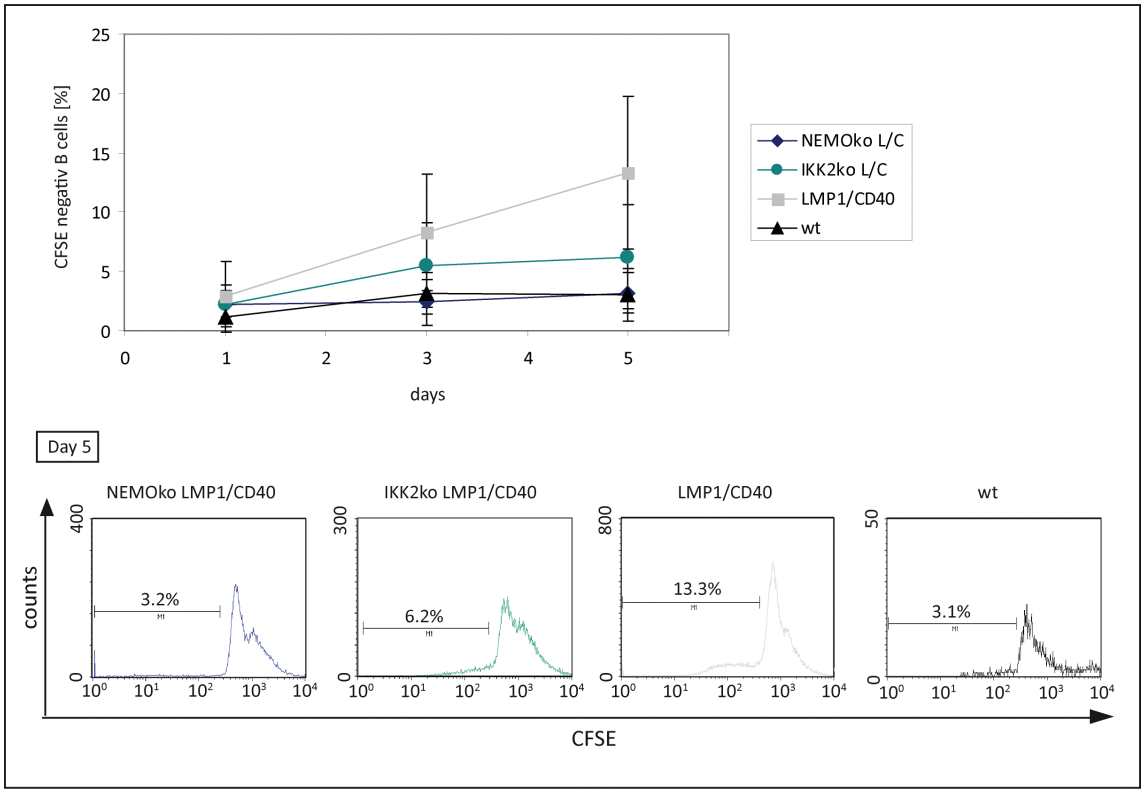

Figure 3.18 The canonical NF-κB pathway is essential for LMP1/CD40 induced proliferation.
B cells of NEMOko LMP1/CD40 (blue rhomb), IKK2ko LMP1/CD40 (green circle), LMP1/CD40 (grey square) and wild type (black triangle) mice were isolated, stained with CFSE and taken in culture for five days. Proliferating cells were detected by measuring the CFSE negative, TOPRO-3 negative B cells via FACS analysis on day 1, 3 and 5. The graph depicted on the upper panel displays the means and associated standard deviations of three independent experiments. The lower panel displays representative CFSE FACS blots of day 5. The gates depicted indicate the percentage of CFSE negative B cells.

3.2.6 Neither NEMO nor IKK2 influence the nuclear shuttling of the NF-κB components

The B cell specific depletion of NEMO and IKK2 was achieved by a Cre-recombinase expression, which deleted the loxP flanked NEMO and IKK2 cassettes. In order to confirm a high deletion efficiency of NEMO and IKK2 in NEMOko LMP1/CD40 and IKK2ko LMP1/CD40 mice, the protein expression levels were detected by Western Blot. In NEMOko LMP1/CD40 B cells only residual NEMO expression was detectable. In LMP1/CD40 mice the NEMO expression was up-regulated, whereas in IKK2ko LMP1/CD40 B cells the NEMO expression was reduced. This could indicate an influence of IKK2 and LMP1/CD40 on NEMO transcription or protein stability. The expression of IKK2 in IKK2ko LMP1/CD40 B cells was also scarcely detectable, confirming a high deletion efficiency of IKK2.

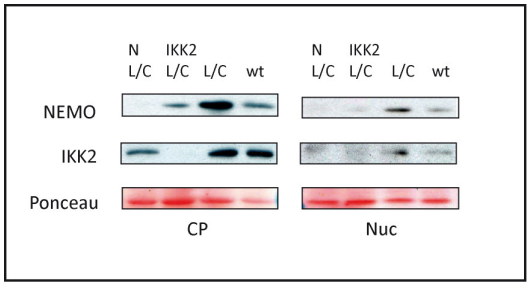

Figure 3.19 Deletion efficiency of NEMO and IKK2.
B cells of NEMOko LMP1/CD40 (N L/C), IKK2ko LMP1/CD40 (IKK2 L/C), LMP1/CD40 (L/C) and wild type (wt) mice were isolated by CD43 depletion and fractionated into the cytoplasm (CP) and nucleus (Nuc). Proteins were analyzed by immunoblotting with antibodies against NEMO (50 kDa) and IKK2 (82 kDa). Equal protein loading was controlled by Ponceau-S staining and antibodies against tubulin (55 kDa) and histone 3 (17 kDa).

In LMP1/CD40 B cells an enhanced nuclear shuttling of p52 and RelB led to the assumption of a hyperactivated non-canonical NF-κB pathway (Hömig-Hölzel et al., 2008). Furthermore, LMP1/CD40 B cells revealed high levels of nuclear p50, which is constitutively prouced in resting B cells by p105 processing. Equal levels of p65 and cRel in wild type and LMP1/CD40 B cells demonstrated that the canonical pathway was not hyperactivated (Hömig-Hölzel et al., 2008). Thus, we were interested to see whether a depletion of NEMO or IKK2 has any influence on the shuttling of the NF-κB components in LMP1/CD40 B cells.

The nuclear fractionation depicted in figure 3.20 displayed the protein levels of the canonical NF-κB subunits. NEMOko LMP1/CD40 B cells revealed slightly reduced levels of p105 in the cytoplasm and p50 in the nucleus compared to LMP1/CD40, whereas IKK2ko LMP1/CD40 B cells demonstrated levels of the canonical NF-κB components in the nucleus and cytoplasm that were similar to LMP1/CD40 B cells. C-Rel levels were comparable in all four genotypes and the subunit p65 was not redistributed to the nucleus, corroborating earlier findings that the canonical NF-κB pathway is not active in LMP1/CD40 cells (Hömig-Hölzel et al., 2008).

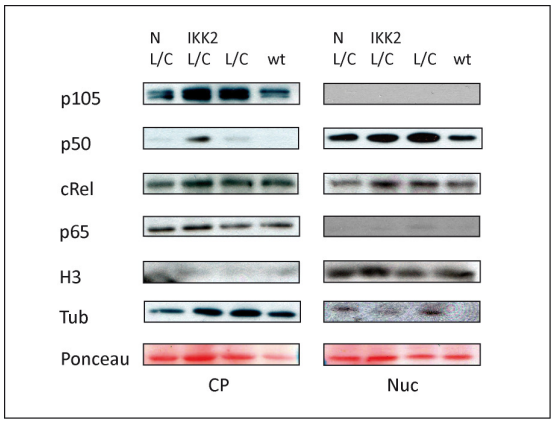

Figure 3.20 Inactivation of the canonical NF-κB pathway slightly influences the LMP1/CD40 induced expression and nuclear localisation of canonical NF-κB components.
B cells of NEMOko LMP1/CD40 (N L/C), IKK2 LMP1/CD40 (IKK2 L/C), LMP1/CD40 (L/C) and wild type (wt) mice were isolated and fractionated into the cytoplasm (CP) and nucleus (Nuc). Proteins were analyzed by immunoblotting with antibodies against p105/p50 (105 kDa/50 kDa), cRel (69 kDa) and p65 (65 kDa). Equal protein loading was controlled by Ponceau-S staining and antibodies against tubulin (55 kDa) and histone 3 (17 kDa). The blot depicted is representative for three independent experiments.

In order to determine whether NEMO or IKK2 influence the LMP1/CD40 induced nuclear shuttling of p52 and RelB, the protein levels of the non-canonical NF-κB pathway were detected by immunoblotting. p100, which is further processed to p52, was diminished in IKK2ko LMP1/CD40 and strongly reduced in NEMOko LMP1/CD40 B cells (Fig. 3.21). This effect could be explained by the known transcriptional regulation of p100 via the canonical NF-κB pathway. However, the p52 levels of NEMOko LMP1/CD40 and IKK2ko LMP1/CD40 were comparable to LMP1/CD40 B cells, indicating the complete processing of all available p100. The non-canonical subunit RelB, also a target of the canonical NF-κB pathway, was still upregulated and efficiently shuttled in IKK2 LMP1/CD40. In NEMO LMP1/CD40 B cells the transcription and therefore the nuclear translocation of RelB was diminished.

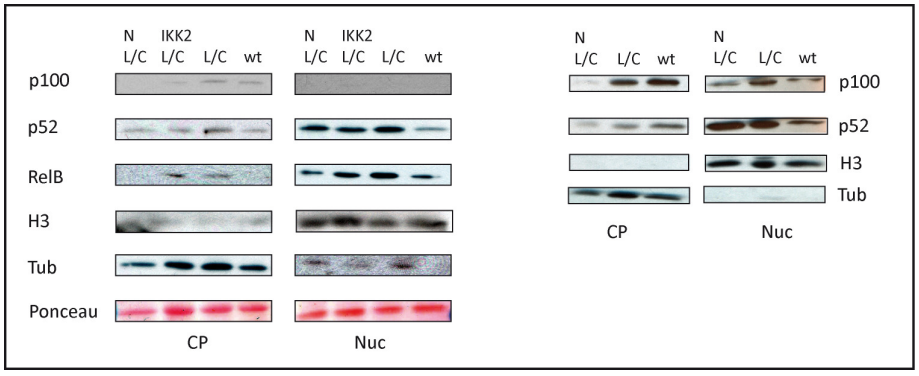

Figure 3.21 The inactivation of the canonical NF-κB pathway slightly influences the LMP1/CD40 induced expression and nuclear localisation of non-canonical NF-κB components.
B cells of NEMOko LMP1/CD40 (N L/C), IKK2 LMP1/CD40 (IKK2 L/C), LMP1/CD40 (L/C) and wild type (wt) mice were isolated and fractionated into the cytoplasm (CP) and nucleus (Nuc). Proteins were analyzed by immunoblotting with antibodies against p100/p52 (100 kDa/ 50 kDa) and RelB (70kDa). Equal protein loading was controlled by Ponceau-S staining and antibodies against tubulin (55 kDa) and histone 3 (17 kDa). The blot depicted is representative for three independent experiments.

In summary, an inactivation of either IKK2 or NEMO slightly reduced the expression of some NF-κB components, but did not impair either the shuttling of canonical or non-canonical NF-κB components into the nucleus. The reduction of RelB seen was not influencing B cell expansion or survival, other data in our lab show, that RelBko LMP1/CD40 B cell had an

enhanced B cell expansion and survival (Kristina Djermanovic, unpublished data). Hence, an altered NF-κB activity in NEMOko LMP1/CD40 and IKK2ko LMP1/CD40 mice cannot be responsible for the impaired proliferation and survival of LMP1/CD40 B cells. Previous data revealed that beside the non-canonical NF-κB pathway the MAPK Erk and JNK are hyperactivated in LMP1/CD40 expressing B cells. A link between NF-κB and the MAPK had been previously published by Waterfield et al. (2004), who demonstrated a NEMO and IKK2 dependent activation of Erk via p105 and Tpl2 in macrophages. So far it has not been shown whether NEMO and IKK2 contribute to CD40 induced MAPK activation. Therefore, we tested the activation status of Erk and JNK in NEMOko LMP1/CD40 and IKK2ko LMP1/CD40 B cells in comparison to LMP1/CD40 B cells.

3.2.7 The canonical NF-κB pathway is important for the LMP1/CD40 induced activation of the MAPKs

In comparison to non-stimulated wild type B cells, LMP1/CD40 expressing B cells demonstrated slightly enhanced levels of Erk and Jnk and high levels of pErk and pJNK (Hömig-Hölzel et al., 2008). To detect whether a depletion of NEMO or IKK2 influences the activation of these MAP kinases, proteins were isolated from NEMOko LMP1/CD40 and IKK2ko LMP1/CD40 B cells and analysed by immunoblotting. The pErk levels of NEMOko LMP1/CD40 and IKK2ko LMP1/CD40 B cells were higher than those in wild type B cells but lower than those in LMP1/CD40 B cells. To corroborate this finding, an intracellular FACS for pErk, Erk, pJNK and Jnk was established. Cells were stained with B220 to gate for the B cell population, and with a primary antibody against the protein of interest. Primary antibody binding was detected with a secondary antibody coupled to a fluorochrome. As a negative control cells were only stained with B220 and the secondary antibody. The intracellular FACS demonstrated lower levels of pErk and pJNK in both NEMOko LMP1/CD40 and IKK2ko LMP1/CD40 in comparison to LMP1/CD40, but higher levels than in wild type, indicating an interaction between NF-κB pathway and MAPK activation. The expression levels of Erk were elevated in IKK2ko LMP1/CD40 and LMP1/CD40 B cells. The JNK expression was slightly enhanced in NEMOko LMP1/CD40, IKK2ko LMP1/CD40 and LMP1/CD40 B cells. The increased expression did not explain the enhanced phosphorylation levels of the MAPKs, since the ratio pMAPK/MAPK in NEMOko LMP1/CD40 and IKK2ko LMP1/CD40 was higher

than in wild type B cells. These data show that in LMP1/CD40 B cells depletion of NEMO or IKK2 led to a reduction of the pErk and pJNK caused by LMP1/CD40 activity.

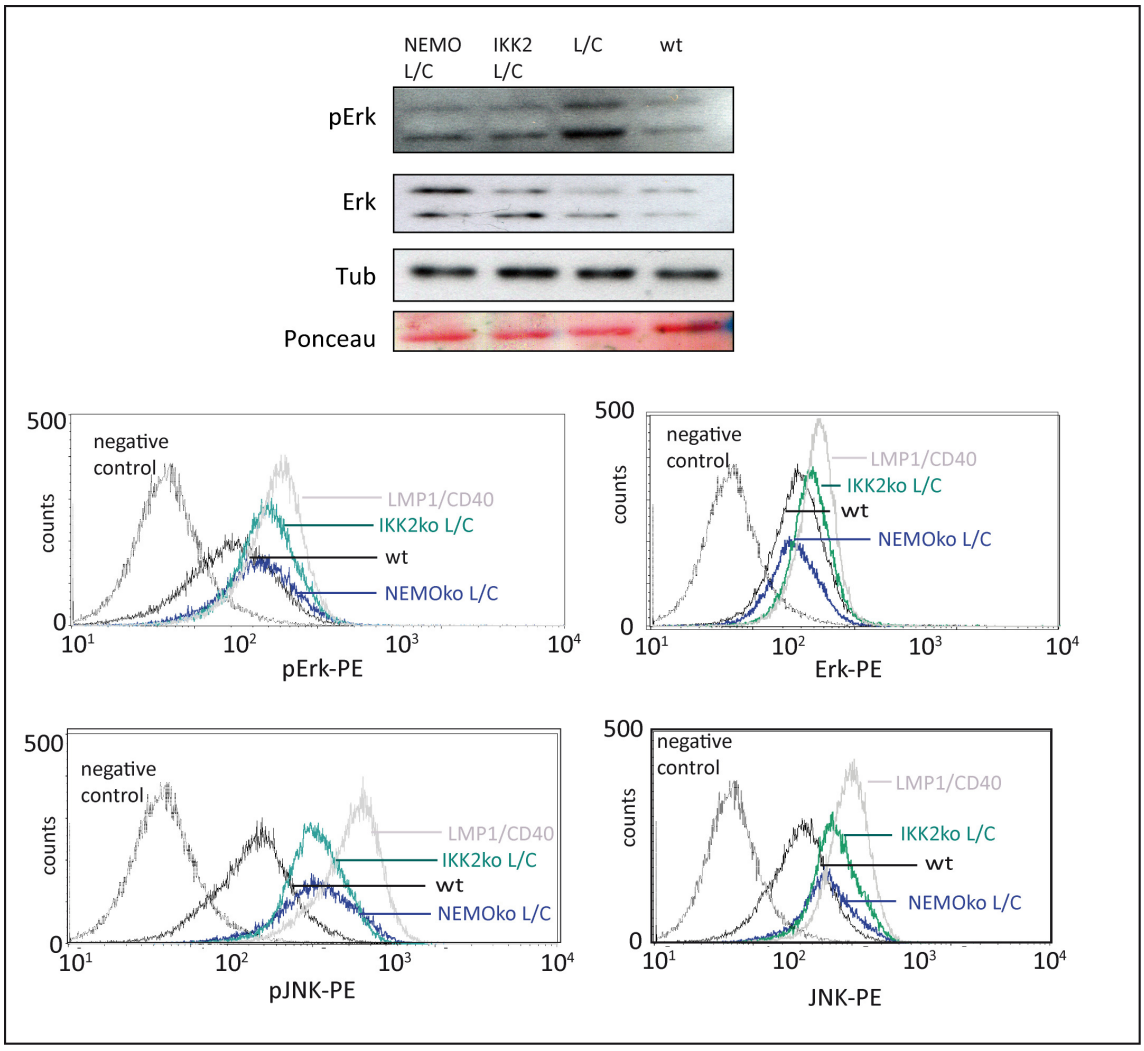

Figure 3.22 The canonical NF-κB pathway plays a role in LMP1/CD40 induced MAPK activation.
Splenic B cells of NEMOko LMP1/CD40 (blue), IKK2ko LMP1/CD40 (green), LMP1/CD40 (grey) and wild type (black) mice were isolated. Protein extracts were prepared of whole cells and analyzed by immunoblotting using antibodies against pErk1/2 (42/44 kDa) and Erk1/2 (42/44 kDa). Equal loading was controlled by tubulin In parallel, splenic cells were stained for B220 in combination with pErk, Erk, pJnk and JNK and analyzed via intracellular FACS.

It has been published in the past that NEMO and IKK2 not only induce the proteasomal degradation of pIκBα, but also the degradation of p105 (Waterfield et al., 2004). This degradation leads to both the release of NF-κB dimers and to a release of Tpl2 (tumour progression locus 2), which is bound to p105. On the other hand Tpl2 has been shown (Eliopoulos et al., 2003) to phosphorylate MEK, leading to the activation of Erk and thereby to an activation of the protein MSK1 (Das et al., 2005). It was shown that MSK1 exclusively

phosphorylates p65 at its serine 276. To detect whether LMP1/CD40 regulates this pathway, we tested the pp65(Ser276) levels in splenic B cells.

3.2.8 The canonical NF-κB pathway is important for the LMP1/CD40 induced phosphorylation of p65(Ser276)

High levels of pErk should lead to an enhanced activation of MSK1 and consequently to increased levels of pp65(Ser276). Expression was studied in LMP1/CD40, NEMOko LMP1/CD40, IKK2ko LMP1/CD40 and a wild type control mice. LMP1/CD40 B cells displayed a robust up-regulation of pp65(Ser276) in compare to wild type B cells. NEMOko LMP1/CD40 and IKK2ko LMP1/CD40 levels of pp65(Ser276) were slightly up-regulated to a level similar to that of than wild type. This indicated that an impaired canonical NF-κB pathway blocks the Erk phosphorylation to some extent, which in turn inhibits the phosphorylation of p65.

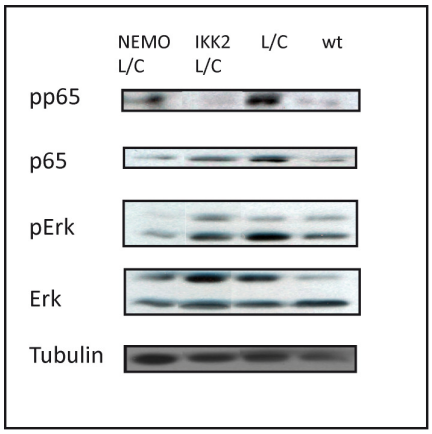

Figure 3.23 LMP1/CD40 induces NF-κB dependent Ser276 phosphorylation of p65.
Splenic B cells of NEMOko LMP1/CD40, IKK2ko LMP1/CD40, LMP1/CD40 and wild type mice were isolated. Protein extracts of whole cells were prepared and analyzed by immunoblotting, using antibodies against pErk1/2 (42/ 44 kDa), Erk (42/44 kDa), pJNK (46/52 kDa) and JNK (46/52 kDa). An antibody against tubulin (55kDa) was used as loading control.

However, residual levels of both pErk and pp65 were present in NEMOko LMP1/CD40 B cells. Therefore, we were interested whether this remaining activity of the canonical NF-κB pathway in the single knock-outs could be inhibited by a deletion of both components at once.

3.2.9 NEMOko IKK2ko LMP1/CD40 mice display an impaired mature B cell development

To create the dual NEMO and IKK2 knock-out mouse model the floxed NEMO, IKK2, LMP1/CD40 and $CD19^{Cre/+}$ genes were all combined in one mouse strain by mouse crossing. Mice with homozygous NEMO and IKK2 floxed genes and heterozygously expressed LMP1/CD40 and $CD19^{Cre/+}$ are referred to in the following as the NEMOko IKK2ko LMP1/CD40 mice. To test whether a depletion of both NEMO and IKK2 influences the LMP1/CD40 induced B cell development, the absolute B cell numbers in the periphery were quantified. The absolute splenic B cell numbers in the NEMOko IKK2ko LMP/CD40 mice were drastically decreased in comparison to either the NEMOko LMP1/CD40 or IKK2ko LMP1/CD40 mice and corresponded to the B cell levels seen in NEMOko or IKK2ko mice. The same phenotype was reflected in FoB and MZB cell numbers, which were reduced to about one third of wild type B cell numbers. This indicated that a depletion of both NEMO and IKK2 has an adverse effect on the LMP1/CD40 induced B cell survival. Therefore we were interested, whether a deletion of both NEMO and IKK2 in LMP1/CD40 mice also influences the MAPK signalling.

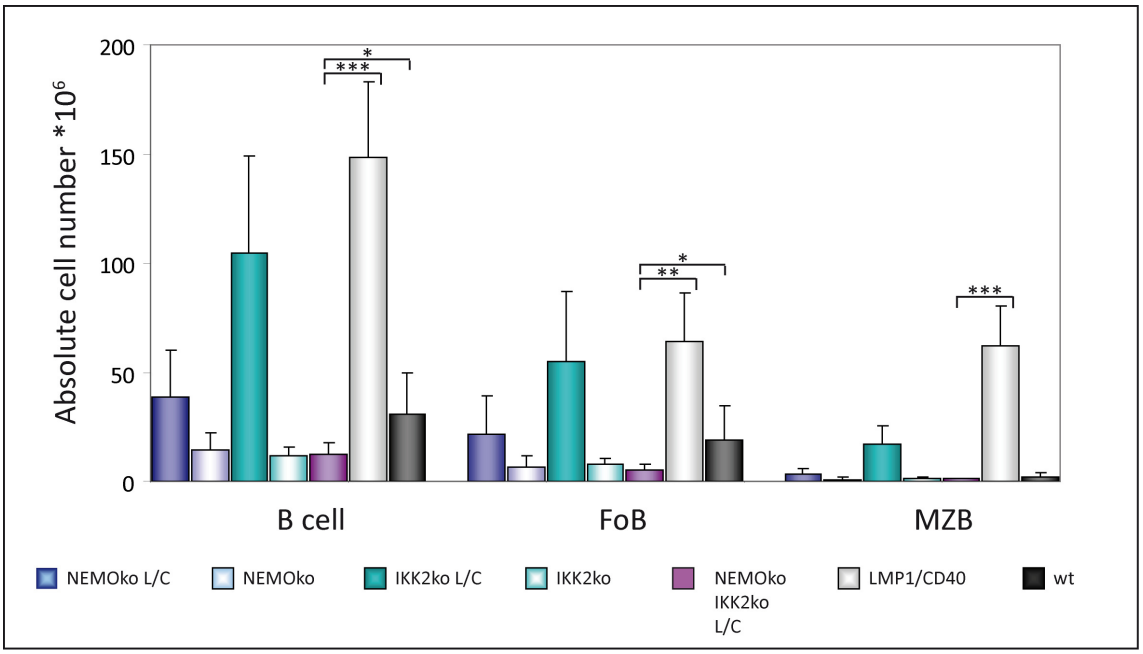

Figure 3.24 NEMOko IKK2ko LMP1/CD40 mice demonstrate a block in B cell expansion and differentiation. Splenic cells of NEMOko LMP1/CD40 (dark blue), NEMOko (light blue), IKK2ko LMP1/CD40 (dark green), IKK2ko (light green), NEMOko IKK2ko LMP1/CD40 (purple), LMP1/CD40 (grey) and wild type (black) mice were isolated, counted and stained with B220, CD21 and CD23 to detect B cells and distinguish follicular (FoB) from

marginal zone B cells (MZB). Depicted mean values and standard deviations were calculated from two independent sets of mice.

3.2.10 NEMOko IKK2ko LMP1/CD40 mice demonstrate an impaired Erk and p65 phosphorylation

In NEMOko LMP1/CD40 and IKK2ko LMP1/CD40 mice, a diminished B cell number correlated with a reduced phosphorylation of Erk (see Fig. 3.22). To test whether the combined deletion of NEMO and IKK2 in LMP1/CD40 mice potentiates this effect, splenic B cells were isolated from NEMOko IKK2ko LMP1/CD40 mice and the phosphorylation of Erk analyzed by immunoblotting and intracellular FACS. In both approaches the pErk levels were seen to be reduced to wild type B cell levels, confirming an important role of NF-κB for Erk activation by LMP1/CD40. Furthermore, the levels of p65 and pp65 in the NEMOko IKK2ko LMP1/CD40 B cells were also diminished to levels comparable to wild type B cells. These results provide additional evidence that the canonical NF-κB pathway is involved in the Tpl2-Erk-p65 pathway in CD40-induced B cells. We assume that a NEMO-IKK2 redundancy is responsible for a remaining Erk activation in NEMOko LMP1/CD40 mice, which was completely lost in NEMOko IKK2ko LMP1/CD40 mice.

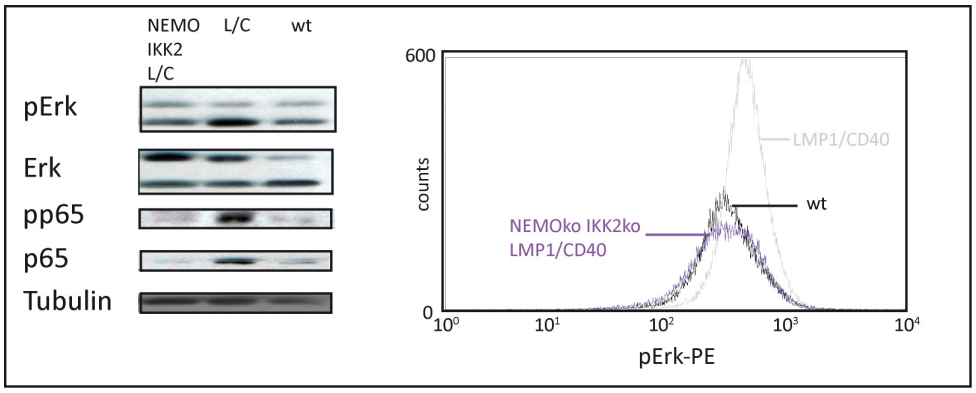

Figure 3.25 NEMOko IKK2ko in LMP1/CD40 mice block Erk and p65 phosphorylation.
Splenic B cells were isolated from NEMOko IKK2ko LMP1/CD40 (purple), LMP1/CD40 (grey) and wild type (black) mice. For immunoblotting protein extracts were prepared and analyzed with antibodies against pErk1/2 (42/44 kDa), Erk1/2 (42/44 kDa), pp65 (65 kDa) and p65 (65kDa). Tubulin (55kDa) was used as a loading control. Additionally, splenic cells were stained with B220, pErk (rabbit) and α-rabbit PE for intracellular FACS.

4. Discussion

4.1 AID targeting to the Ig locus

AID introduces mutations specifically into the Ig loci, thereby enhancing immunoglobulin diversity. It is not clear how this AID mutagenic activity is targeted exclusively to the Ig locus, and which *cis* and *trans* acting factors are involved in this process. A detailed deletion analysis of the Ig locus was performed to detect those regulatory sequences leading to AID recruitment.

4.1.1 *GFP2* as a reporter system to trace AID induced hypermutation

The detection of AID-induced gene mutations could be conducted via three different established assays. In reversion assays an artificially introduced stop codon is mutated by hypermutation, leading to the re-expression of a reporter gene such as IgM or GFP (Arakawa et al., 2006). The disadvantage of this system lies in its dependence on the very restricted area for the detection of AID effects. Furthermore, it is not possible to distinguish between different kinds of mutations or to detect silent mutations. Direct sequencing of the target would solve these problems, but is not practicable for large scale mutation studies. Therefore, the *GFP2* reporter, established by Hiroshi Arakawa (Arakawa et al., 2008) was used for the experiments. Mutations in all regions over the *GFP* gene, including insertions and deletions, can be detected via a loss of GFP fluorescence.

However, even *GFP2* has the disadvantage of not detecting silent mutations. Furthermore, mutations leading to the expression of *GFP* with higher intensity were not considered in the reported deletion series.

To exclude that mutations in *GFP2* cause an expression silencing, Artem Blagodatski performed additional control experiments in our lab (Blagodatski et al., 2009). He sorted GFP^{high} and GFP^{low} cells from a $\psi V^{-}IgL^{GFP2}$ mutation screen and isolated mRNA. The continued transcription of GFP low cells was confirmed by semi-quantitative RT-PCR. This experiment demonstrated that low or high intensities of GFP are not coupled to GFP expression.

4.1.2 The sequence of Igλ is necessary and sufficient to recruit AID

AID is specifically recruited to the Ig locus (Martin et al., 2002). To address the question whether specific sequences, contained in the Ig locus, are responsible for AID recruitment, Hiroshi Arakawa designed a $\psi V^{-}IgL^{-}$ cell line, deleting the Igλ locus. A targeted insertion of the *GFP2* reporter into the deleted Igλ locus led to a reduction of SHM activity from 6.4% to 0.01%, indicating that elements essential for hypermutation are present in the Ig sequence. This result was confirmed by the reinsertion of the 9.8 kb sequence of Igλ coupled to *GFP2* into the $\psi V^{-}IgL^{-}$ cell line, reconstituting the hypermutation rate to 7.4%. So, for the first time, we were able to show that the Ig sequence itself is essential for AID targeting. To test, whether the sequence is also sufficient, Artem Blagodatski introduced the sequence to non-Ig loci such as the BACH2, RDM1 or RAD52 (Blagodatski et al., 2009), which are typically not involved in hypermutation. Even in sequences not usually involved in hypermutation, the Ig sequence was sufficient to induce AID targeting and a hypermutation rate comparable to $\psi V^{-}IgL^{GFP2}$.

To identify and locate potential *cis*-elements essential for AID recruitment overlapping IgL fragments of different sizes were reinserted upstream of the *GFP2* reporter in the $\psi V^{-}IgL^{-}$ cell line. The reinsertion of the first 3 kb ('A', 'B') and the last 2.8 kb ('P') of the 9.8 kb core of the IgL did not induce hypermutation. Further reinsertions demonstrated that several elements upstream and downstream of the enhancer region and the enhancer itself contribute to the AID targeting. By adding the fragment 'S' (3 kb-7 kb) to the non-mutating fragments 'B' or 'P', a mutation rate comparable to the wild type IgL locus was reached. However, the insertion of the core element 'S' itself achieved only one third of SHM activity compared to the complete locus. This indicates a role of 'B' and 'P' in boosting hypermutation. The low hypermutation rate of $\psi V^{-}IgL^{S,GFP2}$ did not result from distance effects, since in 'K' (consisting of 'S' and 'P') the 'S' fragment is also directly located next to the reporter without influencing the hypermutation rate. Nevertheless, 'S' was sufficient to recruit AID and displayed a mutation rate more than 100 times higher than the background level in $\psi V^{-}IgL^{-}$.

To rule out that different mutation rates resulted from variations in the rates of GFP transcription, a semi-quantitative RT-PCR on GFP was performed for cell lines containing the reinserted fragments by Artem Blagodatski (Blagodatski et al., 2009). Again, there were no

obvious differences in GFP transcription levels, confirming the independence between GFP transcription and GFP intensity levels.

4.1.3 The Ig enhancer plays a decisive role in AID targeting

The reinsertion analysis revealed that the hypermutation activity was mainly transmitted via the 'S' fragment, which contains the 3-7 kb of the Ig locus including the enhancer. Therefore, a detailed analysis of this region was performed to identify specific *cis*-elements in the 'S' region. *GFP2* plasmids containing either 1 kb incremental fragments or single 1 kb fragments of 'S' were transfected into the ψV⁻IgL⁻ cell line. The insertion series from the 5'- and 3'-end both indicated an essential role of the region '2-3'. The importance of '2-3' was proven by the analysis of the single fragments, demonstrating an exclusive ability of '2-3' to recruit AID, which is probably enhanced by surrounding elements. Interestingly, the '2-3' region contains the Igλ enhancer.

The role of the Ig enhancer for GCV and SHM has been indicated previously. Xiang et al. 2008 created an Igκ enhancer (Ed) knock-out mouse which revealed a reduced SHM rate. Moreover, Yang et al. (2006) deleted the IgL enhancer in DT40 cells and demonstrated that, whereas the enhancer influenced the transcription of IgL only moderately, the GCV/SHM activities were reduced fivefold. Kothapalli et al. (Kothapalli et al., 2008) described a systematic deletion of the IgL locus in DT40. They showed that a deletion of the enhancer reduced the mutation rate to one half of that of the complete locus. A further deletion of almost the whole IgL locus inhibited mutations completely, which is in accord with our results of the ψV⁻IgL⁻ cell line.

A series of 200 bp internal deletion analysis of the region 'S' was then used to localize smaller essential regions of the enhancer, I performed. This deletion analysis revealed that only one element, the region '2.2-2.4', located at the 5'-end of the enhancer, was important for SHM. An additionally 50 bp staggered-end reinsertion analysis of '2-3' confirmed the previous results. The reinsertion of '2-3' in the ψV⁻IgL⁻ cell line from the 5'-end indicated the existence of an important element located between '2.25' and '2.30', the reinsertion from the 3'-end displayed an important role of '2.20-2.25'. Both series confirmed the exclusive role of '2.2-2.4', focusing on '2.2-2.3'. The fact that the 5'- and 3'- end reinsertions resulted

in two different adjacent elements, essential for AID recruitment, might be explained by a motif repetition or synergistic elements located in '2.00-2.25' and '2.25-2.30'.

4.1.6 The 'HCorE' element '2.2-2.4' is sufficient to target AID

To test the region '2.2-2.4' for its sufficiency to initiate SHM and whether it includes putative motive repetitions, *GFP2* plasmids containing '2.2-2.4' and its multimers were tranfected into the ψV$^-$IgL$^-$ cell line. The hypermutation activity of cells including '2.2-2.4' was 0.6% and therewith 60 times higher than the background activity of IgL$^-$. This is the first demonstration of a 200 bp region sufficient for AID recruitment. A multimerization of '2.2-2.4' increased the hypermutation rate to 4%, which corresponds to more than half of that of the complete IgL locus. This strong effect might be the result of either a motif repetition or a required minimal distance to the reporter. To verify a distance effect it would be necessary to introduce a stuffer fragment between the reporter and '2.2-2.4'. Previous results from different reinsertion series do not suggest a distance effect. However, additional effects due to length-dependent conformational changes or changes in the chromatin structure cannot be excluded.

Further experiments, performed in our lab have confirmed the exclusive role of '2.2-2.4' for SHM. Ulrike Schötz inserted the region '2.2-2.4' in the non-mutating *BACH2* locus. There, '2.2-2.4' induced 1% GFP low cells, which was similar to '2.2-2.4' in the IgL locus (personal communication). Thus, '2.2-2.4' can induce SHM, independent of the chromosomal location, which argues against a potential role of chromatin structures.

Additionally, Arundhathi Sriharshan succeeded in identifying the homologous '2.2-2.4' regions of the closely related species duck and turkey. Transfecting *GFP2* plasmids containing duck '2.2-2.4' or turkey '2.2-2.4' into the ψV$^-$IgL$^-$ cell line induced a GFP low population of 0.9% and 1.0%, respectively (personal communication). This high evolutionary conservation further confirms the core function of '2.2-2.4' in AID targeting.

4.1.7 *In silico* analysis of '2.2-2.4' and localization of transcription factor binding sites

After the identification of the 200 bp fragment, with high activity for SHM, we were interested to identify known transcription factors that can bind to this region. With the help of the bioinformatical tools MEME and MAST, several *cis*- and *trans*-elements were detected. These were predominantly accumulated at the 5'-end of '2.2-2.4'. At the very 5'-end an E2A binding site was identified. E2A has been shown before to be crucial for hypermutation. Thus, Schötz et al. (2006) published that inactivation of E2A in DT40 B cells led to a strong reduction in the number of mutations inserted into the V region. Furthermore, Tanaka et al. (2010) could show that a random integration of E-box motives in the Igκ enhancer, initiated hypermutation, whereas mutation of these E-box motives inhibited AID targeting. Close to the 5' located E2A a MEF an NF-κB binding site were predicted.

The identification of a MEF binding site (A/T rich region) in the λ enhancer was already published in 1998 (Satyaraj et al.). The role of MEF and NF-κB binding sites for AID targeting was only recently published (Kim et al., 2009). A mutation of either the NF-κB or the MEF binding site, or a deletion of NF-κB components c-Rel or p50, decreased AID targeting, detected by gene conversion rate significantly (Kim et al., 2009).

Between '2.35' and '2.4', a binding site for SP-1 (CCAC) was located. SP-1 has been shown to directly interact with an approximately 200 bp distant MEF-2, thereby enhancing the promoter activity synergistically (Grayson et al., 1998). Similar effects have been found for SP-1/NF-κB cooperative promoter activation (Perkins et al., 1993).

At the 3'-end of '2.2-2.4' a Pax5 binding site was identified. Pax5 is a transciption factor essential for cell lineage commitment in the early B cell stage. The role of Pax5 in late B cell development was not established until a Pax5 binding site was found in the murine heavy chain 3' alpha enhancer. Here the Pax5 site had a negative regulatory effect on the enhancer activity (Neurath 1994). Furthermore, depletion of Pax5 in DT40 B cells revealed a promotion of plasma cell differentiation (Nera et al., 2006). Therefore, Pax5 has probably an inhibitory rather than an AID binding function.

An AID targeting model, depicted in Fig. 4.1. has been proposed, knowing that AID can be co-immunoprecipitated with RNA polymerase II (Nambu et al., 2003) and the fundamental role of NF-κB, MEF and E2A transcription factors in the hypermutation process.

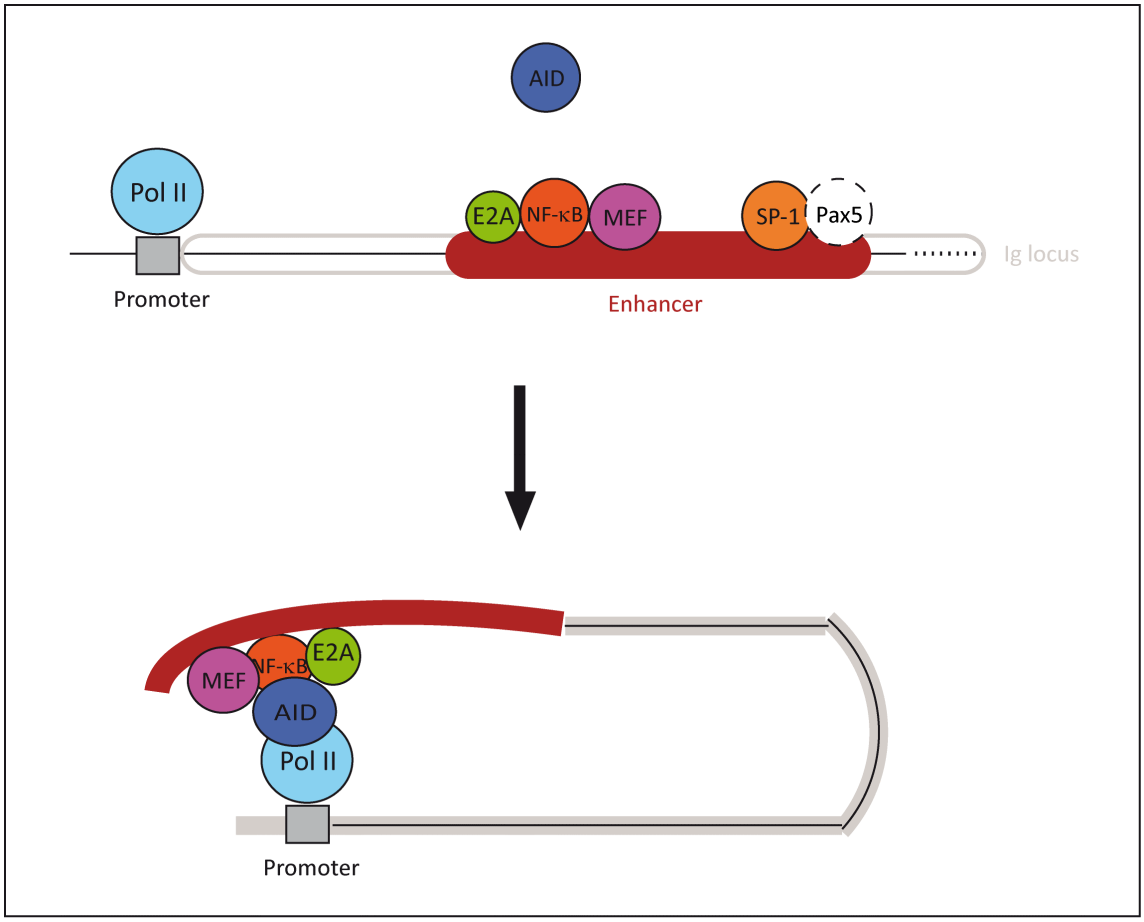

Figure 4.1 AID targeting model.
Transcription factors E2A (green), NF-κB (orange) and MEF (violet) bind to the enhancer (red) and recruit AID (blue). The transcriptions factor complex loops to the promoter region (grey), loading AID onto the RNA polymerase II (light blue).

The transcription factors described above, could bind to the conserved Ig enhancer, interact with each other and AID and loop to the promoter region. Thereby, AID could be loaded on the polymerase, introducing mutations in the transcribed DNA strand. Probably further factors like e.g. SP-1 could be involved in this process enhancing the binding affinity.

4.2 The role of the canonical NF-κB pathway for LMP1/CD40 induced B cell expansion and differentiation

The interaction of CD40/CD40L activates several signalling pathways in B cells, leading to longer survival and enhanced proliferation. *In vitro* analyses of LMP1/CD40 expressing cells

have shown an activation of the MAPK and NF-κB pathways (Hatzivassiliou et al., 1998). *In vivo* data have confirmed these results (Hömig-Hölzel et al., 2008) and in addition deteced a specific activation of the non-canonical NF-κB pathway. To address the role of the canonical NF-κB pathway in constitutive CD40 signalling the effect of B cell specific deletion of NEMO and IKK2 was studied.

4.2.1 The influence of the canonical NF-κB pathway on LMP1/CD40 expressing B cells *in vivo*

In vivo data have shown splenomegaly due to a B cell expansion in the mantle and follicle areas in LMP1/CD40 mice. Moreover a shift in differentiation from Fo to MZ B cells was seen (Hömig-Hölzel et al., 2008). Both, NEMOko LMP1/CD40 and IKK2ko LMP1/CD40 mice displayed a reduced degree of splenomegaly and B cell expansion, revealing a dependence of the LMP1/CD40 mediated B cell expansion on NEMO and IKK2. Furthermore, the seen differentiation shift to the MZ B cell population was blocked in both the NEMOko LMP1/CD40 and IKK2 LMP1/CD40 mice. This establishes that the enhanced MZ B cell differentiation seen in LMP1/CD40 mice is dependent on the activity of the canonical NF-κB pathway. Such a role of the canonical NF-κB pathway for MZ B cell development has already been suggested by previous studies. Thus, p50ko mice displayed a defective MZB development and the absence of p65 or c-Rel also diminished the MZ B cell population (Cariappa et al., 2000).

The enhanced expression levels of surface CD95 and ICAM seen in LMP1/CD40 cells were to some extent maintained after inactivation of NEMO and IKK2. ICAM, an adhesion molecule, has been published as a NF-κB target gene and CD95 has been shown to be up-regulated by CD40 activation (Ribeiro et al., 2002). CD95 usually induces apoptosis, which is inhibited by ligation of CD40 (van Ejik et al., 2001). In activated B cells the non-functional death-inducing signalling complex (DISC) is composed of FAS, FADD and inhibitory cFLIP. CD40 regulates the expression of cFLIP, thereby inhibiting the activation of caspase-8 (van Ejik et al., 2001). Whereas in IKK2ko LMP1/CD40 cells all B cell populations demonstrated the same levels of CD95 and ICAM, in NEMOko LMP1/CD40 only MZ B cells or marginal precursor B cells displayed enhanced levels of CD95 and ICAM, whereas expression on Fo B cells remained at wild type level. The reason for this might be the stronger impairment of the canonical NF-κB

pathway after inactivation of NEMO compared to IKK2. The specific activation of MZ B cells in NEMOko LMP1/CD40 cells is in accordance with earlier publications showing that MZ B cells react rapidly and efficiently to the presence of blood-borne bacteria and have therefore a much lower activation-threshold than follicular B cells (Lopes-Carvalho et al., 2005).
Thus, LMP1/CD40 expressing B cells *in vivo* depend on the canonical NF-κB pathway regarding B cell expansion, differentiation and activation.

4.2.2 The influence of the canonical NF-κB pathway on LMP1/CD40 expressing B cells *in vitro*

In LMP1/CD40 mice the splenic B cells demonstrated a longer survival and an improved spontaneous proliferation in *in vitro* experiments (Hömig-Hölzel et al., 2008). NEMOko LMP1/CD40 and IKK2 LMP1/CD40 B cells survived less efficient than LMP1/CD40 B cells, demonstrated by higher TOPRO levels, but better than wild type controls. This is in accordance with former publications (Zarnegar et al., 2004) showing that both the canonical and the non-canonical NF-κB pathway contribute to the survival of B cells. CD40 stimulated primary B cells derived from p50, c-Rel or p52 knock-out mice were shown to have an impaired survival *in vivo*. The simultaneous inactivation of p50 and cRel reduced the survival to about one half of that seen in wild type mice. Therefore the intermediate survival phenotype of NEMOko LMP1/CD40 and IKK2ko LMP1/CD40 might reflect remaining activity of the non-canonical NF-κB pathway.
Moreover, the proliferation of IKK2ko LMP1/CD40 B cells was reduced and even completely inhibited in NEMOko LMP1/CD40 B cells. These results demonstrate an essential role of the canonical NF-κB pathway for CD40 mediated B cell proliferation that cannot be compensated by an activated alternative NF-κB pathway. In accordance with our data it has been published that CD40 stimulated B cells of c-Rel, p50 or c-Rel/p50 knock-out mice were completely blocked in proliferation (Zarnegar et al., 2004) and that IKK2 played a critical role for B cell proliferation (Li et al., 2003). However, CD40 stimulated p52-/- primary B cells still expressed G1-S cell cycle transition genes, indicating that they are not arrested at the G1-S checkpoint (Zarnegar et al., 2004). These data suggest that the canonical and not the alternative NF-κB pathway plays an essential role for short term CD40 as well as for constitutive CD40 induced proliferation.

4.2.3 The role of NEMO and IKK2 for NF-κB and MAPK activation in LMP1/CD40 mice

LMP1/CD40 expressing B cells have been shown to display an increased translocation of p52, p50 and RelB to the nucleus as well as an overal enhanced expression of p52, p50 and RelB (Hömig-Hölzel et al., 2008). In NEMOko LMP1/CD40 B cells, p50 and p52 levels were still increased, although the expression level of the p52 precursor, p100, was drastically decreased. This is in line with a previous publication, showing that the transcriptional regulation of p100 depends on an active canonical NF-κB pathway (Liptay et al., 1994) and that p100 is completely processed to p52 (de Jong et al., 2010), maintaining p52 levels despite loss of p100 expression. The RelB levels of IKK2ko LMP1/CD40 mice were similar to these seen in LMP1/CD40 but were reduced in NEMOko LMP1/CD40 mice. RelB has also been published to be a target gene of the canonical NF-κB pathway (Bren et al., 2001), which might explain that RelB levels were reduced in NEMOko LMP1/CD40 in comparison to LMP1/CD40 cells. However it is unlikely that the reduced RelB levels are responsible for the reduced proliferation of NEMOko LMP1/CD40 in comparison to LMP1/CD40 B cells, since it is known from RelBko LMP1/CD40 mouse experiments performed by Kristina Djermanovic (personal communication) that RelB does not influence B cell expansion, survival or activation status in LMP1/CD40 mice. This might indicate that enhanced translocation of RelB and p52 could be the result of increased transcription of these components rather than an enhanced activation of the non-canonical NF-κB activator NIK. Surprisingly, the translocation of canonical NF-κB components, which were not overexpressed, was not influenced by the deletion of either NEMO or IKK2.

A recent publication has shown that TNF treated B cells with a specific NEMO mutation were exclusively impaired in p65 nuclear shuttling as well as in their Erk phosphorylation (Owen et al., 2010). The phosphorylation of MAPK Erk and JNK were elevated in LMP1/CD40 mice (Hömig-Hölzel et al., 2006). Thereby, Erk contributed significantly to B cell survival and lymphomagenesis (Hojer 2009). Hence we decided to investigate the influence of NEMO or IKK2 knock-out on the MAPK activation in LMP1/CD40 expressing B cells. The levels of pErk and pJNK were reduced in NEMOko LMP1/CD40 and IKK2ko LMP1/CD40, demontrated in Western Blots and intracellular FACS analyses, and were completely abolished in NEMOko

IKK2ko LMP1/CD40 double knock-out B cells. A link between Erk and NF-κB has been suggested before. Heißmeyer et al. (2001) demonstrated that NEMO and IKK2 are essential for p105 degradation, hence releasing the kinase Tpl2 in 293HEK cells. This was confirmed by Waterfield et al. (2004) in macrophages, showing an Erk phosphorylation by Tpl2 via MEK1. A publication by Eliopoulos et al. (2003) revealed a CD40 dependent Tpl2 activation in B cells, resulting in an Erk phosphorylation. Therefore, the reduced levels of pErk in NEMOko LMP1/CD40 and IKK2ko LMP1/CD40 might be explained by a reduced degradation of p105, inhibiting Tpl2, the MEK1 kinase.

4.2.4 A new role of p65 for LMP1/CD40 induced B cell expansion and activation

In accordance with the publications mentioned before, Das et al. (2005) demonstrated Tpl2 induced phosphorylation of p65 Ser276 via MEK1, Erk and MSK1 in MEF cells. They also described the pp65 independence of IκBα and the independence of nuclear shuttling or DNA tagging. Hence we were interested whether a constitutive CD40 signalling in LMP1/CD40 mice leads to a specific phosphorylation of p65. High levels of pp65(Ser276) were detected in LMP1/CD40, but not in wild type control mice. In NEMOko LMP1/CD40 or IKK2ko LMP1/CD40 mice the level of pp65(Ser276) was strongly diminished. On the other hand we know from RelBko LMP1/CD40 and IKK1ko LMP1/CD40 experiments performed by Kristina Djermanovic, that RelB or IKK1 inactivation does not have any influence on the p65 phosphorylation (personal communication). So the effect strictly depends on the canonical NF-κB pathway. On the basis of these results, we propose a working model which could explain the complete dependence of LMP1/CD40 mediated B cell expansion on the canonical NF-κB pathway. NEMO and IKK2 phosphorylate p105, which is proteasomal degraded. Thereby, NF-κB dimers like p50/p65 and the kinase Tpl2 can be released. The dimers can translocate to the nucleus, Tpl2 can phosphorylate MSK1 via MEK1 and Erk. MSK1 shuttles also to nucleus, where it phosphorylates specifically p65 at serine 276. The phosphorylation induces a conformational change of the dimer, facilitating the binding of additional binding factors like CBP, therewith leading to an enhanced binding affinity to the promoter of specific genes like IL6.

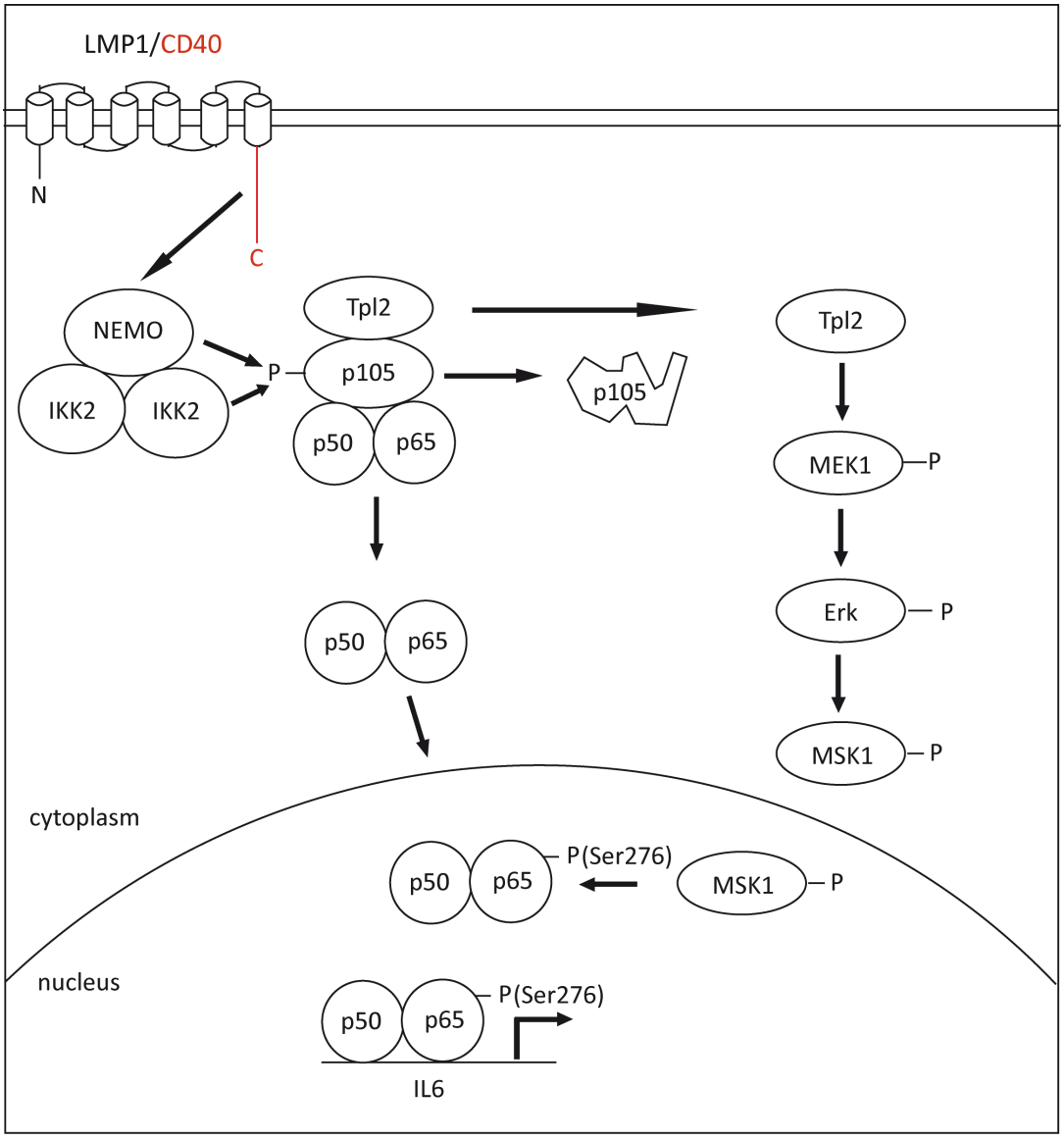

Figure 4.2 Model for LMP1/CD40 signal transduction via NEMO and IKK2.
NEMO and IKK2 phosphorylate p105, initiating a proteasomal degradation of p105. p50/p65 are released, shuttling to the nucleus, Tpl2 is released, phosphorylating MEK1. MSK1 is phosphorylated via MEK/Erk and translocates to the nucleus, where it activates p65 via phosphorylation. pp65(Ser276) initiates the transcription of specific genes like IL6.

5. Materials and Methods

5.1. Materials

5.1.1 Antibodies

Immuno-staining antibodies

Antibody	Ab ID	Source	Size (kDa)	Dilution	Dilutant
IκBα (#371)	Santa Cruz	rabbit	33	1:1000	TBST 5% BSA
pIκBα (#9246)	Cell Signaling	mouse	33	1:1000	TBT 5% Milk
Erk (#9102)	Cell Signaling	rabbit	42, 44	1:1000	TBST 5% BSA
pErk (#9101)	Cell Signaling	rabbit	42,44	1:1000	TBST 5% BSA
JNK (#9258)	Cell Signaling	rabbit	46, 54	1:1000	TBST 5% BSA
pJNK (#4821-50)	Abcam	rabbit	46, 54	1:500	TBST 5% BSA
p65 (#3034)	Cell Signaling	rabbit	65	1:1000	TBST 5% BSA
pp65(Ser276) (#101749)	Santa Cruz	rabbit	65	1:1000	TBST 5% BSA
p52/p100 (#4882)	Cell Signaling	rabbit	52, 100	1:1000	TBST 5% BSA
p50/p105 (#1190)	Santa Cruz	goat	50, 105	1:500	TBST 5% BSA
RelB (#4954)	Cell Signaling	rabbit	70	1:1000	TBST 5% BSA
c-Rel (#6955)	Santa Cruz	mouse	75	1:500	TBST 5% BSA
NEMO (#8330)	Santa Cruz	rabbit	50	1:1000	TBST 5% BSA
IKK2 (#2684)	Cell Signaling	rabbit	87	1:1000	TBST 5% BSA
α-IgG rabbit (#7074)	Cell Signaling	goat		1:2000	TBST 1% Milk
α-IgG mouse (#7076)	Cell Signaling	Goat		1:2000	TBST 1% Milk

Antibodies for intracellular FACS

Antibody	Ab ID	Source	Dilution	Dilutant
Erk (#9102)	Cell Signaling	rabbit	1:50	Cytofix/Cytoperm (BD555028)
pErk (#9101)	Cell Signaling	rabbit	1:50	Cytofix/Cytoperm (BD555028)
JNK (#9258)	Cell Signaling	rabbit	1:50	Cytofix/Cytoperm (BD555028)
pJNK (#4821-50)	Abcam	rabbit	1:50	Cytofix/Cytoperm (BD555028)

α-IgG(rabbit)-PE (#A11008)	Invitrogen	goat	1:100	Cytofix/Cytoperm

5.1.2 Bacterial strains (chemically competent cells)

DH-5α (*Escherichia Coli*): F^-, Δ80dlacZΔM15, Δ(lacZYA$^-$argF)U169, deoR, recA1, endA1, hsdR17(rK^-, mK^+), phoA, supEE44, λ^-, thi-1, gyrA96, relA1.

TOPO TA Cloning® Kit: Top10 One Shot® Cells [Invitrogen Corporation]

5.1.3 Cell culture

Chicken Medium
1xDMEM/F-12 Medium (Gibco™ Invitrogen)
10% FBS (v/v) (Biochrom)
1% Chicken Serum (v/v) (Pan)
200µg/ml Penicillin/Streptomycin (Gibco™ Invitrogen)
0.5 mM (final c) β-Mercaptoethanol (Sigma-Aldrich)

Mouse B cell medium
1xRPMI 1640
1% Penicillin/Streptomycin (v/v) (Gibco™, Invitrogen);
10.000U/ml Pen; 10.000µg/ml Strep
1% (v/v) non-essential amino acids (Gibco™, Invitrogen); 100x
1% L-glutamine (v/v) (Gibco™, Invitrogen); 200 mM stock
1% sodiumpyruvate (v/v) (Gibco™, Invitrogen); 100mM stock
50 µM β-Mercaptoethanol (Gibco™, Invitrogen); 50 mM stock

5.1.4 Cell lines

Mutants of the chicken DT40 B cell line that were used for the transfections of Igλ-containing plasmids.

$\psi V^{-}AID^{RI}$	The AID gene *aicda* was deleted and reconstituted by a randomly integrated AID cDNA cassette driven by a β-actin promoter and coupled to a mycophenolic acid resistance gene (Arakawa et al., 2008). The pseudogenes of the rearranged Ig locus were deleted, thereby impairing gene conversion and enhancing hypermutation.
$\psi V^{-}IgL^{-}$	The rearranged Ig locus was deleted in the $\psi V^{-}AID^{RI}$ cell line and replaced by a puromycin resistance gene (Blagodatskiy et al., 2009).

5.1.5 Consumables

Bacterial culture	Petri dish Falcon Easy Grip™ (Becton Dickinson)
Cell culture	96-, 24-, 6-well plates (Nalge Nunc)
	Tissue culture flasks (Becton Dickinson)
Cuvettes	Electroporation Bio Rad Gene Pulser Cuvette (Bio-Rad)
	Photometry UV-Vis cuvette (Eppendorf)
PCR	8 well strips (ABgene Inc)
	8 cap strips (ABgene Inc)

5.1.6 Enzymes and dNTPs

Calf Intestinal Phosphatase (New England Biolabs)

DNA Polymerases	Expand Long Template PCR System (Roche Diagnostics GmbH)
	Taq Polymerase (New England BioLabs and Invitrogen Life Technologies)

dNTPs (MBI Fermentas GmbH)

Proteinase K (Qiagen)

Restriction endonucleases (New England Biolabs and MBI Fermentas GmbH)

5.1.7 Experimental Kits

DNA cloning	Topo TA Cloning® Kit (Invitrogen GmbH)
DNA purification	Gel extraction (Qiagen GmbH)
	PCR purification (Qiagen GmbH)
Intracellular FACS	Cytofix/Cytoperm Fixation/Permeabilization kit (Becton Dickinson)
Ligation	DNA Ligation Version 2.1 (Takara Bio Inc.)
Plasmid Isolation	Mini (MBI Fermentas GmbH)
	Maxi (Qiagen GmbH)
Sequencing	BigDye Terminator 3.1 Cycle Sequencing Kit (Applied Biosystems)

5.1.8 Instruments

Electroporator	Gene Pulser Xcell™ (Bio-Rad Lab.)
FACS	BD™ LSRII and Calibur Flow Cytometer (Becton Dickinson)
Incubators	Heraeus (Kendro Lab. Products)
Processor (WB-Film)	Cawomat 2000 IR (Ernst Christiansen)
Sequencer DNA	ABI 3730 DNA Analyzer (Applied Biosystems & Hitachi; Hitachi High Tech.Corp.)
UV spectrophotometer	BioPhotometer (Eppendorf GmbH)

5.1.9 Media

2YT Broth

1.6% (w/v) bacto tryptone (Becton, Dickinson and Company Inc.), 1% (w/v) yeast extract (Sigma-Aldrich Chemie GmbH), 0.5% (w/v) NaCl.

LB Agar Plates

2% (w/v) LB broth base (Sigma-Aldrich Chemie GmbH), 1.5% (w/v) Bacto™ Agar (Becton, Dickinson and Company Inc.), antibiotics.

5.1.10 Mouse strains

LMP1/CD40^{flSTOPP} (Hömig-Hölzel et al., 2008)

The transgene LMP1/CD40 is inserted in the r*osa26* locus of a BALB/c mouse strain. A loxP flanked stop cassette, which can be deleted by a Cre recombinase, is positioned upstream of the LMP1/CD40 gene and thus prevents the expression of the chimeric protein.

CD19-Cre (Rickert et al., 1997)
The transgene Cre-recombinase is inserted heterozygously in the *cd19* locusof a C57BL/6 mouse strain, thereby being regulated via the CD19 promoter, but destroying the *cd19* gene.

IKK2$^{fl/fl}$ (Pasparakis et al., 2002)
Exons 6 and 7 of the *IKK2* gene were placed between loxP sites in a C57BL/6 mouse strain. A *Cre*-mediated deletion of these exons leads to an *IKK2* null allele.

NEMOfl/fl (Schmidt-Supprian et al., 2000)
Exon 2 of the *NEMO* gene was placed between loxP sites in a C57BL/6 mouse strain. A Cre-mediated deletion of exon 2 leads to a *NEMO* null allele.

5.1.11 Plasmids

pIgL$^{-,GFP2}$; provided by Hiroshi Arakawa (Blagodatsky et al., 2008)
IgL arm sequences were cloned into the *pBluescriptKS+* (Stratagene, CA). The *GFP2* construct, consisting of the RSV promoter, *GFP* open reading frame of *pHypermut2* (Arakawa et al., 2008), an *IRES* (Arakawa et al., 2004), a *blasticidin resistance gene* and the *SV40* polyadenylation signal (Arakawa et al., 2001), was cloned into the unique *BamHI* restriction sites.

pIgL^{FOI,GFP2}
All reinsertion plasmids were cloned by inserting the PCR amplified fragment of interest (FOI) into pIgL$^{-,GFP2}$ via the unique restriction sites *SpeI/NheI*.

5.1.12 Primer

Oligonucleotides, used for mouse typing, are listed in 5.2 Methods, genotyping.

Oligonucleotides, used for the amplification of reinsertion fragments, are listed in 7 Supplementary Information, List of primers

5.1.13 Software

Statistics	R (http://www.r-project.org/), a freely available program for statistical computing and graphics.
Illustration	Adobe illustrator CS3, Adobe photoshop CS3
Vector design	Clone Manager 9
FACS	CELLQuest (Beckton Dickinson)

5.2 Methods

5.2.1 Vector design of DT40 knock-in cellines

The vector for all knock-in constructs was the pIgL$^{-,GFP2}$ (Blagodatski et al., 2009). The IgL arm sequences were cloned into the *pBluescript II KS (+)* backbone and *GFP2* was inserted into the unique *BamHI* site. *GFP2* contains a chicken β-actin promoter, a SV40 polyA signal, an IRES cassette and a *bsr* drug resistance gene. Unique *NheI* and *SpeI* sites located in the pIgL$^{-,GFP2}$ are used to reinsert IgL fragments.

1 kb reinsertion of IgL	The reinsertion of the complete IgL locus was achieved via pIgL$^{W, GFP2}$. 'W' corresponds to the chicken genome coordinates chr15:8165070-8176699, lacking the region between V and J. The plasmid pIgL$^{W, GFP2}$ was used as precursor for DNA amplification of other IgL fragments. All fragments of this series were inserted into the NheI/SpeI sites of pIgL$^{-, GFP2}$.
1 kb reinsertion of 'S',	All plasmids of the series were designed by inserting the

50 bp end deletion of 'S'	amplified fragments into pIgL$^{-, GFP2}$ *NheI/SpeI* sites. The amplification was performed with primers listed in the supplementary data using pIgL$^{W, GFP2}$ as the precursor.
200 bp internal deletion of 'S'	All plasmids of the series were designed by inserting the amplified fragments into pIgL$^{-, GFP2}$ *NheI/SpeI* sites. The amplification was performed in a two step PCR. In the first PCR two fragments (the 5' fragment and the 3' fragment), flanking the internal deletion, were amplified. The sequence of the reverse primer for the 5' fragment starts with 9 bp complementary to the start of the 3' fragment. Vice versa, the sequence of the forward primer of the 3' fragment starts with 9bp, complementary to the end of the 5' fragment, thereby creating two fragments with an overlapping region of 18 bp. This overlap allowed an annealing of the 5' fragment and the 3' fragment during a second PCR, performed with the forward primer of the 5' fragment and the reverse primer of the 3' fragment. The primers used for this series are listed in the supplementary data.
Multimerization of '2.2-2.4'	The amplified fragments were cloned into the TOPO vector, excised by NheI/Spe/ restriction and successively cloned into pIgL$^{-, GFP2}$.

5.2.2 Standard methods of molecular biology

5.2.2.1 Amplification of knock-in fragments

Fragments for external deletion		**PCR program**		
H_2O	94.5 µl	Denaturation	93°C	2'

Expand Long Buffer I	15 µl	Amplification 34x	93°C	30''
dNTPs (10mM)	3 µl		65°C	30''
Primer for (25mM)	3 µl		68°C	5'*)
Primer rev (25mM)	3 µl	Melting	68°C	7'
Expand Long Polymerase Mix	1.5 µl	Cool	4°C	
DNA (1ng/µl)	15 µl	*) time increases 20 sec each cycle		
Template: pIgL$^{W, GFP2}$				

Fragments for internal deletion		**PCR program**		
H_2O	108.9 µl	Denaturation	93°C	2'
Expand Long Buffer I	15 µl	Amplification 34x	93°C	30''
dNTPs (10mM)	3 µl		65°C	30''
Primer for (25mM)	3 µl		68°C	5'*)
Primer rev (25mM)	3 µl	Melting	68°C	7'
Expand Long Polymerase Mix	1.5 µl	Cool	4°C	
DNA 1 and DNA 2	3 µl	*) time increases 20 sec each cycle		
Template: amplified DNA 1 and DNA 2				

5.2.2.2 Agarose – Gelelectrophoresis

PCR products and restriction-digested DNA fragments were separated on a 0.8-2% (w/v), depending on the fragment size, agarose gel in a gel-electrophoresis chamber (Peqlab) filled with 1xTAE buffer for about 1 hour at 80V. Bands were detected via EtBr treatment and UV light visualization.

TAE buffer: 40 mM Tris/HCl, 20 mM Acetate, 1 mM EDTA, pH 8.5

5.2.2.3 PCR and Gel purification of DNA

PCR amplified products were purified with the Qiagen PCR purification kit according to manufacturer's protocol.

DNA fragments, separated by Gel electrophoresis, were purified from the gel using the Qiagen Gel purification kit according to the manufacturer's protocol.

5.2.2.4 DNA Ligation

The ligation of vector and insert DNA was performed with the Takara Ligation kit according to the manufacturer's protocol. The ligation was kept for 30 min at 16°C.

5.2.2.5 TOPO cloning

The TOPO TA cloning kit (Invitrogen) was used for fragments difficult to clone according to the manual. PCR amplified DNA products were incubated with Taq polymerase and dATPs at 72°C for 20 min to add A-overhangs to the insert DNA. Successfully cloned fragments were excised via *NheI/SpeI* restriction and cloned into the $pIgL^{-,GFP2}$ vector.

5.2.2.6 Transformation

A transformation of plasmid DNA (>1ng) or a ligation mix into 50 µl of *E.coli DH5α* cells was achieved by heat shock. DNA and competent cells were incubated on ice for 20 min, followed by a heat shock at 42°C for 45 seconds followed by 2 minutes on ice. 100 µl of 2YTBroth medium was added an incubated for 30 minutes at 37°C. Afterwards, the bacteria were plated on an agar plate, containing antibiotics, and incubated overnight at 37°C.

5.2.2.7 *E.coli DH5α* competent cell preparation

The DH5α bacteria strain was streaked out on a LB agar plate without antibiotics for single cell separation and incubated overnight at 37°C.
Next day a single cell colony was inoculated in 5 ml SOB Broth and incubated overnight at 37°C.
Next day 2.5 ml of bacteria culture were inoculated into 500 ml SOB broth and incubated at 25°C. One 1 ml of culture was used for OD600 measurement. OD600 measurement was repeated periodically. An OD600 of 0.4 indicates, that bacteria enter the logarithmic growing

scale. Bacteria were cooled immediately on ice and kept on ice for 10 further minutes. The culture was centrifuged at 2000xg for 10 minutes at 4°C. The supernatant was discarded and the cells were gently resuspended in 330 ml ice-cold FTB. The culture was cooled on ice for 10 minutes and centrifuged at 2000xg for 10 minutes at 4°C. The supernatant was discarded and the cells were gently resuspended in 50 ml ice-cold FTB. Afterwards 3.5 ml of DMSO were added. Aliquots of 400 µl were distributed quickly in 1.5 ml tubes and frozen immediately in liquid nitrogen. The cells were kept at -80°C.

The efficiency of competent cells was tested by transforming 1ng of *pBluescript* plasmid to 400 µl of competent cells. Cells were plated in dilution of 1:100, 1:10 and the rest of cells on 3 agar plates. Next day, the titer of competent cells (= number of colonies produced by transformation of 1 µg DNA) was calculated. The titer has to be at least $1x10^6$ colonies.

5.2.2.8 Culture of *E.coli*

E.coli was cultured on LB agar plates in a 37°C incubator or in 2YTBroth medium in a 37°C shaker. Bacteria cultures were stored at -80°C in a dilution 3 vol. culture : 1 vol. 50% glycerol.

5.2.2.9 Plasmid isolation

The plasmid DNA was isolated from 4ml *E.coli* culture using the Fermentas GeneJet™ miniprep kit according the manufacturer's protocol. For large scale plasmid preparation 400ml culture and the Qiagen Maxiprep kit were used.

5.2.2.10 Restriction digestion

A restriction digest of plasmid DNA was performed with 1 µg of DNA according to manufacturer's protocol. The digest was incubated for at least 3 hours and analyzed by gel-electrophoresis.

5.2.2.11 Phenol/Chloroform extraction of DNA

1 vol. of water saturated phenol/chloroform (1:1) was added to plasmid or restricted DNA and mixed vigorously. The sample was centrifuged at 15000 rpm for 5 min at 4°C. The upper aqueous phase, containing the DNA, was transferred to a new tube. The lower organic phase and interface, containing proteins, was discarded. 1 vol of water saturated chloroform was added to the DNA, mixed and centrifuged at 15000 rpm for 5 min at 4°C. The upper aqueous phase was transferred to a new tube and supplemented with an equal amount of isopropanol and 0.1 vol 3M NaOAc. The sample was mixed vigorously and centrifuged at 15000 rpm for 30 min at 4°C. The pellet was washed with 70% ethanol and centrifuged for additional 5 minutes. The pellet was air-dried for 1 hour and dissolved in 1xTE or milliQ water.

5.2.2.12 Determination of DNA concentration

The calculation of DNA concentration was done by UV photospectrometry at wavelength 260 nm which equates to the DNA absorbance maximum wavelength.

5.2.2.13 Sequencing

Sequencing reaction (Big Dye Terminator v3.1 BD)		**PCR program**	
DMSO	0.5 µl	96°C	4’
DEPC H_2O	4.1 µl	95°C	30’’
5x buffer BDT	1 µl	50°C	20’’
BDT	2 µl	60°C	4’
Primer (0.25 µM)	0.4 µl	4°C	∞
Template	2 µl		

After the PCR reaction (manufacturer’s instruction), the DNA had to be purified. 2.5 µl of 125 mM EDTA were added to each PCR reaction and the PCR plate was centrifuged at 900xg for 2 min. 30 µl of 100% Ethanol was added and incubated for 15 minutes at room temperature. Afterwards the plate was centrifuged at 2000xg for 30 minutes at 4°C. The supernatant was discarded by quick spinning the plate upside down. The DNA pellet was washed with 50 µl

70% Ethanol. The supernatant was again removed by quick spinning. The pellet was dried at 70°C for 10 minutes. The DNA pellet was dissolved in 30 µl water and transferred to a sequencing plate.

5.2.3. Cell culture of DT40

5.2.3.1. Basic cell culture conditions of DT40

The optimum culture conditions for DT40 are 41°C with 5% CO_2 and a cell density of 10^6cells/ml. DT40 cells were cultured in flasks, 6-, 24- and 96-well plates in chicken medium (see Material, Media).

5.2.3.2 DT40 cell freeze and thaw

DT40 cells were centrifuged for 5 min at 500xg. 10^7 cells were resuspended in 1 ml freezing medium (70% RPMI, 20% FCS, 10% DMSO) and transferred to freezing vials. Vials were wrapped in tissue to guarantee a slow freezing at -80°C. Next day, cells were transferred to liquid nitrogen for longer storage.
Cells taken from liquid nitrogen were thawed quickly at 41°C. Cells were transferred to 5 ml chicken medium, to dilute the toxic DMSO, and centrifuged at 500xg for 5 minutes. The cells were resuspended in chicken medium and transferred to a culture flask.

5.2.3.3 Transfection of DT40 cells

300 µg of linearized, phenol/chloroform purified plasmid were resuspended in 300 µl water under sterile conditions. 10^7 cells were diluted in 800 µl chicken medium transferred to an electroporation cuvette and supplemented with 40 µg linearized DNA. The electroporation was performed at 25 µF and 700 V.
The electroporated cells were diluted in 10 ml chicken medium and distributed equally (100 µl) to a 96-well plate. Next day (12h after transfection), 100 µl of 2x selection medium were added to each well. 7 to 10 days after transfection, 10 µl of drug resistant colonies were

transferred to 250 µl chicken medium in a 96-well plate for further analysis of targeted integration.

5.2.3.4 Genomic DNA isolation of DT40 cells

100 µl of cell suspension were transferred to a 96 well PCR plate, washed with PBS and centrifuged at 500xg for 5 min. The pellet was resuspended in 10 µl K buffer (1x PCR buffer, 0.1 mg/ml proteinase K, 0.5% Tween20). For proteolysis, the mixture was incubated for 45 min at 56°C and afterwards at 95°C for 10 min to inactivate the proteinase K. This crude extract was used for PCR validation of targeted integration.

5.2.3.5 Validation of targeted integration

The cell line $\psi V^{-}IgL^{-}$ was used for all reinsertion experiments and had a puromycin resistance gene inserted at the deleted IgL position. The transfection of fragment leads to homologues recombination and the deletion of the resistance cassette and therewith to a sensitivity for puromycin. Therefore, all transfected clones were tested for puromycin resistance. 100 µl of cell culture were transferred to a 96 well plate containing 100 µl of 2x puromycin solution (final concentration 1 µg/ml). Puromycin sensitve clones were selected from stock plates and tested in PCR for targeted integration.

To analyze whether the construct was inserted only in the rearranged Ig locus two different PCR approaches were performed. In the first approach, one primer is located in the genome upstream the 5' target arm und the second primer is located in the reporter construct, thereby verifying a targeted integration in the Ig locus. In the second approach the primers were located in the intervening sequence between V and J, which is only present in the non-rearranged Ig locus. If this sequence is not detectable after the PCR reaction it indicates an integration of the construct into the non-rearranged Ig locus and the clone had to be excluded from further analyses.

Targeted integration		**PCR program**		
H_2O	6.3 µl	Denaturation	93°C	2'

Expand Long Buffer I	1 µl	Amplification 34x	93°C	30''
dNTPs (10mM)	0.2 µl		65°C	30''
Primer for (25mM)	0.2 µl		68°C	5'*)
Primer rev (25mM)	0.2 µl	Melting	68°C	7'
Expand Long Polymerase Mix	0.07 µl	Cool	4°C	
Crude extract	1 µl	*) time increases 20 sec each cycle		
Template: Crude extract of genomic DNA				

5.2.3.6 Subcloning of DT40 clones

Subcloning by limited dilution was performed to achieve a single cell population of a heterogeneous bulk population. Cells were diluted to a concentration of either 3, 1 and 0.3 cells per well and distributed on 96 well plates. After incubation for 7 days without medium exchange, colonies could be transferred to a 24 well plate. The 24 subclones were analyzed by FACS after 14 days.

5.2.3.7 FACS analysis of DT40 cells

Cell lines, which tested positive for targeted integration were analyzed for GFP expression by FACS. 250 µl of each cell suspension were centrifuged at 500xg for 5 min at 4°C. Cells were washed with PBS and resuspended in 250 µl PBS. During the FACS analysis, 5000 living cells were detected. Living cells were separated from dead cells by gating on FSC^{high} SSC^{high} cells.

5.3 Mouse analysis of knock-out mice

5.3.1 Mouse breeding

LMP1/$CD40^{flstop}$ $CD19^{Cre/+}$ $NEMO^{fl/fl}$ mice, referred to as NEMOko LMP1/CD40 mice, were achieved by crossing heterozygous LMP1/$CD40^{flstop}$ $CD19^{Cre/+}$ (BALB/c) mice with $NEMO^{fl/fl}$ (C57BL/6) mice. LMP1/$CD40^{flstop}$ $CD19^{Cre/+}$ $IKK2^{fl/fl}$ mice, referred to as IKK2ko LMP1/CD40 mice, were generated by crossing heterozygous LMP1/$CD40^{flstop}$ $CD19^{Cre/+}$ (BALB/c) mice with $IKK2^{fl/fl}$ (C57BL/6) mice. Mouse analyses were performed on mixed background 8-16 weeks

after birth. All mice were bred and kept under pathogen-free conditions. All experiments were performed with the sanction of the German animal welfare law and the institutional committee on animal experimentation.

5.3.2 Mouse tail genomic DNA preparation

Mouse tail tips were lysed in 500 µl lysis buffer including freshly added Proteinase K (100 µg/ml) at 56°C for at least four hours in a thermomixer at 800 rpm. 170 µl saturated (5M) NaCl were added and the sample was centrifuged for 10 minutes at 10000xg to precipitate the protein fraction. The supernatant was transferred to a new tube containing 600 µl 100% Isopropanol to precipitate the DNA. After inverting the tube several times the sample was centrifuged 10 minutes at 10000xg. The supernatant was removed and the DNA pellet was washed with 70% Ethanol. The sample was again centrifuged and the Ethanol was removed carefully with a pipette tip. After drying the DNA at 37°C for at least one hour, the DNA pellet was dissolved in 100 µl TrisHCl buffer by shaking at 37°C.

Lysis buffer: 100 mM Tris/HCl pH 8, 5 mM EDTA, 0.2% SDS, 200 mM NaCl

5.3.3 Genotyping

To detect the murine genotype, different PCRs were performed.

LMP1/CD40		**PCR program**		
H_2O	18.65 µl	Denaturation	95°C	2’30’’
Taq Buffer	2.5 µl	Amplification 31x	94°C	45’’
$MgCl_2$ (50mM)	1 µl		55°C	45’’
dNTPs (10mM)	0.5 µl		72°C	1’15’’
Primer LMP1ex1fw1	0.1 µl	Melting	70°C	10’
Primer CD40 PCR3	0.1 µl	Cool	4°C	
Taq Pol	0.15 µl			
DNA	1 µl			

CD19Cre		**PCR program**		
H_2O	18.6 µl	Denaturation	95°C	2’30’’
Taq Buffer	2.5 µl	Amplification 29x	94°C	45’’
$MgCl_2$ (50mM)	1 µl		59°C	45’’
dNTPs (10mM)	0.5 µl		72°C	2’
Primer CD19c	0.25 µl	Melting	70°C	10’
Primer CD19d	0.25 µl	Cool	4°C	
Primer CD19Cre	0.25 µl			
Taq Pol	0.15 µl			
DNA	1 µl			

Rosa26		**PCR program**		
H_2O	18.15 µl	Denaturation	95°C	5’
Taq Buffer	2.5 µl	Amplification 33x	94°C	45’’
$MgCl_2$ (50mM)	1.5 µl		58°C	45’’
dNTPs (10mM)	0.5 µl		72°C	1’
Primer 60	0.1 µl	Melting	70°C	10’
Primer 62	0.1 µl	Cool	4°C	
DMSO	0.75 µl			
Taq Pol	0.15 µl			
DNA	1 µl			

NEMOfl/fl		**PCR program**		
H_2O	18.1 µl	Denaturation	94°C	2’
Taq Buffer	2.5 µl	Amplification 36x	94°C	45’’
$MgCl_2$ (50mM)	0.5 µl		58°C	45’’
dNTPs (10mM)	0.5 µl		72°C	1’15’’
Primer NEMOfwd	0.25 µl	Melting	70°C	10’
Primer NEMOrev	0.25 µl	Cool	4°C	
Primer NEMOdel	0.25 µl			
Taq Pol	0.15 µl			

DNA	1 µl

IKK2fl/fl		**PCR program**		
H_2O	18.22 µl	Denaturation	95°C	2’30’’
Taq Buffer	2.5 µl	Amplification 34x	94°C	45’’
$MgCl_2$ (50mM)	1 µl		58°C	45’’
dNTPs (10mM)	1 µl		72°C	1’15’’
Primer M96	0.21 µl	Melting	70°C	10’
Primer M97	0.21 µl	Cool	4°C	
Primer M98	0.21 µl			
Taq Pol	0.15 µl			
DNA	1 µl			

Primer	
LMP1ex1fw1	AGGAGCCCTCCT TGTCCTCTA
CD40PCR3	CTGAGATGCGACTCTCTTTGCCAT
Primer 60	CTCTCCCAAAGTCGCTCTG
Primer 62	TACTCCGAGGCGGATCACAAGC
CD19c	AACCAGTCAACACCCTTCC
CD19d	CCAGACTAGATACAGACCAG
CD19Cre	TCAGCTACACCAGAGACGG
NEMOfwd (29)	TTCTTGGAAGGGTATGGCCAG
NEMOrev (30)	TCCGGGCTTCCTGGAATTT
NEMOdel (31)	GGCCTCACACAAGCAAAGCAT
M96 (26)	GTTCAGAGGTTCAGTCCATTATC
M97 (27)	TAGCCTGCAAGAGACAATACG
M98 (28)	TCCTCTCCTCGTCATCCTTCG

5.3.4 Mouse sacrifice and organ removal

The mice were sacrificed by CO_2 gas and organs were isolated under sterile conditions. To educe cells from the peritoneal cavity, the cavity was rinsed with 5% (v/v) FCS B cell medium, which was withdrawn by a syringe. Inguinal lymph nodes and spleens were isolated as complete organs. Pending further processing the lymph nodes were kept in 5% (v/v) medium, the spleens in 1% (v/v) FCS B cell medium. Bone marrow cells were prepared by rinsing the femur with 5% (v/v) FCS B cell medium.

5.3.5 Isolation of primary lymphocytes

The murine spleen and the inguinal lymph nodes were passed through a 70 µm mesh strainer to produce a single cell suspension. The red blood cells in the cell suspensions from spleen, lymph nodes and bone marrow had to be lysed in lysis buffer (manufactorer's manual) for three minutes at room temperature. Splenic B cells were isolated by CD43 depletion via Magnetic Cell Separation (MACS) according to Miltenyi's isolation protocol.

Cell strainer (BD Bioscience), Red blood cell lysis buffer (Mitenyi), CD43 beads (Miltenyi), MACS buffer (Miltenyi).

5.3.6 FACS analysis of primary murine B-cells

Fluorescence activated cell sorting (FACS) was performed on a FACSCalibur™ (BD Bioscience). Cells were washed with MACS buffer and stained for 20 minutes in an adequate concentration of monoclonal antibodies, coupled to FITC, PE, PercP or APC (BD Bioscience). $3x10^4$ viable cells, detected by forward/sideward scatter and TOPRO-3 (Molecular probes) staining, were recorded and analyzed with CellQuest™ software.

Antibody	concentration	Antibody	concentration
AA4.1-PE	1/200	CD44-APC	1/400
B220-FITC	1/200	CD5-APC	1/300
B220-PE	1/600	CD62L-FITC	1/200
B220-PercP	1/100	CD8-PerCP	1/50

B220-APC	1/200	CD86-FITC	1/300
CD21-FITC	1/400	CD95-PE	1/200
CD23-Bio	1/200	IgD-Bio	1/300
CD23-PE	1/200	ICAM-FITC	1/200
CD3-PE	1/200	IgM-APC	1/200
CD4-PE	1/200	IgM-FITC	1/50
CD4-FITC	1/1000	SA-PercP	1/100
CD43-FITC	1/100		

5.3.7 Intracellular FACS of primary murine B cells

Intracellular staining of B cells was performed with the Cytofix/Cytoperm^{TM} Fixation/Permeabilization Kit (BD Bioscience) according to the company's protocol. Notwithstanding with the protocol has been the permeabilization time raised to at least one hour and the staining temperature, changed from 4°C to room temperature.

5.3.8 Protein extraction of splenic B cells

After MACS isolation of B cells and resting for one hour at 37°C in 1% FCS B Cell Medium, proteins were extracted. $5x10^6$ cells were washed once with ice-cold PBS. Afterwards 20 µl 2xNP40 buffer, containing freshly added proteinase- and phosphatase-inhibitor, were added without resuspension and the cells were vortexed 20 minutes at 4°C. To separate the proteins from DNA and cell debris, the samples were centrifuged >12000g for 15 minutes at 4°C. Protein extracts were stored at -80°C.

2xNP40 buffer: 100 mM Tris pH 7.4, 300 mM NaCl, 4mM EDTA, 2% NP40 (v/v), 20% proteinase inhibitor (v/v) (Mini Complete, Roche), 2% phosphatase inhibitor (v/v) (Halt phosphatase inhibitor cocktail, Pierce).

5.3.9 Nuclear fractionation of splenic B cells

After MACS isolation of B cells and resting one hour at 37°C in 1% B-Cell Medium, nuclear fractionation was performed. $2x10^7$ cells were washed once with ice-cold PBS, resuspended in 100 µl buffer A, supplemented freshly with DTT and proteinase-inhibitor, and incubated on ice for 15 minutes. 6.75 µl 10% NP40 were added and the sample was vortexed for 5 minutes at 4°C. To separate the cell nuclei from the cytoplasm, the sample was centrifuged at maximal speed for 10 minutes. The cytoplasm (supernatant) was transferred to a new tube and stored at -80°C. The nuclei were washed in buffer A and resuspended in 40 µl buffer C by vortexing for 30 minutes at 4°C. To separate nuclear proteins from cell debris and DNA, the sample was centrifuged at maximal speed for 10 minutes at 4°C. Nuclear proteins were stored at -80°C.

Buffer A (10 mM HEPES pH 7.9, 10 mM KCl, 0.1 mM EDTA, 0.1 mM EGTA, 1 mM DTT, 1x protease inhibitors).
Buffer C (20 mM HEPES pH 7.9, 0.4 M NaCl, 1 mM EDTA, 1 mM EGTA, 1 mM DTT, 1x protease inhibitors).

5.3.10 Immunoblotting

The protein concentration was detected using the Bradford reagent and an albumin calibration curve. 10-20 µg of protein solution supplemented with 5x Laemmli buffer (300 mM Tris pH 6.8, 7.5% SDS (w/v), 50% Glycerin (v/v), 0.01% bromphenol blue, 1% β-Mercaptoethanol) were denaturated at 70°C for 10 minutes. Proteins were loaded onto a SDS polyacrylamide gel and separated according to size by gel electrophoresis. A protein standard was used to determine protein sizes (Benchmark™, Invitrogen). The gel-running was performed in a Bio-Rad elecrophoresis chamber using Laemmli running buffer (25 mM Tris base, 0.2 M glycine, 0.1% SDS). The electrophoresis of the gel, consisting of a stacking gel (5% acrylamide (v/v), 0.625 mM Tris pH6.8, 0.1% SDS (w/v), 0.1% APS (w/v), 0.006% TEMED (w/v)) and a resolving gel (12% acrylamide (v/v), 3.75mM Tris pH 8.8, 0.1% SDS (w/v), 0.1% APS (w/v), 0.004% TEMED (w/v)), was carried out at 20-40 mA depending on the number of gels. After the separation the resolving gel was transferred on a polyvinylidenfluoride (PVDF) membrane (Immobilon™ P membrane, Millipore) and blotted in a transfer buffer (25 mM Tris base, 0.2 M glycine, 20% Methanol (v/v)) using a Bio-Rad mini tank blotting chamber for 2 hours at 250 mA. Afterwards, the membrane was incubated in Ponceau S to stain the proteins loaded on the gel and to control for an equal loading. To

avoid unspecific binding of antibodies the membrane was blocked with TBST (TBS: 0.1 M Tris/HCl pH 7.5, 0.1 M NaCl; Tween 0.02% (v/v)) 5% BSA (w/v) for at least one hour or over night at 4°C. The primary antibody was incubated in TBST 5% BSA (w/v) or TBST 5% milk powder (w/v) according the protocol for 2 hours or at 4°C overnight. The membrane was washed three times with TBST for 5 minutes. Then the membrane was incubated in the secondary antibody in TBST 1% milk powder (w/v) for 1.5 hours and washed three times in TBST. To detect proteins, the membrane was covered with ECL™ detection reagent (GE healthcare) for 1 minute. Chemiluminescence was detected by exposing the membrane to a photosensitive film (CEA RP nem, Ernst Christiansen) and developing the film in a processor. To probe the membrane with antibodies of similar size, the membrane was stripped in between with stripping buffer (62.5 mM Tris/HCl pH 6.8, 2% SDS (w/v), 100 mM β-Mercaptoethanol) for 30 minutes at 56°C.

5.3.11 *Ex vivo* survival test

For a B cell survival assay, B cells were isolated via CD43 depletion and diluted in 10% FCS B cell medium to the concentration $5x10^6$ cells/ml. The cells were cultured for 5 days in a 96 well plate ($5x10^5$ cells/well). TOPRO-3 binds to the DNA and was used to stain for dead cells. The cell number and TOPRO-3 negative cells were detected by FACSCalibur™.

5.3.12 *Ex vivo* proliferation test

For a B cell proliferation assay, isolated B cells were stained in FCS free medium with 5 µM 5-(and 6)-carboxyfluorescein diacetate N-succinimidyl ester (CFSE) (Molecular Probes) for 5 min at 37°C. CFSE binds to proteins on the inner membrane and is distributed equally to the daughter cells with every cell division. The reaction was stopped with 10% B cell medium and cells were cultured in a concentration of $5x10^5$ cells/well for 5 days. The cell number and CFSE negative cells were detected by FACSCalibur™.

5.3.13 Immunohistochemistry

For the immunohistochemistry of spleens, a section of the spleen of approximately 5 mm was embedded in O.C.T. Tissue Tek (Sakura), frozen in liquid nitrogen for a few seconds and stored at -20°C. For storage, the spleen was wrapped in aluminium foil to avoid oxygen contact. Using a cryostat (Leica Microsystems), sections of 6 µm thickness were cut, fixed on a cryo microscope slide and stored at -20°C. Before staining, the sections were thawed and dried for 30 minutes at RT and fixed in 100% (v/v) Acetone for 5 minutes at -20°C. Afterwards, the sections were washed with PBS and incubated for 20 minutes in quenching buffer (PBS containing 10 % (v/v) goat serum, 0.1 % (v/v) H_2O_2, 1 % (w/v) BSA) to block non-specific antibody binding. In the next step, the sections were incubated in two different blocking buffers (Avidin/Biotin Blocking Kit; Vector Laboratories) for 15 minutes each. Between all blocking and staining steps, the sections were washed three times for 5 minutes in PBS. All incubations were performed at RT in a humidified chamber. The sections were incubated with antibodies either coupled to streptavidin or peroxidase for 1 hour. The antibody development occurred via treatment with Blue Alkaline Phosphatase
Substrate Kit III (Vector laboratories) or with Red Peroxidase Substrate Kit AEC (3-amino-9-ethylcarbazole) (Vector laboratories). The staining was stopped by washing with PBS. The sections were air-dried and embedded in gelatine. The slides were stored at RT in the dark and analyzed by a fluorescent microscope (Zeiss). Pictures were taken by a digital camera (RS Photometrics).

Antibody/Reagent	Source	Conjugate	Dilution	Manufactor
α-Mouse IgM	Goat	Peroxidase	1:100	Sigma (A-8786)
α-MOMA-1 IgG2	Rat		1:100	Biomedicals (T-2011)
α–rat IgG2	Mouse	Bio	1:250	Jackson (212-066-082)
Streptavidin-Alkaline Phosphatase				Sigma (S-2890)

6. References

Agathanggelou A., Niedobitek G., Chen R., Nicholls J., Yin W. and Young L. (1995). Expression of immune regulatory molecules in Epstein-Barr virus-associated nasopharyngeal carcinomas with prominent lymphoid stroma. Evidence for a functional interaction between epithelial tumor cells and infiltrating lymphoid cells. Am J Pathol *147(4)*, 1152-1160.

Agrawal A. and Schatz D. (1997). RAG1 and RAG2 form a stable postcleavage synaptic complex with DNA containing signal ends in V(D)J recombination. Cell *89*, 43-53.

Aldinucci D., Poletto D., Nanni P., Degan M., Rupolo M., Pinto A. and Gattei V. (2002). CD40L induces proliferation, self-renewal, rescue from apoptosis, and production of cytokines by CD40-expressing AML blasts. Exp Hematol *30(11)*, 1283-1292.

Alt F., Yancopoulos G., Blackwell T., Wood C., Thomas E., Boss M., Coffman R., Rosenberg N., Tonegawa S., Baltimore D. (1984). Ordered rearrangement of immunoglobulin heavy chain variable region segments. EMBO J. *3(6)*, 1209-1219.

Altenburg A., Baldus S., Smola H., Pfister H. and Hess S. (1999) CD40 ligand-CD40 interaction induces chemokines in cervical carcinoma cells in synergism with IFN-gamma. J Immunol *162(7)*, 4140-4147.

Arakawa H., Saribasak H. and Buerstedde J. (2004). Activation-induced cytidine deaminase initiates immunoglobulin gene conversion and hypermutation by a common intermediate. PLoS Biol. *2(7)*, E179.

Arakawa H. (2006). Immunoglobulin gene conversion and hypermutation assay by FACs. Subcell Biochem. *40*, 351-352.

Arakawa H., Kudo H., Batrak V., Caldwell R., Rieger M., Ellwart J. and Buerstedde J. (2008) Protein evolution by hypermutation and selection in the B cell line DT40. Nucleic Acids Res. *36(1)*:e1.

Arenzana-Seisdedos F., Turpin P., Rodriguez M., Thomas D., Hay R., Virelizier J. and Dargemont C. (1997). Nuclear localization of I kappa B alpha promotes active transport of NF-kappa B from the nucleus to the cytoplasm. J Cell Sci *110 (Pt 3)*, 369-378.

Baba T. and Humphries E. (1985). Formation of a transformed follicle is necessary but not sufficient for development of an avian leukosis virus-induced lymphoma. Proc Natl Acad Sci U S A *82(1)*, 213-216.

Banchereau J., Brière F., Liu Y. and Rousset F. (1994). Molecular control of B lymphocyte growth and differentiation. Stem Cells *12(3)*, 278-288.

Barreto V., Reina-San-Martin B., Ramiro A., McBride K. and Nussenzweig M. (2003). C-terminal deletion of AID uncouples class switch recombination from somatic hypermutation and gene conversion. Mol Cell *12(2)*, 501-508.

Barrett T., Shu G. and Clark E. (1991). CD40 signaling activates CD11a/CD18 (LFA-1)-mediated adhesion in B cells. J Immunol *146(6)*, 1722-1729.

Beale R., Petersen-Mahrt S., Watt I., Harris R., Rada C. and Neuberger M. (2004). Comparison of the differential context-dependence of DNA deamination by APOBEC enzymes: correlation with mutation spectra in vivo. J Mol Biol *337(3)*, 585-596.

Beinke S., Robinson M., Hugunin M. and Ley S. (2004). Lipopolysaccharide activation of the TPL-2/MEK/extracellular signal-regulated kinase mitogen-activated protein kinase cascade is regulated by IkappaB kinase-induced proteolysis of NF-kappaB1 p105. Mol Cell Biol *24(21)*, 9658-9667.

Besmer E., Market E. and Papavasiliou F. (2006). The transcription elongation complex directs activation-induced cytidine deaminase-mediated DNA deamination. Mol Cell Biol *26(11)*, 4378-4385.

Betz A., Neuberger M and Milstein C. (1993). Discriminating intrinsic and antigen-selected mutational hotspots in immunoglobulin V genes. Immunol Today *14(8)*, 405-411.

Bishop G., Moore C., Xie P., Stunz L. and Kraus Z. (2007). TRAF proteins in CD40 signaling. Adv Exp Med Biol *597*, 131-151.

Blagodatski A., Batrak V., Schmidl S., Schoetz U., Caldwell R., Arakawa H. and Buerstedde J. (2009). A cis-acting diversification activator both necessary and sufficient for AID mediated hypermutation. PLoS Genet. 5(1):e1000332. Epub 2009 Jan 9.

Bonizzi G. and Karin M (2004). The two NF-kappaB activation pathways and their role in innate and adaptive immunity. Trends Immunol *25(6)*, 280-288.

Bourgeois C., Rocha B. and Tanchot C. (2002). A role for CD40 expression on CD8+ T cells in the generation of CD8+ T cell memory. Science *297(5589)*, 2060-2063.

Brandsteitter R., Pham P., Scharff M. and Goodman M. (2003). Activation-induced cytidine deaminase deaminates deoxycytidine on single-stranded DNA but requires the action of RNase. Proc Natl Acad Sci USA *100(7)*, 4102-4107.

Bren G., Solan N., Miyoshi H., Pennington K., Pobst L. and Paya C. (2001) Transcription of the RelB gene is regulated by NF-kappaB. Oncogene *20(53)*, 7722-7733.

Buerstedde J., Reynaud C., Humphries E., Olson W., Ewert D. and Weill J. (1990). Light chain gene conversion continues at high rate in an ALV-induced cell line. EMBO J. *9(3)*, 921-927.

Buerstedde J. and Takeda S. (1991). Increased ratio of targeted to random integration after transfection of chicken B cell lines. Cell *67(1)*, 179-188.

Callard R., Armitage R., Fanslow W. and Spriggs M. (1993). CD40 ligand and its role in X-linked hyper-IgM syndrome. Immunol Today. *14(11)*, 559-564.

Cariappa A., Liou H., Horwitz H. and Pillai S. (2000). Nuclear factor □B is required for the development of marginal zone B lymphocytes. J. Exp. Med. *192*, 1175-1182.

Carlson L., McCormack W., Postema C., Humphries E. and Thompson C. (1990). Templated insertions in the rearranged chicken IgL V gene segment arise by intrachromosomal gene conversion. Genes Dev *4(4)*, 536-547.

Chaudhuri J., Tian M., Khuong C., Chua K., Pinaud E. and Alt F. (2003). Transcription-targeted DNA deamination by the AID antibody diversification enzyme. Nature *422(6933)*, 726-730.

Chaudhuri J., Khoung C. and Alt F. (2004). Replication protein A interacts with AID to promote deamination of somatic hypermutation targets. Nature *430(7003)*, 992-998.

Chen L., Fischle W., Verdin E. and Greene W. (2001). Duration of Nuclear NF-κB Action Regulated by Reversible Acetylation. Science *293(5535)*, 1653 – 1657.

Chesi M., Robbiani D., Sebag M., Chng W., Affer M., Tiedemann R., Valdez R., Palmer S., Haas S., Stewart A., Fonseca R., Kremer R., Cattoretti G. and Bergsagel P. (2008). AID-dependent activation of a MYC transgene induces multiple myeloma in a conditional mouse model of post-germinal center malignancies. Cancer Cell *13(2)*, 167-180.

Cohen S. and Porter R. (1964). Structure and biological activity of immunoglobulins. Adv Immunol. *27*, 287-349.

Conticello S., Thomas C., Petersen-Mahrt S. and Neuberger M. (2005). Evolution of the AID/APOBEC family of polynucleotide (deoxy)cytidine deaminases. Mol Biol Evol *22(2)*, 367-377.

Cooper M., Peterson R., South M. and Good R. (1966). The functions of the thymus system and the bursa system in the chicken. J Exp Med *123(1)*, 75-102.

Das S., Cho J., Lambertz I., Kelliher M., Eliopoulos A., Du K. and Tsichlis (2005). Tpl2/Cot Signals Activate ERK, JNK, and NF-kB in a Cell-type and Stimulus- specific Manner. J Biol. Chem. *280(25)*, 23748-23757.

Davies C., Mak T., Young L. and Eliopoulos (2005). TRAF6 is required for TRAF2-dependent CD40 signal transduction in nonhemopoietic cells. Mol Cell Biol *25(22)*, 9806-9819.

Déchanet J., Grosset C., Taupin J., Merville P., Banchereau J., Ripoche J. and Moreau J. (1997). CD40 ligand stimulates proinflammatory cytokine production by human endothelial cells. J Immunol *159(11),* 5640-5647.

Dedeoglu F., Horwitz B., Chaudhuri J., Alt F. and Geha R. (2004). Induction of activation-induced cytidine deaminase gene expression by IL-4 and CD40 ligation is dependent on STAT6 and NFkappaB. Int Immunol *16(3)*, 395-404.

de Jong S., Albrecht J., Schmidt M., Müller-Fleckenstein I. and Biesinger B. (2010). Activation of noncanonical NF-kappaB signaling by the oncoprotein Tio.J Biol Chem. *285(22)*, 16495-16503.

Dickerson S., Market E., Besmer E. and Papavasilou F. (2003). AID mediates hypermutation by deaminating single stranded DNA. J Exp Med *197(10)*, 1291-1296.

Dobrzanski P., Ryseck R. and Bravo R. (1995). Specific inhibition of RelB/p52 transcriptional activity by the C-terminal domain of p100. Oncogene *10(5)*, 1003-1007.

Durandy A., Revy P., Imai K. and Fischer A. (2005). Hyper-immunoglobulin M syndromes caused by intrinsic B-lymphocyte defects. Immunol Rev *203*, 67-79.

Early P., Huang H., Davis M., Calame K. and Hood L. (1980), An immunoglobulin heavy chain variable gene is generated from three segments of DNA: VH, D, and JH. Cell 19, 981-992.

Ehrlich A. and Kuppers R. (1995). Analysis of immunoglobulin gene rearrangements in single B cells. Curr Opin Immunol *7*, 281-284.

Eliopoulos A. and Young L. (2001) LMP1 structure and signal transduction. Semin Cancer Biol. *11(6)*, 435-444.

Eliopoulos A., Wang C., Dumitru C. and Tsichlis P. (2003). Tpl2 transduces CD40 and TNF signals that activate ERK and regulates IgE induction by CD40. EMBO *22(15)*, 3855-3864.

Fu Y. and Chaplin D. (1999). Development and maturation of secondary lymphoid tissues. Annu Rev Immunol *17*, 399-433.

Gallagher N., Eliopoulos A., Agathangelo A., Oates J., Crocker J. and Young L**.** (2002). CD40 activation in epithelial ovarian carcinoma cells modulates growth, apoptosis, and cytokine secretion. Mol Pathol *55(2)*, 110-120.

Gordon M., Kanegai C., Doerr J. and Wall R. (2003). Somatic hypermutation of the B cell receptor genes B29 (Igbeta, CD79b) and mb1 (Igalpha, CD79a). Proc Natl Acad Sci U S A *100(7)*, 4126-4131.

Ghosh S., May M. and Kopp E. (1998). NF-kappa B and Rel proteins: evolutionarily conserved mediators of immune responses**.** Annu Rev Immunol. *16*, 225-260.

Gosh S. and Karin M. (2002). Missing pieces in the NF-κB puzzle. Cell 109, 81-96.

Grayson J. Bassel-Duby R. and Williams R. (1998). Collaborative interactions between MEF-2 and Sp1 in muscle-specific gene regulation. J Cell Biochem. *70(3)*, 366-375.

Gu Z., Jin S., Gao Y., Weaver D. and Alt F. (1997). Ku70-deficient embryonic stem cells have increased ionizing radiosensitivity, defective DNA end-binding activity, and instability to support V(D)J recombination. Proc Natl Acad Sci USA *94*, 8076-8081.

Hardy R., Carmack C., Shinton S., Kemp J. and Hayakawa K. (1991). Resolution and characterization of pro-B and pre-pro-B cell stages in normal mouse bone marrow. J Exp Med *173*, 1213-1225.

Hatzivassiliou E., Miller W., Raab-Traub N., Kieff E. and Mosialos G. (1998). A Fusion of the EBV Latent Membrane Protein-1 (LMP1) Transmembrane Domains to the CD40 Cytoplasmic Domain Is Similar to LMP1 in Constitutive Activation of Epidermal Growth Factor Receptor Expression, Nuclear Factor-□B, and Stress-Activated Protein Kinase. The Journal of Immunology *(160)*, 1116-1121.

Hayward A., Levy J., Facchetti F., Notarangelo L., Ochs H., Etzioni A., Bonnefoy J., Cosyns M. and Weinberg A (1997). Cholangiopathy and tumors of the pancreas, liver, and biliary tree in boys with X-linked immunodeficiency with hyper-IgM. J Immunol *158(2)*, 977-983.

He J., Saha S., Kang J., Zarnegar B., Cheng G. (2007). Specificity of TRAF3 in its negative regulation of the noncanonical NF-kappa B pathway. J Biol Chem *282(6)*, 3688-3694.

Heissmeyer V., Krappmann D., Hatada E. and Scheidereit C. (2001). Shared pathways of IkappaB kinase-induced SCF(betaTrCP)-mediated ubiquitination and degradation for the NF-kappaB precursor p105 and IkappaBalpha. Mol Cell Biol *21(4)*, 1024-1035.

Hoffmann A., Levchenko A., Scott M. and Baltimore D. (2002). The IkappaB-NF-kappaB signaling module: temporal control and selective gene activation. Science *298(5596)*, 1241-1245.

Hojer C. (2009). Mechanisms of B cell activation and lymphomagenesis. Dissertation LMU Munich.

Hömig-Hölzel C., Hojer C., Rastelli J., Casola S., Strobl L., Müller W., Quintanilla-Martinez L., Gewies A., Ruland J., Rajewsky K. and Zimber-Strobl U. (2008) Constitutive CD40 signaling in B cells selectively activates the noncanonical NF-kappaB pathway and promotes lymphomagenesis. J Exp Med *205(6)*, 1317-1329.

Hostager B., Haxhinasto S., Rowland S. and Bishop G. (2003). Tumor necrosis factor receptor-associated factor 2 (TRAF2)-deficient B lymphocytes reveal novel roles for TRAF2 in CD40 signaling. J Biol Chem *278(46)*, 45382-45390.

Hozumi N and Tonegawa S. (1976). Evidence for somatic rearrangement of immunoglobulin genes coding for variable and constant regions. Proc Natl Acad Sci USA *73*, 3628-3632.

Hu Y., Baud V., Delhase M., Zhang P., Deerinck T., Ellisman M., Johnson R. and Karin M. Abnormal morphogenesis but intact IKK activation in mice lacking the IKKalpha subunit of IkappaB kinase. Science *284(5412)*, 316-320.

Ito S., Nagaoka H., Shinkura R., Begum N., Muramatsu M., Nakata M. and Honjo T. (2004). Activation-induced cytidine deaminase shuttles between nucleus and cytoplasm like apolipoprotein B mRNA editing catalytic polypeptide 1. Proc Natl Acad Sci USA *101(7)*, 1975-1980.

Jabara H., Fu S., Geha R. and Vercelli D. (1990). CD40 and IgE: synergism between anti-CD40 monoclonal antibody and interleukin 4 in the induction of IgE synthesis by highly purified human B cells. J Exp Med *172(6)*, 1861-1864.

Janeway C., Travers P., Walport M. and Shlomchik M. (2002). Immunologie. 5. Auflage Spektrum, Akad. Verl. 2002, ISBN 3-8274-1079-7.

Kaisho T., Takeda K., Tsujimura T., Kawai T., Nomura F., Terada N. and Akira S. (2001). IkappaB kinase alpha is essential for mature B cell development and function. J Exp Med. *193(4)*, 417-426.

Karin M, Ben-Neriah Y. (2000). Phosphorylation meets ubiquitination: the control of NF-[kappa]B activity. Annu Rev Immunol *18*, 621-663.

Karin M. and Greten F. (2005). NF-kappaB: linking inflammation and immunity to cancer development and progression. Nat Rev Immunol *5(10)*, 749-759.

Kato K., Cantwell M., Sharma S. and Kipps T. (1998). Gene transfer of CD40-ligand induces autologous immune recognition of chronic lymphocytic leukemia B cells. J Clin Invest. *101(5)*, 1133–1141.

Kawabe T., Naka T., Yoshida K., Tanaka T., Fujiwara H., Suematsu S., Yoshida N., Kishimoto T. and Kikutani H. (1994). The immune responses in CD40-deficient mice: impaired immunoglobulin class switching and germinal center formation. Immunity *1(3)*, 167-178

Kim Y. and Tian M. (2009). NF-kappaB family of transcription factor facilitates gene conversion in chicken B cells. Mol Immunol. *46(16)*, 3283-3291.

Komori T., Okada A., Stewart V. and Alt F. (1993). Lack of N regions in antigen receptor variable genes of TdT-deficient lymphocytes. Science *261*, 1171-1175.

Kothapalli N., Norton D. and Fugmann S. (2008). Cutting Edge: A *cis*-Acting DNA Element Targets AID-Mediated Sequence Diversification to the Chicken Ig Light Chain Gene Locus. The Journal of Immunology 180, 2019 -2023.

Landowski T.**,** Qu N.**,** Buyuksal I.**,** Painter J. and Dalton W. (1997). Mutations in the Fas Antigen in Patients With Multiple Myeloma. Blood *90(11)*, 4266-4270.

Lee SY, Reichlin A, Santana A, Sokol KA, Nussenzweig MC, Choi Y. TRAF2 is essential for JNK but not NF-kappaB activation and regulates lymphocyte proliferation and survival.
Immunity *7(5)*, 703-713.

Li Z., Otevrel T., Gao Y., Cheng H., Seed B., Stamato T., Taccioli G. and Alt F. (1995). The XRCC4 gene encodes a novel protein involved in DNA double-strand break repair and V(D)J recombination. Cell *83*, 1079-1089.

Li Z., Chu W., Hu Y., Delhase M., Deerinck T., Ellisman M., Johnson R. and Karin M. (1999). The IKKbeta subunit of IkappaB kinase (IKK) is essential for nuclear factor kappaB activation and prevention of apoptosis. J Exp Med *189(11)*, 1839-1845.

Li Z., Omori S., Labuda T., Karin M. and Rickert R. (2003). IKK beta is required for peripheral B cell survival and proliferation. J Immunol. *170(9)*, 4630-4637.

Liou H., Nolan G., Ghosh S., Fujita T. and Baltimore D. (1992). The NF-kappa B p50 precursor, p105, contains an internal I kappa B-like inhibitor that preferentially inhibits p50. EMBO *11(8)*, 3003-3009.

Liptay S., Schmid R., Nabel E. and Nabel G. (1994). Transcriptional regulation of NF-kappa B2: evidence for kappa B-mediated positive and negative autoregulation. Mol Cell Biol *14(12)*, 7695-7703.

Loffert D., Ehlich A., Müller W. and Rajewsky K (1996). Surrogate light chain expression is required to establish immunoglobulin heavy-chain allelic exclusion during early B-cell development. Immunity *4*, 133-144.

Lopes-Carvalho T., Foote J. and Kearney JF (2005). Marginal zone B cells in lymphocyte activation and regulation. Current Opinion in Immunology *17 (3)*, 244-250.

Martin A. and Scharff M. (2002). Somatic hypermutation of the AID transgene in B and non-B cells. Proc Natl Acad Sci USA *99(19)*, 12304-12308.

Max E., Seidman J. and Leder P. (1979). Sequences of five potential recombination sites encoded close to an immunoglobulin kappa constant region gene. Proc Natl Acad Sci USA *76*, 3450-3454.

McBride K., Barreto V., Ramiro A., Stavropoulos P. and Nussenzweig M (2004). Somatic hypermutation is limited by CRM1-dependent nuclear export of activation-induced deaminase. J Exp Med *199(9)*, 1235-1244.

Melchers F., Karasuyama H., Haasner D., Bauer S., Kudo A., Sakaguchi N., Jameson B. and Rolink A. (1993). The surrogate light chain in B-cell development. Immunol Today *14(2)*, 60-68.

Melchers F., Ten-Boeckel E., Yamagami T., Andersson J. and Rolink A. (1999). The roles of pre-B and B-cell receptors in the stepwise allelic exclusion of mouse IgH and L chain gene loci. Semin Immunol *11*, 307-317.

Melchers F., Ten Boeckel E., Seidl T., Kong X., Yamagami T., Onishi K., Shimizu T., Rolink A., Andersson J. (2000). Repertoire selection by pre-B-cell-receptors, and genetic control of B-cell development from immature to mature B-cells. Immunol Rev. *135*, 5-242.

Mercurio F., DiDonato J., Rosette C. and Karin M. (1993). p105 and p98 precursor proteins play an active role in NF-kappa B-mediated signal transduction. Genes Dev *7(4)*, 705-718.

Muramatsu M., Sankaranand V., Anant S., Sugai M., Kinoshita K., Davidson N. and Honjo T. (1999). Specific expression of activation-induced cytidine deaminase (AID), a novel member of the RNA-editing deaminase family in germinal center B cells. J Biol Chem *274 (26)*, 18470-18476.

Muramatsu M., Kinoshita K., Fagarasan S., Yamada S., Shinkai Y. and Honjo T. (2000). Class switch recombination and hypermutation require activation-induced cytidine deaminase (AID), a potential RNA editing enzyme. Cell *102*, 553-563.

Müschen M., Re D., Jungnickel B., Diehl V., Rajewsky K. and Küppers R. (2000). Somatic mutation of the CD95 gene in human B cells as a side-effect of the germinal center reaction. J Exp Med *192(12)*, 1833-40.

Nambu Y., Sugai M., Gonda H., Lee C., Katakai T., Agata Y., Yokota Y. and Shimizu A. (2003). Transcription-coupled events associating with immunoglobulin switch region chromatin. Science *302(5653)*, 2137-2140.

Nera K., Kohonen P., Narvi E., Peippo A., Mustonen L., Terho P., Koskela K., Buerstedde J. and Lassila O. (1996). Loss of Pax5 promotes plasma cell differentiation. Immunity *24(3)*, 283-293.

Neuberger M. and Milstein C. (1995). Somatic hypermutation. Curr Opin Immunol *7(2)*, 248-254.

Neurath M., Strober W. and Wakatsuki Y. (1997). The murine Ig 3' alpha enhancer is a target site with repressor function for the B cell lineage-specific transcription factor BSAP (NF-HB, S alpha-BP). The Journal of Immunology *153(2)*, 730-742.

Okazaki I., Kotani A. and Honjo T. (2007). Role of AID in tumorigenesis. Adv Immunol *94*: 245-273.

Okazaki I., Kinsoshita K., Muramatsu M., Yoshikawa K. and Honjo T. (2002). The AID enzyme induces class switch recombination in fibroblasts. Nature *416(6878)*, 340-345.

Olins D., Edelman G. (1962). The antigenic structure of the polypeptide chains of human gamma-globulin. J Exp Med *116*, 635-651.

Palombella V., Rando O., Goldberg A. and Maniatis T. (1994). The ubiquitin-proteasome pathway is required for processing the NF-kappa B1 precursor protein and the activation of NF-kappa B. Cell *78(5)*, 773-785.

Pasparakis M., Schmidt-Supprian M. and Rajewsky K. (2002). IkappaB kinase signaling is essential for maintenance of mature B cells. J Exp Med *196(6)*, 743-752.

Pasqualucci L., Migliazza A., Fracchiolla N., William C., Neri A., Baldini L., Chaganti R., Klein U., Küppers R., Rajewsky K. and Dalla-Favera R. (1998). BCL-6 mutations in normal germinal center B cells: evidence of somatic hypermutation acting outside Ig loci. Proc Natl Acad Sci USA *95(20)*, 11816-11821.

Pasqualucci L., Guglielmino R., Houldsworth J., Mohr J., Aoufouchi S., Polakiewicz R., Chaganti R. and Dalla-Favera R. (2004). Expression of the AID protein in normal and neoplastic B cells. Blood *104(10)*, 3318-3325.

Paulie S., Rosén A., Ehlin-Henriksson B., Braesch-Andersen S., Jakobson E., Koho H. and Perlmann P. (1989). The human B lymphocyte and carcinoma antigen, CDw40, is a phosphoprotein involved in growth signal transduction. J Immunol *142(2)*, 590-595.

Pauling L., Campbell D. and Pressman D (1943). The nature of the forces between antigen and antibody and of the precipitation reaction. Physiological Reviews *23*, 203-219.

Pellat-Deceunynck C., Amiot M., Robillard N., Wijdenes J. and Bataille R. (1996). CD11a-CD18 and CD102 interactions mediate human myeloma cell growth arrest induced by CD40 stimulation. Cancer *Res 56(8)*, 1909-1916.

Perkins N., Edwards N., Duckett C., Agranoff A., Schmid R. and Nabel G. (1993). A cooperative interaction between NF-kappa B and Sp1 is required for HIV-1 enhancer activation. EMBO J. *12(9)*, 3551–3558.

Petersen-Mahrt S. and Neuberger M. (2003). In vitro deamination of cytosine to uracil in single-stranded DNA by apolipoprotein B editing complex catalytic subunit 1 (APOBEC1). J Bio Chem *278(22)*, 19583-19586.

Pham P., Bransteitter R., Petruska J. and Goodman M. (2003). Processive AID-catalysed cytosine deamination on single-stranded DNA simulates somatic hypermutation. Nature *424(6944)*, 103-107.

Pillai S. and Cariappa A. (2009). The follicular versus marginal zone B lymphocyte cell fate decision. Nat Rev Immunol. 9(*11*),767-777.

Pullen S., Miller H., Everdeen D., Dang T., Crute J. and Kehry M. (1998). CD40-tumor necrosis factor receptor-associated factor (TRAF) interactions: regulation of CD40 signaling through multiple TRAF binding sites and TRAF hetero-oligomerization.
Biochemistry *37(34)*, 11836-18845.

Pullen S., Dang T., Crute J. and Kehry M (1999). CD40 signaling through tumor necrosis factor receptor-associated factors (TRAFs). Binding site specificity and activation of downstream pathways by distinct TRAFs. J Biol Chem *274(20)*, 14246-14254.

Rada C., Williams G., Nilsen H., Barnes D., Lindahl T. and Neuberger M. (2002). Immunoglobulin isotype switching is inhibited and somatic hypermutation perturbed in UNG-deficient mice. Curr Biol *12(20)*: 1748-1755.

Rada C., Jarvis J. and Milstein C. (2002). AID-GFP chimeric protein increases hypermutation of Ig genes with no evidence of nuclear localization. Proc Natl Acad Sci USA *99(10)*, 7003-7008.

Revy P., Muto T., Levy Y., Geissmann F., Plebani A., Sanal O., Catalan N., Forveille M., Dufourcq-Lagelouse R., Gennery A., Tezcan I., Ersoy F., Kayserili H., Ugazio AG., Brousse N., Muramatsu M., Notarangelo L., Kinoshita K., Honjo T., Fischer A. and Durandy A. (2000). Activation-induced cytidine deaminase (AID) deficiency causes the autosomal recessive form of the Hyper-IgM syndrome (HIGM2). Cell *102*, 565-575.

Reynaud C., Anquez V., Grimal H. and Weill J. (1987). A hyperconversion mechanism generates the chicken light chain preimmune repertoire. Cell *48(3)*, 379-388.

Reynaud C., Dahan A., Anquez V. and Weill J. (1989). Somatic hyperconversion diversifies the single Vh gene of the chicken with a high incidence in the D region. *Cell 59(1)*, 171-183.

Ribeiro P., Renard N., Warzocha K., Charlot C., Jeandenant L., Callet-Bauchu E., Coiffier B. and Salles G. (2002). CD40 regulation of death domains containing receptors and their ligands on lymphoma B cells. British Journal of Haematology 103(3), 684-689.

Rickert R., Roes J. and Rajewsky K. (1997). B lymphocyte-specific, Cre-mediated mutagenesis in mice. Nucleic Acids Res *25*, 1317-1318.

Rogozin I. and Klochanov N. (1992). Somatic hypermutagenesis in immunoglobulin genes. II. Influence of neighbouring base sequences on mutagenesis. Biochim Biophys Acta *1171*, 11-18.

Rowland S., Tremblay M., Ellison J., Stunz L., Bishop G., Hostager B. (2007). A novel mechanism for TNFR-associated factor 6-dependent CD40 signaling. J Immunol. *179(7)*: 4645-4653.

Sale J. (2004). Immunoglobulin diversification in DT40: a model for vertebrate DNA damage tolerance. DNA repair *3(7)*, 693-702.

Satyaraj and Storb U. (1998). Mef2 proteins, required for muscle differentiation, bind an essential site in the Ig lambda enhancer. J Immunol*. 161 (1998)*, 4795–4802.

Schmidt-Supprian M., Bloch W., Courtois G., Addicks K., Israel A., Rajewsky K. and Pasparakis M. (2000). NEMO/IKK gamma-deficient mice model incontinentia pigmenti. Mol. Cell *5(6)*, 981-992.

Schoetz U., Cervelli M., Wang Y., Fiedler P. and Buerstedde J. (2006). E2A expression stimulates Ig hypermutation. J Immunol. 177(*1*), 395-400..

Sen R. and Baltimore D (1986). Multiple nuclear factors interact with the immunoglobulin enhancer sequences. Cell 1986 *46(5)*, 705-716.

Sen R. and Baltimore D (1986). Inducibility of kappa immunoglobulin enhancer-binding protein Nf-kappa B by a posttranslational mechanism. *Cell 47(6)*, 921-928.

Senftleben U., Cao Y., Xiao G., Greten F., Krähn G., Bonizzi G., Chen Y., Hu Y., Fong A., Sun S. and Karin M. (2001). Activation by IKKalpha of a second, evolutionary conserved, NF-kappa B signaling pathway. Science *293(5534)*, 1495-1499.

Sharpe M., Milstein C., Jarvis J. and Neuberger M. (1991). Somatic hypermutation of immunoglobulin kappa may depend on sequences 3' of C kappa and occurs on passenger transgenes. EMBO J. *10(8)*, 2139-2145.

Shen H., Peters A., Baron B., Zhu X. and Storb U. (1998). Mutation of BCL-6 gene in normal B cells by the process of somatic hypermutation of Ig genes. Science *280(5370)*, 1750-1752.

Shinkura R., Ito S., Begum N., Nagaoka H., Muramatsu M., Kinoshita K., Sakakibara Y., Hijikata H. and Honjo T. (2004). Separate domains of AID are required for somatic hypermutation and class-switch recombination. Nat Immunol *5(7)*, 707-712.

Shokett P. and Schatz D. (1999). DNA hairpin opening mediated by the RAG1 and RAG2 proteins. Mol Cell Biol *19*, 4159-4166.

Siggs O., Berger M., Krebs P., Arnold C., Eidenschenk C., Huber C., Pirie E., Smart N., Khovananth K., Xia Y., McInerney G., Karlsson Hedestam G., Nemazee D. and Beutler B. (2010). A mutation of Ikbkg causes immune deficiency without impairing degradation of IκBα. Proc Natl Acad Sci U S A. *107(7)*:3046-3051.

Solan N., Miyoshi H., Carmona E., Bren G. and Paya C. (2002). RelB cellular regulation and transcriptional activity are regulated by p100. J Biol Chem. *277(2)*, 1405-1418.

Stavnezer J. (1996). Immunoglobulin class switching. Curr Opin Immunol *8*, 199-205.

Ta V., Nagaoka H., Catalan N., Durandy A., Fischer A., Imai K., Nonoyama S., Tashiro J., Ikegawa M., Ito S., Kinoshita K., Muramatsu M. and Honjo T. (2003). AID mutant analyses indicate requirement for class-switch-specific cofactors. Nat Immunol *4(9)*, 843-848.

Tanaka A., Shen H., Ratnam S., Kodgire P. and Storb U. (2010). Attracting AID to targets of somatic hypermutation. JEM (*207)2*, 405-415.

Ten-Boeckel E., Melchers F. and Rolink A. (1995). The status of ig loci rearrangements in single cells from different stages of B-cell development. Intl Immunol *7*, 1013-1019.

Teoh G., Tai Y., Urashima M., Shirahama S., Matsuzaki M., Chauhan D., Treon S., Raje N., Hideshima T., Shima Y. and Anderson K. (2000). CD40 activation mediates p53-dependent cell cycle regulation in human multiple myeloma cell lines. Blood *95(3)*, 1039-46.

Van Eijk M., Defrance T., Hennino A. and de Groot C. (2001). Death-receptor contribution to the germinal-center reaction . Trends in Immunology *22 (12)*, 677-682.

Van Kooten C., Galibert L., Seon B., Garrone P., Liu Y. and Banchereau J. (1997). Cross-linking of antigen receptor via Ig-beta (B29, CD79b) can induce both positive and negative signals in CD40-activated human B cells. Clin Exp Immunol *110(3)*, 509-15.

Vince J., Pantaki D., Feltham R., Mace P., Cordier S., Schmukle A., Davidson A., Callus B., Wong W., Gentle I., Carter H., Lee E., Walczak H., Day C., Vaux D. and Silke J. (2009). TRAF2 must bind to cellular inhibitors of apoptosis for tumor necrosis factor (tnf) to efficiently activate nf-{kappa}b and to prevent tnf-induced apoptosis. J Biol Chem. *284(51)*, 35906-35915.

Waterfield M., Jin W., Reiley W., Zhang M. and Sun S. (2004). IkappaB kinase is an essential component of the Tpl2 signaling pathway. Mol Cell Biol *24(13)*, 6040-6048.

Winau F., Westphal O. and Winau R. (2004). Paul Ehrlich – in search of the magic bullet. Microbes and Infection *6*, 786-789.

Xiang Y. and Garrard W. (2008). The downstream transcriptional enhancer, Ed, positively regulates mouse Ig gene expression and somatic hypermutation. The journal of immunology *180*, 6725-6732.

Xiao G., Harhaj E. and Sun S. (2001). NF-kappaB-inducing kinase regulates the processing of NF-kappaB2 p100. Mol Cell *7(2)*, 401-409.

Yang S., Fugmann S. and Schatz D. (2006). Control of gene conversion and somatic hypermutation by immunoglobulin promoter and enhancer sequences. JEM *203(13)*, 2919-2928.

Yilmaz Z., Weih D., Sivakumar V., Weih F. (2003). RelB is required for Peyer's patch development: differential regulation of p52-RelB by lymphotoxin and TNF. EMBO J *22(1)*, 121-130.

Yoshikawa K., Okazaki I., Eto T., Kinoshita K., Muramatsu M., Nagaoka H. and Honjo T. (2002). AID enzyme-induced hypermutation in an actively transcribed gene in fibroblasts. Science *296(5575)*, 2033-2036.

Zarnegar B., He J., Oganesyan G, Hoffmann A., Baltimore D. and Cheng G. (2004) Unique CD40-mediated biological program in B cell activation requires both type 1 and type 2 NF-kappaB activation pathways. Proc Natl Acad Sci U S A *101(21)*, 8108–8113.

Zhou C., Saxon A. and Zhang K. (2003). Human activation-induced cytidine deaminase is induced by IL-4 and negatively regulated by CD45: implication of CD45 as a Janus kinase phosphatase in antibody diversification. J Immunol *170(4)*, 1887-1893.

7. Supplementary data

7.1 List of primers

All primers are designated in 5’ -> 3’ direction

Primer for PCR screening for targeted integration:
Forward: AGCTTGGAATTTAACCTCTCCTGTAAA
Reverse: CCCACCGACTCTAGAGGATCATAATCAGCC
VJ intervening sequence of unrearranged IgL locus:
Forward: GGGGGATCCAGATCTGTGACCGGTGCAAGTGATAGAAAACT
Reverse: TACAAAAACCTCCTGCCACTGCAAGGAGCGAGCTGATGGTTTTTACTGTCT

Targeting Arms for the plasmid pIgL$^{-,GFP2}$:
5’-arm Forward: GGGCTCGAGGGTACTGCGTTTTCCACAAAATTCTCACAG
5’-arm Reverse: GGGAGATCTCTGCACTCTGGCACCGTTAAGCACCATCAC
3’-arm Forward: GGGTGATCAAGATCTGCTAGCACTAGTGGATCCGTCGA
3’-arm Reverse: GGGGAAAAGCGGCCGCCACTGGAAGGAGCTGAAGGCCAC

DNA fragments belonging to the IgL 1kb staggered end deletion series:

***‘A’*:** Forward: GAAGCTAGCTTCCGCCATGGCCTGGGCTCCTCTCC
Reverse: GAAACTAGTATTTTTTGACAGCACTTACCTGGACAGCTGAAAAACTGAA

***‘B’*:** Forward: GGGGCTAGCGGTGGATGTGTTTGTTTTACAGAGG
Reverse: GAAGCTAGCGCAAATCTCTGCTAGGGACCTGGCG

***‘C’*:** Forward: GGGGCTAGCGGTGGATGTGTTTGTTTTACAGAGG
Reverse: GAAGCTAGCGTGTGGCAGAGAGTCTACACATGGC

***‘D’*:** Forward: GGGGCTAGCGGTGGATGTGTTTGTTTTACAGAGG
Reverse: GAAGCTAGCATGGAGCTGTACCATGCGGCCTGCT

***‘E’*:** Forward: GGGGCTAGCGGTGGATGTGTTTGTTTTACAGAGG
Reverse: GAAGCTAGCAAGCTCAGGGTCTCAGTTTGGAGCT

***‘F’*:** Forward: GGGGCTAGCGGTGGATGTGTTTGTTTTACAGAGG
Reverse: GAAGCTAGCATTGCTGCAGTGCAAACGCCCTGGT

***‘G’*:** Forward: GGGGCTAGCGGTGGATGTGTTTGTTTTACAGAGG
Reverse: GGGACTAGTTGTTCAGATGGAACTTCTTATGTTC

***‘I’*:** Forward: GGGGCTAGCGGTGGATGTGTTTGTTTTACAGAGG
Reverse: GAAGCTAGCATGGGATGGAAGGGCCCGTCTGGCC

***‘K’*:** Forward: GAAGCTAGCTTTATGCTGGGAACAGGGGGAGTTC
Reverse: GAAGCTAGCATGGGATGGAAGGGCCCGTCTGGCC

***‘L’*:** Forward: GAAGCTAGCAGGACTGTGCTGTCCTCATGCCCCT
Reverse: GAAGCTAGCATGGGATGGAAGGGCCCGTCTGGCC

***‘M’*:** Forward: GAAGCTAGCCACGACAGCTGGGGCCACACAAAGA
Reverse: GAAGCTAGCATGGGATGGAAGGGCCCGTCTGGCC

***‘N’*:** Forward: GAAGCTAGCGTCACAGGTTGTAACAGGCTGACAT
Reverse: GAAGCTAGCATGGGATGGAAGGGCCCGTCTGGCC

***‘P’*:** Forward: GGGGCTAGCTCACAGAAACATTGAAATGGCTCCT
Reverse: GAAGCTAGCATGGGATGGAAGGGCCCGTCTGGCC

***'S'*:** Forward: GAAGCTAGCTTTATGCTGGGAACAGGGGGAGTTC
Reverse: GAAACTAGTATTGCTGCAGTGCAAACGCCCTGGT

DNA fragments belonging to the 'S' 1kb deletion series

***'0-1'*:** Forward: GAAGCTAGCTTTATGCTGGGAACAGGGGGAGTTC
Reverse: GAAACTAGTGTGTGGCAGAGAGTCTACACATGGC

***'0-2'*:** Forward: GAAGCTAGCTTTATGCTGGGAACAGGGGGAGTTC
Reverse: GAAACTAGTATGGAGCTGTACCATGCGGCCTGCT

***'0-3'*:** Forward: GAAGCTAGCTTTATGCTGGGAACAGGGGGAGTTC
Reverse: GAAACTAGTAAGCTCAGGGTCTCAGTTTGGAGCT

***'0-4'*:** Forward: GAAGCTAGCTTTATGCTGGGAACAGGGGGAGTTC
Reverse: GAAACTAGTATTGCTGCAGTGCAAACGCCCTGGT

***'1-2'*:** Forward: GAAGCTAGCAGGACTGTGCTGTCCTCATGCCCCT
Reverse: GAAACTAGTATGGAGCTGTACCATGCGGCCTGCT

***'2-3'*:** Forward: GAAGCTAGCCACGACAGCTGGGGCCACACAAAGA
Reverse: GAAACTAGTAAGCTCAGGGTCTCAGTTTGGAGCT

***'3-4'*:** Forward: GAAGCTAGCGTCACAGGTTGTAACAGGCTGACAT
Reverse: GAAACTAGTATTGCTGCAGTGCAAACGCCCTGGT

***'2-4'*:** Forward: GAAGCTAGCCACGACAGCTGGGGCCACACAAAGA
Reverse: GAAACTAGTATTGCTGCAGTGCAAACGCCCTGGT

***'1-4'*:** Forward: GAAGCTAGCAGGACTGTGCTGTCCTCATGCCCCT
Reverse: GAAACTAGTATTGCTGCAGTGCAAACGCCCTGGT

DNA fragments belonging to the 'S' 200 bp internal deletion series

Forward primer for hybrid PCR: GAAGCTAGCTTTATGCTGGGAACAGGGGGAGTTC
Reverse primer for hybrid PCR: GAAACTAGTATTGCTGCAGTGCAAACGCCCTGGT

'SΔ0.0-0.2': Forward: GAAGCTAGCTGGCCCCTGTAGGAGCTTTTAGCAC
Reverse: GAAACTAGTATTGCTGCAGTGCAAACGCCCTGGT

'SΔ0.2-0.4':

0.0-0.2: Forward: GAAGCTAGCTTTATGCTGGGAACAGGGGGAGTTC
Reverse: GGATGAATGCATATGCTGCAAAATCTCCCTGGGGAGCGGG

0.4-4.0: Forward: ATTTTGCAGCATATGCATTCATCCCACCCACCCAAACATG
Reverse: GAAACTAGTATTGCTGCAGTGCAAACGCCCTGGT

'SΔ0.4-0.6':

0.0-0.4: Forward: GAAGCTAGCTTTATGCTGGGAACAGGGGGAGTTC
Reverse: CTGGATGGACATATGGAGATGTTGGTGTAGATGGAATAG

0.6-4.0: Forward: CAACATCTCCATATGTCCATCCAGCCACTGGTGGGGTGCA
Reverse: GAAACTAGTATTGCTGCAGTGCAAACGCCCTGGT

'SΔ0.6-0.8':

0.0-0.6: Forward: GAAGCTAGCTTTATGCTGGGAACAGGGGGAGTTC
Reverse: TGCCTGCCACATATGAGACATAGGGTGGGTGGGATGGCTG

0.8-4.0: Forward: CCTATGTCTCATATGTGGCAGGCATTCATGACACTGGGTT
Reverse: GAAACTAGTATTGCTGCAGTGCAAACGCCCTGGT

***'SΔ0.8-1.0'*:**

0.0-0.8: Forward: GAAGCTAGCTTTATGCTGGGAACAGGGGGAGTTC
Reverse: CACAGTCCTCATATGTGGAGCTGGGAGATCCCAGCCCATCT

1.0-4.0: Forward: CCCAGCTCCACATATGAGGACTGTGCTGTCCTCATGCCCCT
Reverse: GAAACTAGTATTGCTGCAGTGCAAACGCCCTGGT

'SΔ1.0-1.2':

0.0-1.0: Forward: GAAGCTAGCTTTATGCTGGGAACAGGGGGAGTTC
Reverse: TGAGCAGCTCATATGGTGTGGCAGAGAGTCTACACATGGC

1.2-4.0: Forward: CTGCCACACCATATGAGCTGCTCATGCTGGATAAAGTCAC
Reverse: GAAACTAGTATTGCTGCAGTGCAAACGCCCTGGT

'SΔ1.2-1.4':

0.0-1.2: Forward: GAAGCTAGCTTTATGCTGGGAACAGGGGGAGTTC
Reverse: ATTCAGCACCATATGGCCTCAGGGACAGTTTGGTAAATCC

1.4-4.0: Forward: CCCTGAGGCCATATGGTGCTGAATTATACATCACAGCTCC
Reverse: GAAACTAGTATTGCTGCAGTGCAAACGCCCTGGT

'SΔ1.4-1.6':

0.0-1.4: Forward: GAAGCTAGCTTTATGCTGGGAACAGGGGGAGTTC
Reverse: GCTGCAGCTCATATGATGCTCCTCAGTGGGTTGTTGCTTC

1.6-4.0: Forward: GAGGAGCATCATATGAGCTGCAGCTCTTGCTCTGTCGTGT
Reverse: GAAACTAGTATTGCTGCAGTGCAAACGCCCTGGT

'SΔ1.6-1.8':

0.0-1.6: Forward: GAAGCTAGCTTTATGCTGGGAACAGGGGGAGTTC
Reverse: GGATATCAGCATATGGGGTAGCCTGGGGTTGCTTTCTATC

1.8-4.0: Forward: AGGCTACCCCATATGCTGATATCCTCACTAGCAGATACAC
Reverse: GAAACTAGTATTGCTGCAGTGCAAACGCCCTGGT

'SΔ1.8-2.0':

0.0-1.8: Forward: GAAGCTAGCTTTATGCTGGGAACAGGGGGAGTTC
Reverse: GCTGTCGTGCATATGCTCCCTGTGCGATCCAGGCCCCACG

2.0-4.0: Forward: CACAGGGAGCATATGCACGACAGCTGGGGCCACACAAAGA
Reverse: GAAACTAGTATTGCTGCAGTGCAAACGCCCTGGT

'SΔ2.0-2.2':

0.0-2.0: Forward: GAAGCTAGCTTTATGCTGGGAACAGGGGGAGTTC
Reverse: CTCACAGCTCATATGATGGAGCTGTACCATGCGGCCTGCT

2.2-4.0: Forward: CAGCTCCATCATATGAGCTGTGAGGCCGGGGCATCCCCAA
Reverse: GAAACTAGTATTGCTGCAGTGCAAACGCCCTGGT

'SΔ2.2-2.4':

0.0-2.2: Forward: GAAGCTAGCTTTATGCTGGGAACAGGGGGAGTTC
Reverse: GCAGCAAAGCATATGGCATGGTGGGGCTGAGCGTGCTGCA

2.4-4.0: Forward: CCACCATGCCATATGCTTTGCTGCTGCTGCTCGGGGTGGG
Reverse: GAAACTAGTATTGCTGCAGTGCAAACGCCCTGGT

'SΔ2.4-2.6':

0.0-2.4: Forward: GAAGCTAGCTTTATGCTGGGAACAGGGGGAGTTC
Reverse: TGGGAGCGGCATATGACTCAGTCTGCAAAGGCCCCAACCT

2.6-4.0: Forward: AGACTGAGTCATATGCCGCTCCCACCACGCGTCAACCCAA
Reverse: GAAACTAGTATTGCTGCAGTGCAAACGCCCTGGT

'SΔ2.6-2.8':

0.0-2.6: Forward: GAAGCTAGCTTTATGCTGGGAACAGGGGGAGTTC
Reverse: TAATTCCTCCATATGGCAGGGGTGGCACATGGGGACAGAG

2.8-4.0: Forward: CCACCCCTGCCATATGGAGGAATTAAATTAAATCAATAAAT
Reverse: GAAACTAGTATTGCTGCAGTGCAAACGCCCTGGT

'SΔ2.8-3.0':

0.0-2.8: Forward: GAAGCTAGCTTTATGCTGGGAACAGGGGGAGTTC
Reverse: ACCTGTGACCATATGTTTAATTGCTGTGTGATGGCTCTGA
3.0-4.0: Forward: GCAATTAAACATATGGTCACAGGTTGTAACAGGCTGACAT
Reverse: GAAACTAGTATTGCTGCAGTGCAAACGCCCTGGT

'SΔ3.0-3.2':
0.0-3.0: Forward: GAAGCTAGCTTTATGCTGGGAACAGGGGGAGTTC
Reverse: TGTCAGTGTCATATGAAGCTCAGGGTCTCAGTTTGGAGCT
3.2-4.0: Forward: CCTGAGCTTCATATGACACTGACAACACAATGTGAGCTGA
Reverse: GAAACTAGTATTGCTGCAGTGCAAACGCCCTGGT

'SΔ3.2-3.4':
0.0-3.2: Forward: GAAGCTAGCTTTATGCTGGGAACAGGGGGAGTTC
Reverse: TGCTGGCTGCATATGGCATCTTGTGGCCCTCCTGCATCGG
3.4-4.0: Forward: ACAAGATGCCATATGCAGCCAGCAGCTGCCCTGCACTAAG
Reverse: GAAACTAGTATTGCTGCAGTGCAAACGCCCTGGT

'SΔ3.4-3.6':
0.0-3.4: Forward: GAAGCTAGCTTTATGCTGGGAACAGGGGGAGTTC
Reverse: ATCTGGGAGCATATGCATCCCCCCACCTCCTCTGTGTGTG
3.6-4.0: Forward: GGGGGGATGCATATGCTCCCAGATGTGCTGACCGCAGCCA
Reverse: GAAACTAGTATTGCTGCAGTGCAAACGCCCTGGT

'SΔ3.6-3.8':
0.0-3.6: Forward: GAAGCTAGCTTTATGCTGGGAACAGGGGGAGTTC
Reverse: CTGGCTCTGCATATGAGTGCAGGCTCAGCTGTGGGGCTGG
3.8-4.0: Forward: GCCTGCACTCATATGCAGAGCCAGGAGCAGGAAATGCTGA
Reverse: GAAACTAGTATTGCTGCAGTGCAAACGCCCTGGT

'SΔ3.8-4.0': Forward: GAAGCTAGCTTTATGCTGGGAACAGGGGGAGTTC
Reverse: GAAACTAGTGTTGCTGCTGTGCCGGGCAGCGGCG

DNA fragments belonging to the '2-3' 50 bp fragment end deletion series

'2.00-2.05': Forward: GAAGCTAGCCACGACAGCTGGGGCCACACAAAGA
Reverse: GGGACTAGTCTGCCCACAGTAACCCAGCTCTTTG

'2.00-2.10': Forward: GAAGCTAGCCACGACAGCTGGGGCCACACAAAGA
Reverse: GGGACTAGTGCTCCCGGGGCTATTCTGAGCCCCCA

'2.00-2.15': Forward: GAAGCTAGCCACGACAGCTGGGGCCACACAAAGA
Reverse: GGGACTAGGCTGTGTGGCCCTGGGCCTGGTGCT

'2.00-2.20': Forward: GAAGCTAGCCACGACAGCTGGGGCCACACAAAGA
Reverse: GGGACTAGTGGTGGGGCTGAGCGTGCTGCACCCT

'2.00-2.25': Forward: GAAGCTAGCCACGACAGCTGGGGCCACACAAAGA
Reverse: GGGACTAGAGACTGAGAAGTAAATTTAGCTTGG

'2.00-2.30': Forward: GAAGCTAGCCACGACAGCTGGGGCCACACAAAGA
Reverse: GGGACTAGCGTTTCCTTTTTTTGGCCGGCGTGGG

'2.00-2.35': Forward: GAAGCTAGCCACGACAGCTGGGGCCACACAAAGA
Reverse: GGGACTAGGCGCGGCGCTCGCTCTGCTTCACAC

'2.00-2.40': Forward: GAAGCTAGCCACGACAGCTGGGGCCACACAAAGA
Reverse: GGGACTAGGCTCAGTCTGGCAAAGCCCCAACCTG

'2.00-2.45': Forward: GAAGCTAGCCACGACAGCTGGGGCCACACAAAGA
Reverse: GGGACTAGCCCATCCCATGTGCCCAGGCCGTGG

'2.00-2.50': Forward: GAAGCTAGCCACGACAGCTGGGGCCACACAAAGA
Reverse: GGGACTAGTCACCTGAAGTGTTGGGGTGTGGGTG

‘2.00-2.55’: Forward: GAAGCTAGCCACGACAGCTGGGGCCACACAAAGA
Reverse: GGGACTAGAGGCCCATGCGTGGGGGGGTCAGC
‘2.00-2.60’: Forward: GAAGCTAGCCACGACAGCTGGGGCCACACAAAGA
Reverse: GGGACTAGGGCAGGGGTGGCACATGGGGACAGAG
‘2.00-2.65’: Forward: GAAGCTAGCCACGACAGCTGGGGCCACACAAAGA
Reverse: GGGACTAGCAGGAGTCGTGGGATTAACTCAGG
‘2.00-2.70’: Forward: GAAGCTAGCCACGACAGCTGGGGCCACACAAAGA
Reverse: GGGACTAGCTGCTCTGCATTTTGGGCATCTCCAG
‘2.00-2.75’: Forward: GAAGCTAGCCACGACAGCTGGGGCCACACAAAGA
Reverse: GGGACTAGTCCGCAGGGGAACACCCATAACTCC
‘2.00-2.80’: Forward: GAAGCTAGCCACGACAGCTGGGGCCACACAAAGA
Reverse: GGGACTAGCTCTTTAATTGCTGTGTGATGGCTCTG
‘2.00-2.85’: Forward: GAAGCTAGCCACGACAGCTGGGGCCACACAAAGA
Reverse: GGGACTAGGGTGCTGGCAGCTGAGCCCGCCTAAAAC
‘2.00-2.90’: Forward: GAAGCTAGCCACGACAGCTGGGGCCACACAAAGA
Reverse: GGGACTAGACAGCCATGCAAATGCTCTCCTCTTTGC
‘2.00-2.95’*:* Forward: GAAGCTAGCCACGACAGCTGGGGCCACACAAAGA
Reverse: GGGACTAGTTTCCAGATAACACCATCCCAGCTGC
‘2.05-3.00’: Forward: GACGCTAGCGAAACCCGAAAACAAGAGCTGGGGGCTC
Reverse: GAAACTAGTAAGCTCAGGGTCTCAGTTTGGAGCT
‘2.10-3.00’: Forward: GACGCTAGCCACCAGGCCCAGGGCCACACAGCCC
Reverse: GAAACTAGTAAGCTCAGGGTCTCAGTTTGGAGCT
‘2.15-3.00’: Forward: GACGCTAGCAGGAAGGCACAGCGCTGTCAGGGTGC
Reverse: GAAACTAGTAAGCTCAGGGTCTCAGTTTGGAGCT
‘2.20-3.00’: Forward: GACGCTAGCCTGTGCGGCCGGGGCATCCCCAAGC
Reverse: GAAACTAGTAAGCTCAGGGTCTCAGTTTGGAGCT
‘2.25-3.00’: Forward: GACGCTAGCAGAAACTGAAGCTGAGGGGCCCACG
Reverse: GAAACTAGTAAGCTCAGGGTCTCAGTTTGGAGCT
‘2.30-3.00’: Forward: GACGCTAGCGTCTCCAGAAAGCACTGACGTGTGA
Reverse: GAAACTAGTAAGCTCAGGGTCTCAGTTTGGAGCT
‘2.35-3.00’: Forward: GACGCTAGCGCCGCCATGTCACACACCTCAGGTT
Reverse: GAAACTAGTAAGCTCAGGGTCTCAGTTTGGAGCT
‘2.40-3.00’: Forward: GACGCTAGCTGCTGCTCGGGGTGGGTGCCCACGG
Reverse: GAAACTAGTAAGCTCAGGGTCTCAGTTTGGAGCT
‘2.45-3.00’: Forward: GACGCTAGCCACGTACACACACTTGCACACCCACACC
Reverse: GAAACTAGTAAGCTCAGGGTCTCAGTTTGGAGCT
‘2.50-3.00’: Forward: GACGCTAGCGCAGATGGGTGCCCCCCAGGCTGACC
Reverse: GAAACTAGTAAGCTCAGGGTCTCAGTTTGGAGCT
‘2.55-3.00’: Forward: GACGCTAGC CACTGCTCCATCCGTGTCTCTGTCC
Reverse: GAAACTAGTAAGCTCAGGGTCTCAGTTTGGAGCT
‘2.60-3.00’: Forward: GACGCTAGC ACCACGCGTCAACCCAAATCCTGAG
Reverse: GAAACTAGTAAGCTCAGGGTCTCAGTTTGGAGCT
‘2.65-3.00’: Forward: GACGCTAGC CCAGCGTCCATGGCAGACTGGAGAT
Reverse: GAAACTAGTAAGCTCAGGGTCTCAGTTTGGAGCT
‘2.70-3.00’: Forward: GACGCTAGC CTGAATCTGAGAGATGAAATGGAGT
Reverse: GAAACTAGTAAGCTCAGGGTCTCAGTTTGGAGCT
‘2.75-3.00’: Forward: GACGCTAGC CCAGCTGTAGGAAGCTCAGAGCCATC
Reverse: GAAACTAGTAAGCTCAGGGTCTCAGTTTGGAGCT

‘2.80-3.00’: Forward: GACGCTAGC ATTAAATCAATAAATGTTTTAGGCG
Reverse: GAAACTAGTAAGCTCAGGGTCTCAGTTTGGAGCT
‘2.85-3.00’: Forward: GACGCTAGC CGAAACAGCCCGCTTGCAAAGAGG
Reverse: GAAACTAGTAAGCTCAGGGTCTCAGTTTGGAGCT
‘2.90-3.00’: Forward: GACGCTAGC CAGCAACCGCCTGTTGTGCAGCTGG
Reverse: GAAACTAGTAAGCTCAGGGTCTCAGTTTGGAGCT
‘2.95-3.00’: Forward: GACGCTAGC AGCCCAGGAGGGGTAAACAGCTCC
Reverse: GAAACTAGTAAGCTCAGGGTCTCAGTTTGGAGCT

DNA fragment ‘2.2-2.4’ for reconstitution and multimerization

‘2.2-2.4’: Forward: GAGGCTAGCAGCTGTGCGGCCGGGGCATCCCCAA
Reverse: GAGACTAGTGGCGCGCCAGCTCAGTCTGGCAAAGCCCCAACCT

7.2 R program

For the statistical analysis of *cis*-elements, I developed following program in collaboration with Herbert Braselmann.

```
setwd("Path…/R")

dframe<- read.table(file="template.txt",header=TRUE,sep="\t",na.strings="")
nrow(dframe)
ncol(dframe)
names(dframe)
attach(dframe)

clone<- factor(c(rep("ref",24),rep("R",24)))
x<- c(rep(1,24),rep(2,24))
y<- as.vector(rbind(ref,ClR))
plot(clone,y)
plot(x,y,xlim=c(0,3))

wilcox.test(ref,clR)
```

Acknowledgements

Mein besonderer Dank gilt Herrn Prof. Horst Zitzelsberger und Frau PD Dr. Ursula Zimber-Strobl, die mich intensiv betreut und mir große Perspektiven eröffnet haben und damit ganz besonders zum Gelingen dieser Arbeit beigetragen haben.

Weiterhin möchte ich mich herzlichst bei Herrn Prof. Jerzy Adamski für seine große Unterstützung und seine Betreuung an der TU München bedanken. Bei Herrn Prof. Michael Atkinson bedanke ich mich für die zusätzliche Betreuung und das Korrekturlesen meiner Arbeit, die mir eine große Hilfe waren.

Ich möchte mich an dieser Stelle auch bei Marc Schmidt-Supprian für die Überlassung der $NEMO^{fl/fl}$ und $IKK2^{fl/fl}$ Mausstämme und viele fruchtbare Diskussionen bedanken.

Mein ganz besonderer Dank geht an Frau Dr. Ulrike Schötz, die mir durch die wunderbare Zusammenarbeit und die fachlichen Diskussionen immer wieder die Freude an der Wissenschaft aufgezeigt hat.

Des Weiteren möchte ich mich ganz herzlich bei Frau Kristina Djermanovic für die belebende Zusammenarbeit, die vielen spannenden Diskussionen und ihre Unterstützung, die mir meine Arbeit sehr erleichtert hat, danken.

Vielen Dank möchte ich auch all denen aussprechen, die mit ihrer Arbeit zum Gelingen dieses Projektes beigetragen haben. Vielen Dank Steffen Heuer, Ursula Holter, Arundhathi Sriharshan und allen Maustierpflegern, insbesondere Manfred Felbermeyer, Andy Kühn und Undine Hurt.

Ich möchte mich auch bei allen Kollegen und ehemaligen Kollegen bedanken, die mich immer wieder unterstützt und neu motiviert haben. Vielen Dank für Eure fachlichen Ratschläge, aber auch dafür, dass Ihr eine so wunderbar freundschaftliche Atmosphäre geschaffen habt. Viele Ideen wären ohne Euch nicht entstanden.

Ein ganz besonderer Dank geht an all jene Freunde, die mich immer wieder unterstützt und aufgebaut, mit mir jede Lebenslage gemeistert haben und immer zu mir standen. Insbesondere möchte ich dabei Frau Tina Limmer danken.

Meinen größten Dank möchte ich meiner Familie aussprechen, die mich in allen schwierigen Stunden mit großem Einsatz und viel Liebe unterstützt haben und ohne die diese Arbeit

niemals entstanden wäre. Dabei danke ich ganz besonders meinen Eltern Christa und Karl, meinen Geschwistern Tanja und Sebastian und meinem Partner Christian.

Erklärung

Ich erkläre an Eides statt, dass ich die der Fakultät Wissenschaftszentrum Weihenstephan für Ernährung, Landnutzung und Umwelt er technischen Universität München zur Promotionsprüfung vorgelete Arbeit mit dem Titel:

„The role of AID and NF-κB for B cell development and lymphomagenesis“

am Institut für Experimentelle Genetik

unter der Anleitung und Betreuung durch Herrn Prof. Dr. Jerzey Adamski

ohne sonstige Hilfe erstellt und bei der Abfassung nur die gemäß § 6 Abs. 5 angegebenen Hilfsmittel benutzt habe.

Ich habe diese Dissertation in dieser oder ähnlicher Form in keinem anderen Prüfungsverfahren als Prüfungsleistung vorgelegt.

Ich hab den angestrebten Doktorgrad noch nicht erworben und bin nicht in einem früheren Promotionsverfahren für den angestrebten Dorktorgrad endgültig gescheitert.

Die Promotionsordnung der Technischen Universität München ist mir bekannt.

München, den…… ……
Unterschrift